PROCESS MODELING AND ANALYSIS OF CO_2 PURIFICATION FOR OXY-COAL COMBUSTION

By

Chukwunwike Ogbonnia Iloeje

B.Eng. Mechanical Engineering
University of Nigeria, Nsukka, 2004

SUBMITTED TO THE DEPARTMENT OF MECHANICAL ENGINEERING IN PARTIAL FULFILLMENT OF THE REQUIREMENTS FOR THE DEGREE OF

MASTER OF SCIENCE IN MECHANICAL ENGINEERING
AT THE
MASSACHUSETTS INSTITUTE OF TECHNOLOGY

JANUARY 2011
[February 2011]

Signature of Author . . . . . .
Department of Mechanical Engineering
January 14, 2011

Certified by. 1/25/11
Ahmed F. Ghoniem
Ronald C. Crane Professor
Thesis Supervisor

Accepted by. . . . . .
Dave E. Hardt
Chairman, Department Committee on Graduate Students

PROCESS MODELING AND ANALYSIS OF CO_2 PURIFICATION FOR OXY-COAL COMBUSTION

By

Chukwunwike Ogbonnia Iloeje

Submitted to the Department of Mechanical Engineering
on January 14, 2011 in Partial Fulfillment of the
Requirements for the degree of Master of Science in
Mechanical Engineering

ABSTRACT

Oxy-coal combustion technology has great potential as one of the major CO_2 capture technologies for power generation from coal. The distinguishing feature of oxy-coal combustion is that the oxygen source is a high concentration oxygen stream and the product flue gas consists primarily of CO_2 and H_2O with contaminants like NO_x, SO_x, and non-condensable gases like argon, oxygen and nitrogen. For carbon sequestration and Enhanced Oil Recovery (EOR) applications, pipeline transport standards as well as storage specifications impose concentration limits on these contaminants. These must be removed to ensure that the transported CO_2-rich stream stays within specified limits to prevent aqueous phase separation, hydrate formation, and corrosion due to acids, water or oxygen. The purification process however constitutes additional energy consumption and lowers overall cycle efficiency. Purification options like traditional flue gas desulfurization (FGD), selective catalytic reduction (SCR), catalytic O_2 consumption, packed bed adsorption and low temperature flash separation have been proposed. In this thesis, we develop a novel CO_2 purification process model for oxy combustion systems that utilizes high-pressure reactive absorption columns for NO_x and SO_x rem oval and distillation strategies for non-condensable gas removal. This process results in significant cost savings and lower energy consumption compared to the traditional systems. We conduct a sensitivity analysis NO_x and SO_x removal system to determine the key performance parameters and based on the results present a modification to the base case that results in further cost and energy savings. Different strategies for the removal of non-condensable gases are developed and compared. This study also explores opportunities for integrating the CO_2 purification unit (CPU) with the base cycle and the impacts of the different strategies on the overall oxy combustion cycle efficiency are presented. A cost analysis for the proposed purification process is also presented.

Thesis Supervisor: Ahmed F. Ghoniem
Title: Ronald C. Crane Professor of Mechanical Engineering

Acknowledgements

I would thank my advisor, Professor Ghoniem, first for the opportunity to do this research and even more for his guidance, support and encouragement throughout my Masters Program.

I am also grateful to Randall Field who has been extremely helpful in my research and provided me with necessary direction and support in all aspects of the research.

I am grateful to my colleagues in the ENEL oxy-coal combustion project team, James Hong, Lei Chen and Sze Zheng Yong, for their help and enthusiasm. My thanks also go out to my lab-mates in the Reacting Gas Dynamics group and to Lorraine Rabb who has been very helpful.

I would not forget the encouragement and support I have received from my family and for that I am very grateful.

I would also like to acknowledge Total Corporation for the Fellowship I received for this Masters Program and ENEL for sponsoring my research.

Not least are all the friends who have made life at MIT so much fun. Thank you all for being there.

And a final thanks to God whose care I can always rely on.

Contents

Acknowledgements 4

Chapter 1 Introduction 9

1.1. Motivation 9

1.2. Oxy-Combustion Power Cycle 10

1.3. Characteristics of Oxy-Combustion Flue Gas 12

1.4. CO_2 Disposal Strategies 14

1.5 Purity Specs for Geological Sequestration 18

1.6. CO_2 Purification Process for Oxy-Combustion Systems 20

1.6.1. NO_X and SO_X Removal 20

1.6.2. Non Condensable Gas Removal 26

1.7. The Proposed System 27

1.7.1. NO_X & SO_X Removal (Single Column) System 27

1.7.2. Non Condensable Gas Removal 27

1.8. Conclusion 29

Chapter 2 CO_2 Purification Unit Analysis 31

2.1. SO_X and NO_X Removal Unit 31

2.2. Lead Chamber Chemistry 33

2.3. Nitric Acid Chemistry 57

2.4. Non-condensable Gas Removal Unit 60

2.4.1. Configuration A 61

2.4.2. Configuration B 64

2.5. Conclusion 66

Chapter 3 Results and Sensitivity Analysis 69

3.1 NO_X and SO_X Removal Unit 69

3.1.1. Chemistry 69

3.1.2. Thermodynamic Property Method 71

3.1.3 Column Specifications 71
3.1.4 Stream Results 72
3.1.5. Stage Composition Profiles 73
3.1.6 Sensitivity analysis 78
3.2 Non-condensable Gas Removal Unit 88
3.2.1. Thermodynamic Property Method 88
3.2.2. Model Results 90
3.3. Conclusion 91
Chapter 4 Analysis of Cycle Integration Options 93
4.1. Integration Options 93
4.2. Results 95
4.3. Conclusion 101
Chapter 5 Cost Estimation 103
5.1. Overview 103
5.2. Methodology 104
5.2.1. Pressure vessels, Compressors and Turbines 104
5.2.2. Shell and Tube Heat Exchangers 104
5.2.3. Multi-stream Plate-Fin Heat exchangers 105
5.2.4. Molecular Sieve Dryers 105
5.3. Material Selection 106
5.3.1. SO_2 Equipment 106
5.3.2. Acid Equipment 107
5.3.3. Low Temperature equipment 108
5.3.4. Others 108
5.4. Cost Estimation Basis 109
5.4.1. Basis for capital cost 109
5.5. Cost Estimation Results 111
5.5.1. Results Discussion 111
5.5.2. Cost Comparison 116

5.6. Conclusion....118
Chapter 6 Conclusion....119
6.1. Summary....119
6.2. Future Work and Challenges....120
6.2.1. Detailed Kinetics for NO_X and SO_X removal....120
6.2.2. Cycle Integration....120
6.2.3. Acid Disposal....121
6.2.4. Cost Estimation....121
6.2.5. Process Optimization....122
Appendix....123
References....129

Chapter 1 Introduction

1.1. Motivation

Fossil fuels remain by far the dominant source of energy in the world, accounting for over 80% of world energy supply and over 68% of electricity generation [1]. However, continued use of fossil fuel without care for CO_2 abatement will result in an increase in CO_2 emission from the current level of about 30Gt-CO_2/year to over 60Gt-CO_2/year by 2050[2]. Therefore, in order to achieve significant reduction in green house gas (GHG) emissions, CO_2 abatement strategies need to be deployed on a global scale. Carbon dioxide capture and sequestration from power plants and large stationary facilities provides a means of utilizing the world's abundant fossil fuel resources while staying on track to meet short to medium term Green House Gas emission targets.

Oxy-combustion technology has great potential as one of the major CO_2 capture technologies for power generation from coal and other fossil fuels. In recognition of this fact, the United States government recently announced the awarding of one billion dollars to the FutureGen 2.0 project, which is set to be the world's first commercial scale oxy-combustion power plant with CO_2 capture and sequestration[3].The distinguishing feature of oxy-coal combustion is that the oxygen source is a high concentration oxygen stream and the product flue gas consists primarily of CO_2 and H_2O with contaminants like NO_X, SO_X, and non-condensable gases like argon, oxygen and nitrogen. For carbon sequestration and Enhanced Oil Recovery (EOR) applications, pipeline transport standards as well as storage specifications impose concentration limits on these contaminants. Impurities like NO_X, SO_X, O_2 and H_2O need to be removed to ensure that the transported CO_2-rich stream stays

within specified limits to prevent issues like phase separation, hydrate formation, and corrosion due to acids, water or oxygen. Removal of non-condensable gases ensures lower effective compression work for pipeline transportation and increases the miscibility of CO_2 with oil for EOR applications [4].

Purification of CO_2 stream increases the parasitic energy consumption of the power plant and increases the overall capital and operating cost. The challenge then is to design a purification system that achieves the required purity specification while minimizing energy consumption and cost penalty. This is achieved through novel process design and by exploring options for integrating the purification system with the base power plant.

1.2. Oxy-Combustion Power Cycle

Traditional air-fired plants burn the fossil fuel in an air stream to produce power, with the air stream serving as both oxidant and diluent in the combustor. In oxy-combustion, an air separation unit (ASU) is installed upstream of the combustor to deliver relatively pure (about 95%) oxygen to the combustor. Temperature control is achieved by recycling some of the flue gas back into the combustor [5]. The flue gas stream leaving the combustor consists primarily of CO_2 and H_2O. The H_2O is easily condensed out by cooling, leaving a relatively pure CO_2 stream ready for sequestration or enhanced oil recovery applications after cleaning. This process eliminates the need for the complex and relatively more expensive post combustion capture of CO_2 from the nitrogen-rich flue gas of a conventional air-fired system. Figure 1.1 shows a high level process layout of the MIT-ENEL pressurized oxy-combustion system [6] .

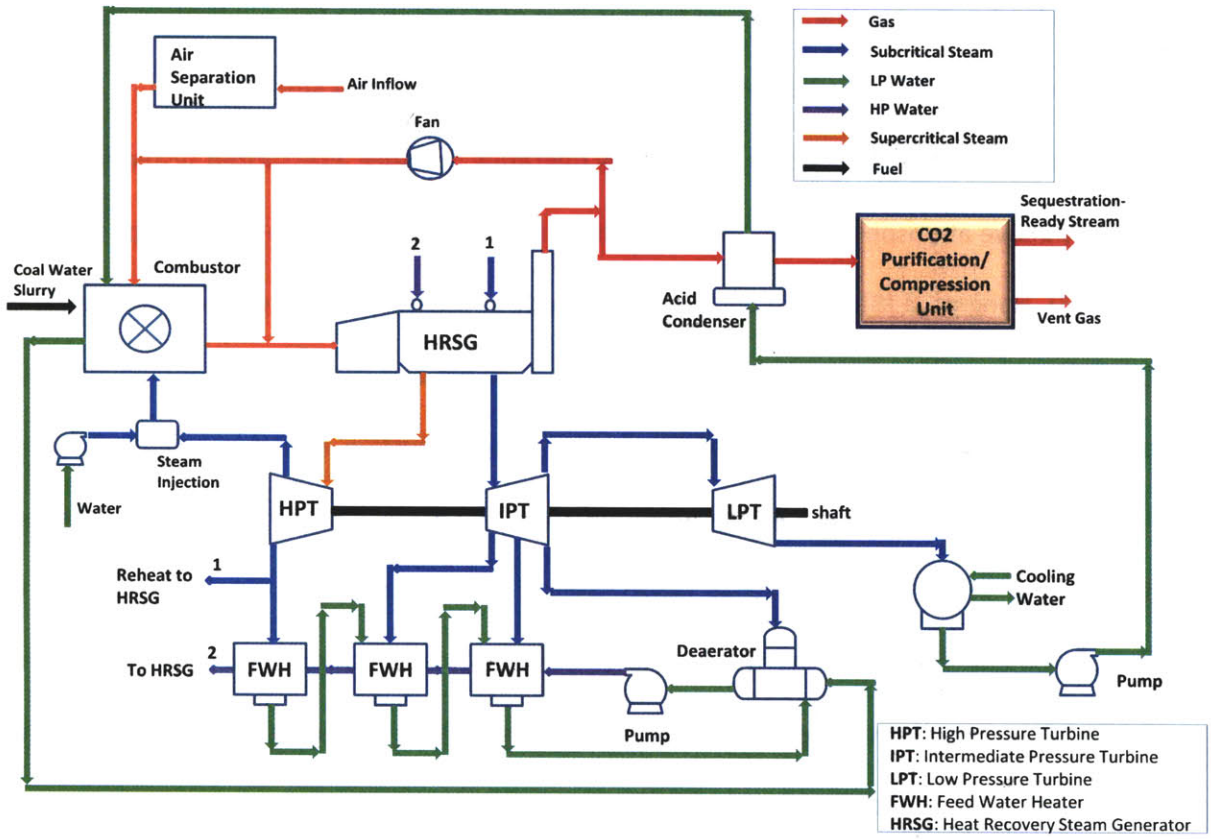

Figure 1.1: Pressurized oxy-combustion system schematic layout.

The air separation unit is fed with inlet air and delivers a high purity oxygen stream to the combustor. Coal water slurry is fed into the combustor and reacts with the oxygen with temperature regulation provided by the recycled CO_2 stream. The flue gas stream exits the combustor and enters the heat recovery steam generator (HRSG) where steam is generated for the steam power cycle. Part of the recycled flue gas stream is used to regulate the temperature at the inlet of the HRSG. The non-recycled portion of the gas stream leaving the HRSG passes through the acid condenser where the water vapor in the flue gas is condensed out. The thermal energy recovered from this condensation is used to preheat the steam cycle feed water, eliminating part of

the required feed-water heating. The cool flue gas then proceeds to the CO_2 purification section for removal of contaminants and other inert gases after which it is ready for storage.

Oxy-combustion systems are typically classified by operating pressure. Pressurized systems operate significantly above atmospheric pressure and studies have been published on systems operating up to 80 bar [7]. Hong et al [8] carried out a detailed study of the operating pressure dependence of the oxy-combustion system for a pressure range of 1 to 30 bar and suggested an optimal pressure closer to 10bar. The main advantage of pressurized oxy-combustion is that it enables a higher quality thermal energy recovery in the acid condenser since the water in the flue gas stream condenses at a higher temperature at higher pressures. Also, the elevated pressure requires smaller equipment sizes, reducing the overall plant capital cost. Atmospheric pressure systems operate at atmospheric pressure and the main advantage of this system is that existing air-fired power plants can be retrofitted to operate as atmospheric oxy-combustion plants. Other classification criteria include recycle strategy, fuel type, fuel feed strategy and process configuration. These will not be discussed here but interesting details can be found in referenced documents.

1.3. Characteristics of Oxy-Combustion Flue Gas

Oxy-combustion takes place in an environment consisting mainly of oxygen and recycled combustion gases. Flue gas recycling is employed in oxy-combustion systems because burning fossil fuels like coal in pure oxygen results in a combustion temperature of up to 3500C [9] which poses material challenges for standard power plant materials. Also, current design of oxy-fuel combustors tries to mimic as closely as possible the combustion conditions of air fired furnaces for which

extensive experience exists and this is achieved by controlling the proportion of the flue gas recycled to the combustor [10-12] .

The recycled flue gas, which therefore serves primarily as thermal capacity, consists primarily of CO_2 and H_2O. However, other contaminants like nitrogen oxides (NO_X), Sulfur oxides (SO_X) and non-condensable gases like argon, oxygen and nitrogen are also present in the flue gas stream. Table 1.1 compares the mole fractions of the major flue gas components for a pressurized oxy-coal combustion system to that of a conventional air fired system.

Table 1.1: Comparison of major flue gas components for oxy-coal and an air-fired coal systems

Component	CO_2	H_2O	O_2	N_2
Oxy-coal @ combustor exit (mole fraction)	0.46	0.48	0.03	0.009
Air-fired @ combustor exit (mole fraction)	0.15	0.06	0.03	0.76

It can be seen from table 1.1 that H_2O and CO_2 mak e up over 90% of the flue gas for oxy-combustion while the dominant component in the flue gas of the conventional air-fired power plant is Nitrogen comprising about 76%. Table 1.2 shows a typical composition of the oxy-combustion flue gas stream at the exit of the acid condenser. At this stage, most of the H_2O has been removed, resulting in a flue gas stream with over 86% proportion of CO_2.

Table 1.2: Typical flue gas composition for a pressurized oxy-coal combustion system @ exit of acid condenser

Component	CO_2	H_2O	O_2	N_2	Ar	CO	NO	NO_2	SO_2
Mole fraction	0.86	.015	.057	.015	.047	.0004	.0003	.00008	.002

This 86% pure CO_2 stream is however not ready for pipeline transport or sequestration. Since pipeline transport standards as well as storage specifications impose concentration limits on

components of the flue gas stream, the gas needs to be further purified to ensure that the transport-ready CO_2-rich stream stays within specified limits.

1.4. CO_2 Disposal Strategies

An adequate sequestration strategy must satisfy the important criteria of safety, environmental sustainability, affordability and can be deployed on a large scale. This section presents a brief overview of available strategies and more detailed information can be found in the referenced literature. A number of storage strategies have been proposed for CO_2 sequestration and the prominent options include mineral carbonization using accelerated chemical processes, deep ocean storage and geological sequestration.

1.4.1. Mineral Carbonation

Mineral carbonation involves the reaction of CO_2 with metal oxide bearing materials like to form carbonates. Suitable materials include naturally occurring silicate rocks and serpentine, as well as slag and fly ash from combustion processes. For large scale deployments, this option requires the availability of the metal oxide mineral materials, involves large scale mining and significant energy input into raw material preparation and in providing heating to accelerate the carbonation process. To this will be added the energy and cost requirement of transporting large quantities of carbonate rock that are produced in this process [9, 13] The technology is also very much in the budding

stages and is not yet likely to play a major role as a disposal option for CO_2 from power plants and industrial processes.

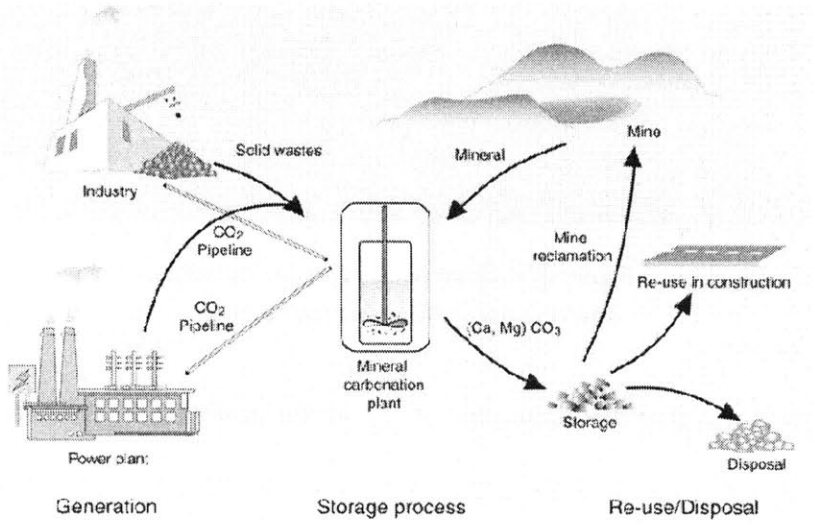

Figure 1.2: Ex-situ mineral carbonation of silicate rocks or industrial residues
Source: Energy Research Centre of the Netherlands (ECN)).

1.4.2. Deep Ocean Storage

In deep ocean storage, dense phase CO_2 is injected into the oceans at considerable depth where it is expected to dissolve or sink to the bottom of the ocean because of its density at those depths.

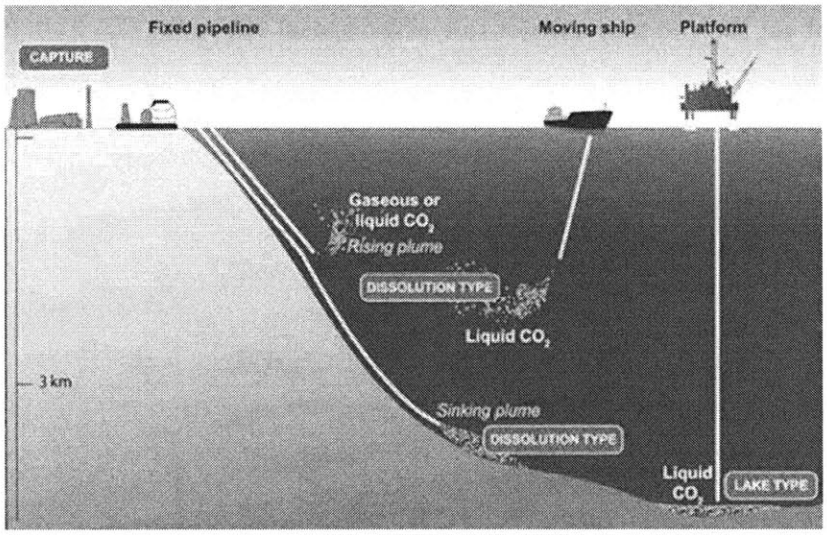

Figure 1.3: Deep ocean storage options
Source: http://www.powerplantccs.com

Studies have also shown that the dissolution of CO_2 in the ocean bed is typically inhibited by the formation of hydrates which limit the activity of the dense CO_2 [14, 15]. Therefore, there is a greater likelihood that the CO_2 will form 'lakes' on the ocean bed. Global oceans by far have the largest capacity for CO_2 storage [9], with an estimated potential of up over 70 million gigatons [16]. The major technical challenge to deep ocean disposal is the relatively limited understanding of the physical and chemical processes that take place in the sea bed. Some studies suggest that deep ocean injection will result in pH changes in the ocean which might be detrimental to marine life [9, 17]. Though deep ocean storage is a promising option for CO_2 mitigation, the scientific understanding of the process as well as the costs involved still has to mature. In addition, opposition from public and environmental NGOs and the bottleneck of international legal and political issues pose formidable obstacles to the adoption of this strategy [13].

1.4.3. Geological Disposal

This is the most developed of the options for CO_2 sequestration. It involves injecting dense phase (supercritical) CO_2 from major stationary sources like power plants into deep rock formations. Studies have shown that geological sequestration has sufficient capacity for the disposal of CO_2 generated globally at least in the short to medium term [9]. The major advantage of this option compared to others is that a lot of experience of injecting high pressure fluid streams into geological formations has been gained in other industries, especially in the oil and gas industry. Large scale CO_2 pipelines have been deployed for years in the US, CO_2 injection for enhanced oil recovery (EOR) has been practiced for years in the North America and the capacity for high-fidelity geophysical surveying is at an advanced stage in the oil and gas industry [13]. Also, geological sequestration sites are more geographically distributed and typically closer to the CO_2 source than would be the case for deep ocean injection. Possible geological formations for CO_2 storage include depleted oil and gas reservoirs, deep saline aquifers and deep unminable coal seams. Enhanced oil recovery and enhanced coal bed methane are also options for CO_2 disposal in this category. Geological disposal is by far the most generally accepted of all the available strategies and is the default storage option assumed in this study.

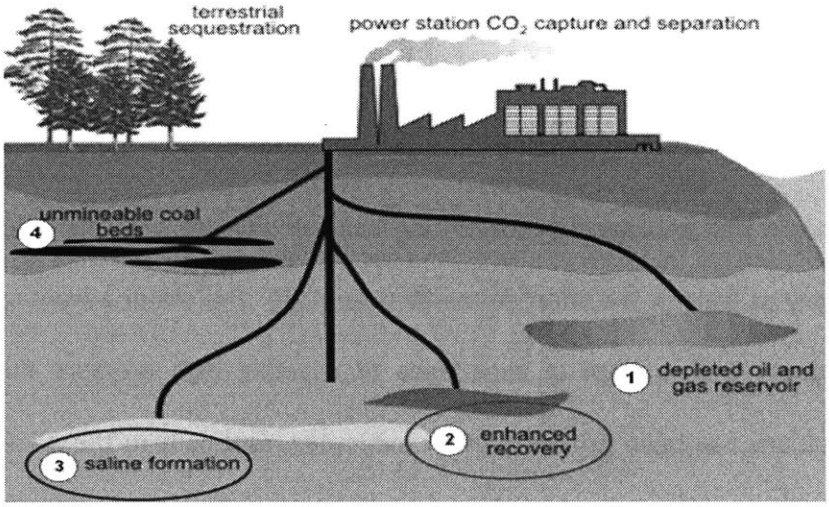

Figure 1.4: Geological CO2 storage options
Source: http://coreenergyholdings.com

1.5 Purity Specs for Geological Sequestration

The purity requirements for CO_2 transport and storage are typically determined by technical, economic and environmental considerations. These considerations often impose restrictions on the amount of contaminants present in the sequestration-ready CO_2 stream. These restrictions aim to prevent issues like aqueous phase separation, hydrate formation and corrosion in CO_2 transport pipelines as well as complex formation and miscibility problems in storage and in EOR applications. In addition, limiting the amount of additional components in the CO_2 stream results in a reduction in the energy input per kg of CO_2 transported for sequestration. For example, the presence of non-condensable contaminants increase compression work per kg of CO_2 transported and increases the minimum miscibility pressure for reservoir oil recovery applications. High oxygen concentrations can result in overheating at injection point, high argon concentration may give rise to CO_2-Ar

complex formation in storage and the presence of water can cause hydrate formation [4, 18]. There is no general agreement on the contribution of NO_2 and SO_2. They nevertheless will be considered as impurities in this study and typical environmental standards will be applied to them.

There are no generally accepted standards for the purity of CO_2 stream for transportation and storage. Most of the existing standards were developed from trade agreements and are typically specific to a given project and as such cannot be applied on a broader scale. The source of the CO_2 and the application (sequestration or enhanced oil recovery) also play a major role in determining the specification for different components. For example, standards developed for CO_2 from non-combustion sources (e.g. oil and gas exploration) will typically have specifications for H_2S and not for SO_2 or even NO_2. Differences in specification requirements seen in different standards are largely a reflection of the lack of a cohesive and comprehensive scientific basis for setting those standards in applications specific to CO_2 transport and storage. A good number of those standards, especially for pipeline transport, were simply taken from the experience with natural gas transportation and do not take into account the physical and chemical property differences between supercritical CO_2 and pipeline natural gas.

Given the lack of consensus amongst experts on required specifications, the purification model in this study utilizes a selection of reasonable standards from existing purity specifications as target product composition. Table 2 shows the specifications selected for this study and a number of sources from which it was selected.

Table 2: Pipeline Specifications

Component	Kinder Morgan*	Weyburn*	Dynamis*	Dakota Gasif.*	FutureGen*	Gulfaks*	Target Specs for this study
H_2O	< 690ppm	< 20ppm	< 500ppm	< 345ppm	< 100ppm	saturation @ 5C	< 500ppm
CO_2	> 95%	> 96%	> 95.5%	> 95%	> 95%	99.50%	> 95.5%
CO		< 0.1%	< 0.2%			< 10ppm	< 20ppm
H_2, N_2, Ar	< 4%	< 300ppm	< 4%	< 2%	< 0.5%	< 0.48%	<4%
NO_2						< 50ppm	< 20ppm
SO_2						< 10ppm	< 10ppm
O_2	< 10ppm	< 50ppm		25-50ppm	< 15ppm	< 10ppm	< 10ppm

* **Source**: Dynamis CO_2 quality recommendations, International Journal of Greenhouse Gas Control 2 (2008)

1.6. CO_2 Purification Process for Oxy-Combustion Systems

1.6.1. NO_X and SO_X Removal

The purification process for oxy-combustion-derived CO_2 streams typically involves two stages. In the first stage, nitrogen and sulfur oxides, together with other contaminants like mercury are removed. This can be achieved using traditional flue gas desulfurization (FGD) and selective catalytic reduction (SCR) processes or via novel strategies that utilize lead chamber chemistry for SOX removal. Other proposed process do exist but will not be discussed here.

1.6.1.1. Traditional FGD and SCR

FGD and SCR are used to remove sulfur oxides and nitrogen oxides respectively from the flue gas. The SCR consists primarily of a storage vessel for the ammonia, an ammonia injection system and a

reactor vessel. The reactor vessel provides sufficient reaction time as well as catalyst beds to enhance the reaction of ammonia with NO_X. Typical SCR systems are designed for 86% reduction [19]. Higher removal efficiencies can be obtained but will require significantly larger capital costs as the purity specifications become more stringent. Figure 1.5 shows a schematic representation of the SCR system. The primary reactions that take place in an ammonia-based SCR are shown below.

$$4NO + 4NH_3 + 3O_2 \rightarrow 4N_2 + 6H_2O \quad (1)$$

$$2NO_2 + 4NH_3 + O_2 \rightarrow 3N_2 + 6H_2O \quad (2)$$

$$NO + NO_2 + 2NH_3 \rightarrow 2N_2 + 3H_2O \quad (3)$$

The FGD utilizes limestone slurry or lime to remove SO_X from the flue gas stream. The two major types are the wet and the dry FGD systems. Wet FGD systems make up over 80% of installed systems in the US largely because they take up less space and are easier to retrofit to existing power plants [20]. The primary equipment in the wet FGD system is the scrubber where the SO_2 is absorbed to and reacts with the limestone slurry (or lime or magnesium hydroxide) to ultimately form gypsum which is often a marketable product. A limestone system also includes the limestone storage silos, dust filters, crushers, feeders, slurry tank, recirculation pumps and heat exchangers. Typical representation of an FGD is shown in figure 1.6. Key reactions in a typical FGD system are shown below:

$$CaCO_3 \text{ (solid)} + SO_2 \text{ (gas)} \rightarrow CaSO_3 \text{ (solid)} + CO_2 \text{ (gas)} \quad (4)$$

$$CaSO_3 \text{ (solid)} + H_2O \text{ (liquid)} + \tfrac{1}{2}O_2 \text{ (gas)} \rightarrow CaSO_4 \text{ (solid)} + H_2O \quad (5)$$

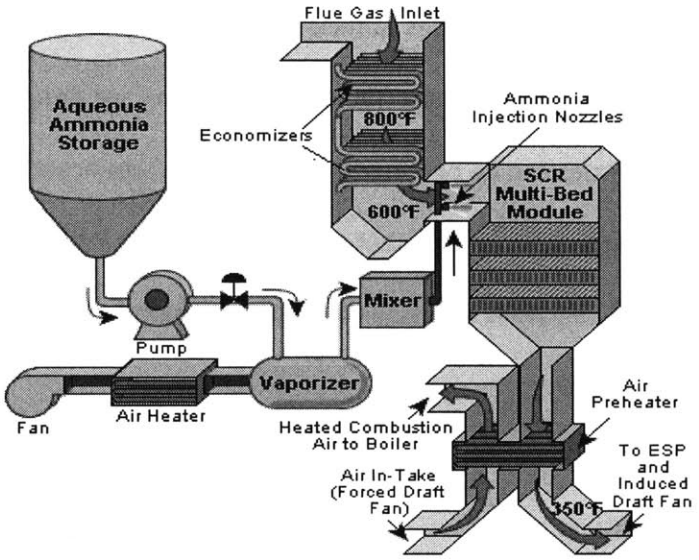

1.5 Selective Catalytic Reduction (SCR) system. Source: http://www.babcock.com

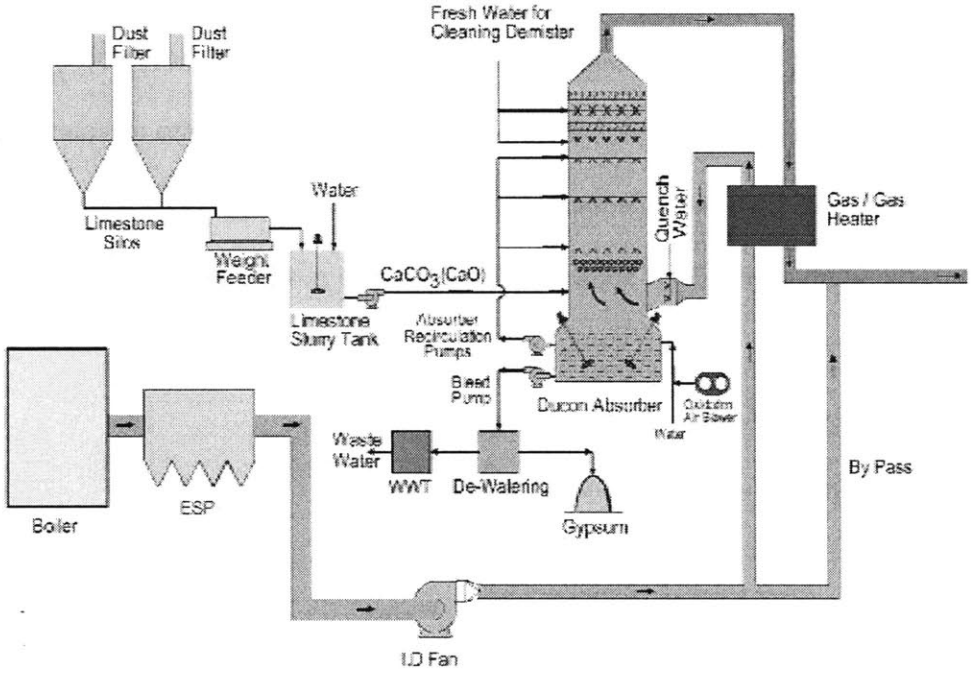

1.6 Limestone based Flue Gas Desulfurization (FGD) Unit (source: http://www.eandj-intl.com)

1.6.1.2. Lead Chamber/Nitric acid chemistry based Processes

These processes utilize the lead chamber and nitric acid chemistry (discussed in chapter two) for the removal of NO_X and SO_X as nitric and sulfuric acid from the flue gas of industrial plants. The name "lead chamber" is purely historical as chambers in the earliest configurations were made of lead. Presented in this study are the Keilin process, the double column (Air Products Concept) and the Single column process.

Keilin & Wallit Process

The first important configuration in this category was suggested by Keilin & Wallit [21], though not specifically for oxy combustion. A detailed discussion of method can be found the referenced document and only a brief sketch will be presented here. This process involves the oxidation of SO_2 to SO_3 in the reactor which contacts with water to form sulfuric acid (see figure 1.7). It starts up with an external supply of NO_2 but subsequently, NO_2 is furnished from the catalytic oxidation of NO in the catalytic stripper. Excess NO_X in the flue gas exiting the reactor is absorbed by the recycled sulfuric acid in the isothermal scrubber and excess NO_2 from the catalytic stripper is removed in the HNO_3 absorber.

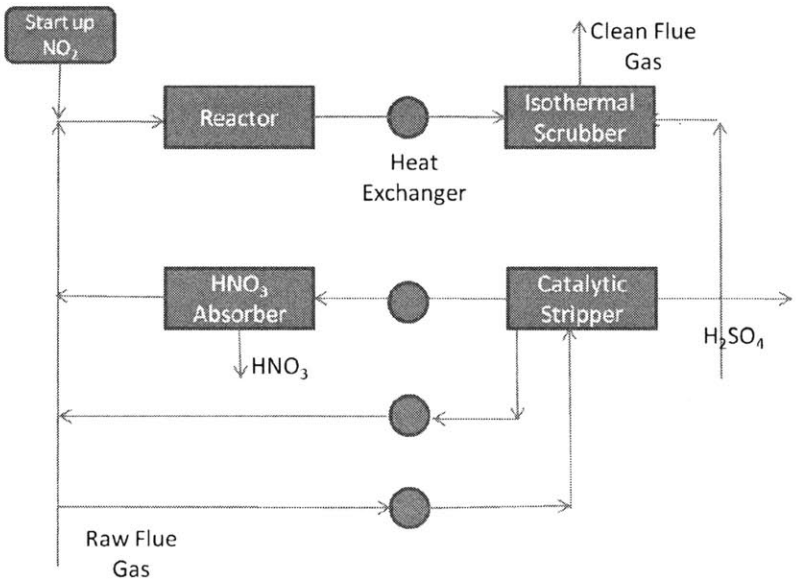

Figure 1.7: schematic diagram of the Keilin & Wallit Process

New Double Column (Base Case) Process:

A newer configuration is the double column process proposed by Air Products[22] which involves the removal of nitrogen oxides and sulfur oxides as nitric and sulfuric acid in two high pressure reactive absorber columns utilizing the lead chamber and nitric acid chemistry. This method was suggested specifically for oxy combustion systems. It does away with the catalytic oxidation of NO as seen in Keilin's case and instead achieves this via the pressure enhanced direct oxidation of NO to NO_2 by oxygen in the flue gas stream. This configuration is selected as the base case model for NO_X and SO_X removal in this study and is shown as part of the overall CO_2 purification system in figure 1.8.

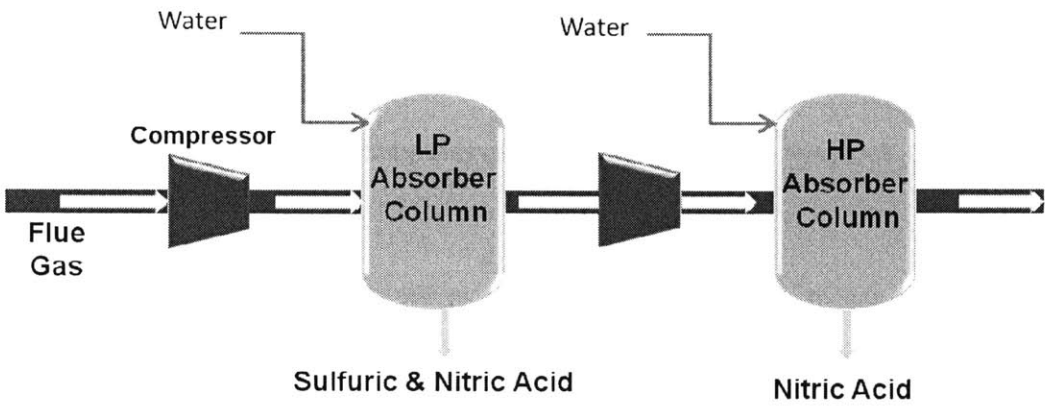

Figure 1.8: Air Products double column process

In this base case option, the oxy-combustion flue gas stream is first compressed to about 15 bar then fed into the low pressure (LP) column where all the SO_X and some of the NO_X is removed as sulfuric and nitric acid. The exit gas is further compressed to about 30 bar and flows into the high pressure (HP) column where further removal of NO_X takes place.

1.6.1.3. Benefits of Novel NO_X & SO_X removal unit over Traditional FGD

- The major advantage of the new purification process is that it eliminates the raw material requirements of the desulfurization process. Limestone, which is the raw material for over 80% of FGD, costs about $15 per ton and the Gypsum product can only sell at about $0 to a maximum of $3 per ton [20]. Therefore this new process avoids about $15/ton of limestone, not including the other associated handling and storage costs in the plant.
- Secondly, the complexity of the system is reduced, eliminating all equipment from the limestone silos and slurry tanks to the gas heaters and slurry pump. Also, a simpler absorber column is required. This leads to a significant decrease in capital cost investment for the desulfurization unit.

- In wet FGD, limestone is dissolved in the aqueous phase and in the process releases CO_2. This process increases the CO_2 concentration in the flue gas stream and will result in a higher CO_2 footprint in the plant or could increase parasitic power to capture the additional CO_2.
- Lastly, the use of air to facilitate oxidation in the desulfurization plant will involve the dilution of the CO_2 stream with nitrogen. To avoid this, a high purity oxygen stream could be utilized but this will increase the parasitic power requirement of the air separation unit.

1.6.2. Non Condensable Gas Removal

The second stage involves the removal of non condensable gases like oxygen, argon and nitrogen from the NO_X and SO_X-free flue gas. This can be achieved through low temperature phase separation in flash drums. The major limitation of using flash drums is that for a typical oxy-combustion flue gas stream, oxygen can only be reduced to about 1% [18]. This value is considerably higher than the 10ppm sequestration specification for oxygen. Other methods can be used in combination with this to achieve lower oxygen concentrations. Some of these include reducing excess oxygen by using optimized combustors, catalytic consumption by adding fuel downstream of the combustor and packed bed oxygen adsorption. Instead of using flash drums, a distillation column is utilized to achieve this stringent oxygen specification. Modeling of various strategies to achieve the O_2 target demonstrated that a distillation column is the only practical option for a separation design based on vapor-liquid equilibrium.

1.7. The Proposed System

The purification system presented in this study employs the lead chamber and nitric acid process for the removal of sulfur and nitrogen oxides (NO_X and SO_X) and a distillation based system for the removal of non condensable gases. It was developed for a coal based oxy-combustion system but can be easily adapted for natural gas oxy-combustion flue gas.

1.7.1. NO_X & SO_X Removal (Single Column) System

This NO_X and SO_X removal section is based on a modification of the base case double column process suggested by Air Products. It arises from sensitivity studies on the impact of key process parameters on the lead chamber chemistry and process conditions and takes advantage of the dominance of pressure as the chief control parameter. This process uses a single reactive absorber column at high pressure to achieve the similar separation efficiencies as the double column case. This leads to significant savings in capital cost and also provides small savings in energy because of the lower pressure drop involved. This method is advantageous for pressurized systems since the underlying chemistry is enhanced by elevated pressure and the flue gas leaving the base power cycle is already at pressure.

1.7.2. Non Condensable Gas Removal

The flue stream leaving the NO_X and SO_X removal section proceeds to the non-condensable gas removal unit where moisture is removed in a molecular sieve dryer and gases like O_2, N_2 and Ar are removed via a low temperature phase separation in a distillation system. Two configurations for this unit were explored in this study: one uses the process stream for providing the energy to drive

the system and delivers a high purity gas phase CO_2 stream while the other utilizes an external cooling unit and delivers a high purity liquid CO_2 stream. The exit 99.99% pure CO_2 stream is then pumped or compressed and pumped up to pipeline pressure of about 110bar in the final compression train and subsequently transported for sequestration or enhanced oil recovery application. A high level schematic diagram of the CO_2 purification system is shown in figure 1.9.

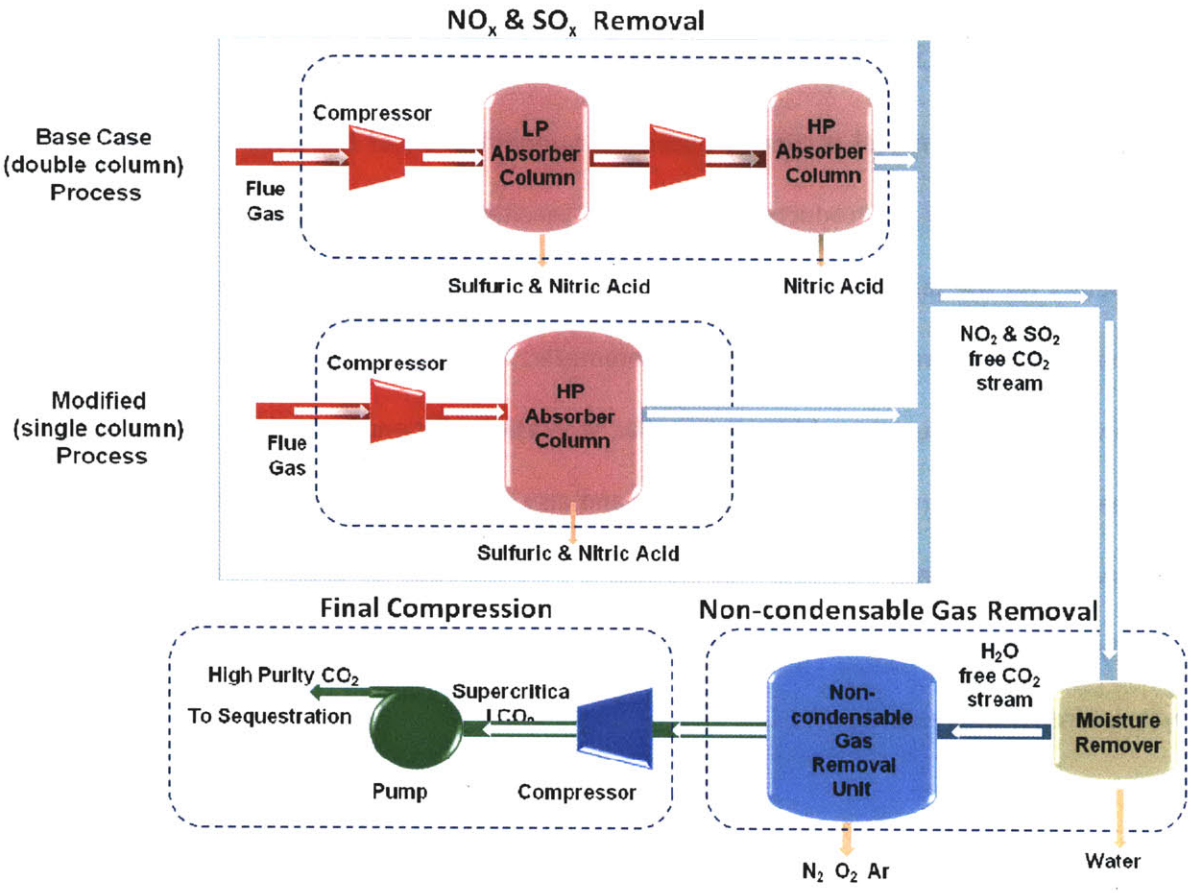

Figure 1.9: Schematic of oxy-coal combustion purification train

1.8. Conclusion

Fossil fuels still remain the dominant source of energy in the world and are projected to stay so in the near future. This will lead to an increase in CO_2 emissions if no action is taken to abate it. For this reason, technologies that enable the carbon capture from fossil plants need to be deployed to reduce Green House Gas emission. Oxy combustion has emerged as an important technology which delivers a CO_2 rich flue gas stream for sequestration or EOR. However, especially for coal based systems, this flue gas stream contains other impurities which need to be removed efficiently and economically.

A CO_2 purification system that is able to deliver high purity CO_2 from oxy combustion systems is presented in this study. The work done here improves on a previous process for SO_X & NO_X removal based on lead chamber and nitric acid chemistry and explores unique configurations for optimal removal of non condensable gases. A more in-depth discussion of the lead chamber and nitric acid chemistry that take place in the NO_X and SO_X removal section is presented in chapter two. The non condensable gas removal section is also discussed in detail in chapter two. Results from simulation of the purification process and sensitivity analysis on the impact of key process parameters on the performance of the system are reported in chapter three. Chapter four then explores opportunities for integrating the purification unit with the base power cycle and the impact of each integration option on cycle performance and efficiency. Cost estimates for the various purification process configurations developed are presented in chapter 5 and chapter 6 wraps up with the conclusion.

Chapter 2 CO_2 Purification Unit Analysis

2.1. SO_X and NO_X Removal Unit

The base case process configuration for the removal of nitrogen and sulfur oxides from the oxy-combustion flue gas, shown in figure 2.1, is based on a process suggested by Air Products [22] in which sulfur dioxide is removed as sulfuric acid and the nitrogen oxides are removed as nitric acid.

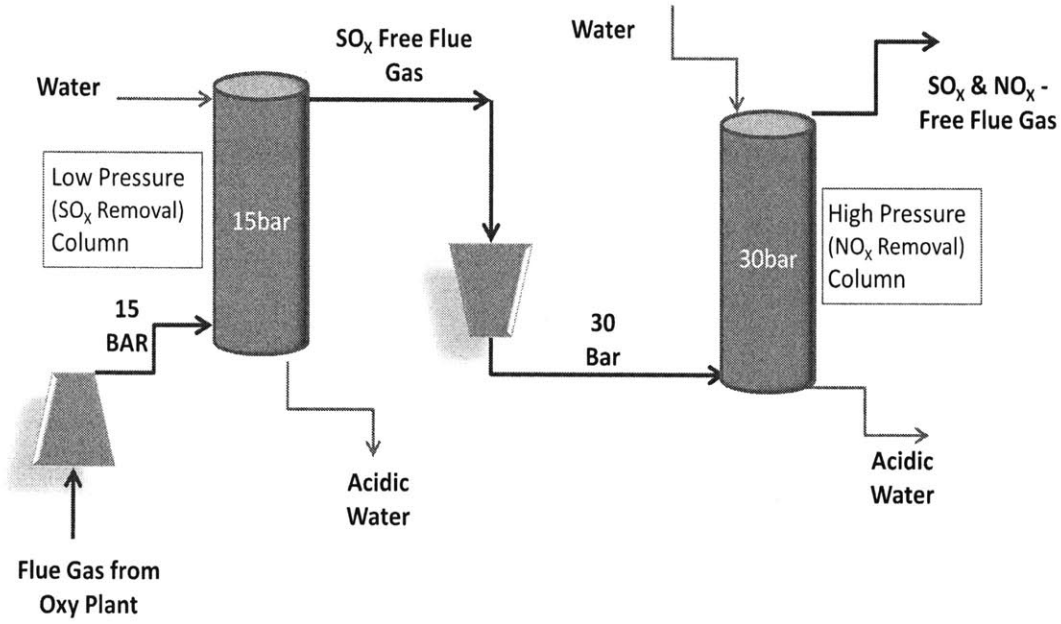

Figure 2.1: SO_X and NO_X Removal Unit

In this process, the flue gas exiting the acid condenser of the base power cycle is compressed up to 15bar and then fed into a reactive absorber column where sufficient residence time and contact with water is provided to remove all the sulfur dioxide as sulfuric acid. The sulfur dioxide-free flue gas is then further compressed up to 30bar and enters the second reactive absorber column where

most of the nitrogen oxides are removed as nitric acid. The cleaned flue gas leaving this column is then dried in a molecular sieve dryer and proceeds to the non-condensable gas removal unit. Operation of this SO_X and NO_X removal columns at elevated pressure is essential because the key rate limiting reaction, which is the oxidation of nitrogen oxide to nitrogen dioxide, is a third order reaction and only achieves sufficient reaction velocity at elevated pressures.

The process for the removal of SO_2 as sulfuric acid and NO_X as Nitric acid in countercurrent reactive absorber columns is known to proceed based on chemistry associated with the lead chamber and nitric acid processes. The proposed reaction pathway for the nitric acid chemistry - which will be presented shortly - has been studied in detail by D. Miller [23] and the rates and phases of all relevant reaction steps are well documented. The lead chamber chemistry however does not share the same fate. The real bone of contention is the SO_2 oxidation reaction 1 which is often assumed to take place exclusively in the gas phase:

$$NO_2 + SO_2 + H_2O \rightarrow H_2SO_4 + NO \qquad (1)$$

Most recent publications referencing this reaction in the context of SO_2 purification from oxy-combustion flue gas streams have unanimously assumed that this reaction is a rapid homogeneous gas phase reaction. However, documented evidence and experimental results are not conclusive regarding the mechanism and kinetics of this reaction. Most studies have assumed that this is a gas phase reaction and that it is fast enough to be modeled as an equilibrium reaction [22]. In a few cases, the overall SO_2 removal rates predicted by these models have been more or less supported by experimental measurements [24]. Though such an assumption may be sufficient for overall process design, it does not provide sufficient insight required for very detailed engineering design

and performance analysis of the removal equipment. For example, it is important to know the actual composition of the bottoms acid from the absorber column as well as the dominant mechanism of SO_2 removal. It makes a difference whether the sulfuric acid is produced mostly in the gas phase or in the liquid phase. Knowing whether NO_2 acts as a catalyst or is directly consumed in the reactions or a mixture of both is relevant in understanding the process and how to control it. As important as all these might be, the absence of any documented detailed reaction pathway with associated reaction rates remains a formidable hindrance to fully understanding and controlling this process. Nevertheless, we will try to present a synopsis of some of the important published data on the chemistry of the lead chamber sulfuric acid process to help provide better understanding and deeper insight into the process and to validate modeling assumptions.

2.2. Lead Chamber Chemistry

The lead chamber process for the manufacture of sulfuric acid was first developed in 1746 by John Roebuck and has experienced performance enhancing modifications over the years. It dominated the sulfuric acid industry for nearly two centuries before being superseded by the contact process. The lead acid process consists of reactions involving sulfur oxides, nitrogen oxides and water. The end product is a dilute sulfuric acid solution which is then further concentrated for industrial applications. According to general wisdom, nitrogen dioxide and sulfur dioxide either react in the gas phase, in the gas – liquid interface, or are first absorbed into the liquid phase and then react to form sulfuric acid, nitric oxide and nitric acid. The sparingly soluble nitric oxide returns to the gas chamber where it is oxidized and re-introduced into the process to complete the loop [25]. The key

components of a typical modern Lead chamber process are the sulfur burners (for producing SO_2), dust collectors, Glover tower, the lead chambers , the Gay Lussac towers, acid circulating system and apparatus for introducing oxides of nitrogen. The composition of the inlet gas to the Glover tower is about 5-10% SO_2, 8-12% oxygen with nitrogen making up the balance. In this tower, the hot inlet air stream is cooled from 530C to about 90C and in the process denitrates the recirculated acid while forming some sulfuric acid. The gas stream leaves the Glover tower for the lead chambers arranged in series where atomized water or steam is introduced to facilitate the production of sulfuric acid by reactions between SO_2, nitrogen oxides, oxygen and water. The chamber walls are cooled to ensure the temperature does not exceed 100C so as to protect the lead walls. The main function of the Gay Lussac towers is to recover nitrogen oxides leaving with the gas stream from the last chamber before it is discharged to the atmosphere [26]. This process typically operates at or near atmospheric pressure.

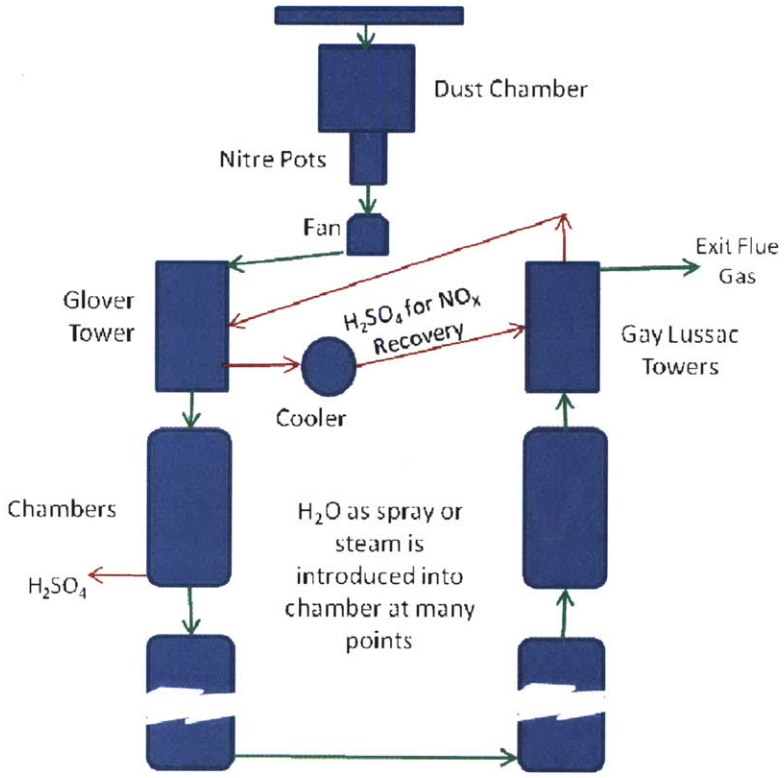

Figure 2.2. Lead Chamber Process: adapted from [26]

2.2.1. Chemistry

The exact chemistry of the lead chamber process remains largely unsettled mainly because the design of the process had been highly empirical and also due to waning interest since the development of the contact process for the manufacture of sulfuric acid. The two important questions that need to be resolved are what reaction steps characterize the process and which reaction route is dominant. The focus of this section will be more on the route question as gleaned from the reaction steps proposed by some prominent authors in this area. Note that there will be no attempt to settle the question here. Rather it is hoped that this presentation will provide the context for justifying the reaction assumptions made in the NO_X and SO_X removal equipment of the CO_2 Purification Unit model which employs lead chamber chemistry.

Three major reaction routes have been suggested for the lead chamber process:

- Gas phase route (figure 2.3): The sulfur dioxide oxidation takes place mainly via homogeneous gas phase reactions.
- Interfacial route (figure 2.4): The sulfur dioxide oxidation takes place mainly via interfacial reactions
- Liquid phase route (figure 2.5): The sulfur dioxide oxidation takes place mainly via liquid phase reactions

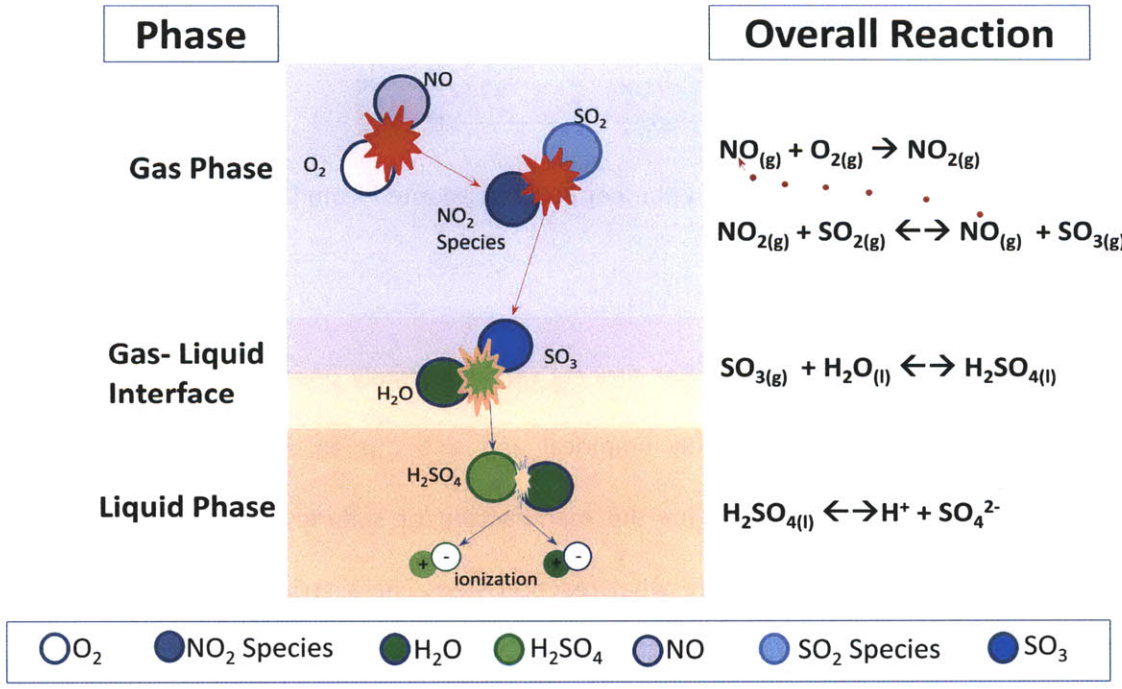

Figure 2.3. Gas Phase oxidation route

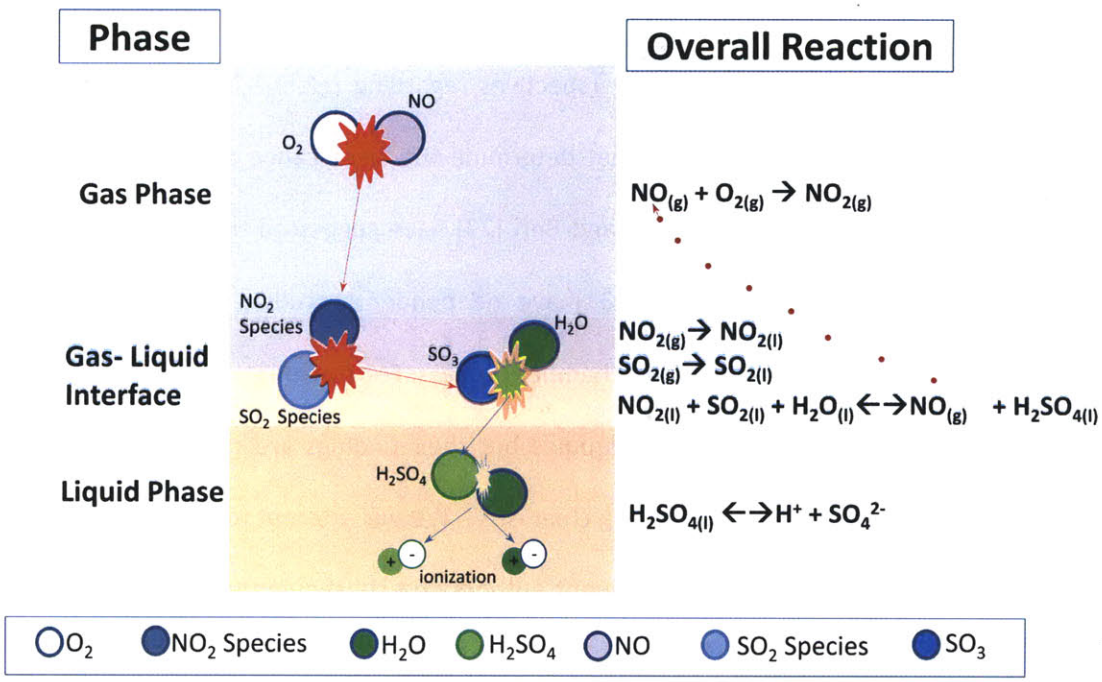

Figure 2.4. Interfacial oxidation route

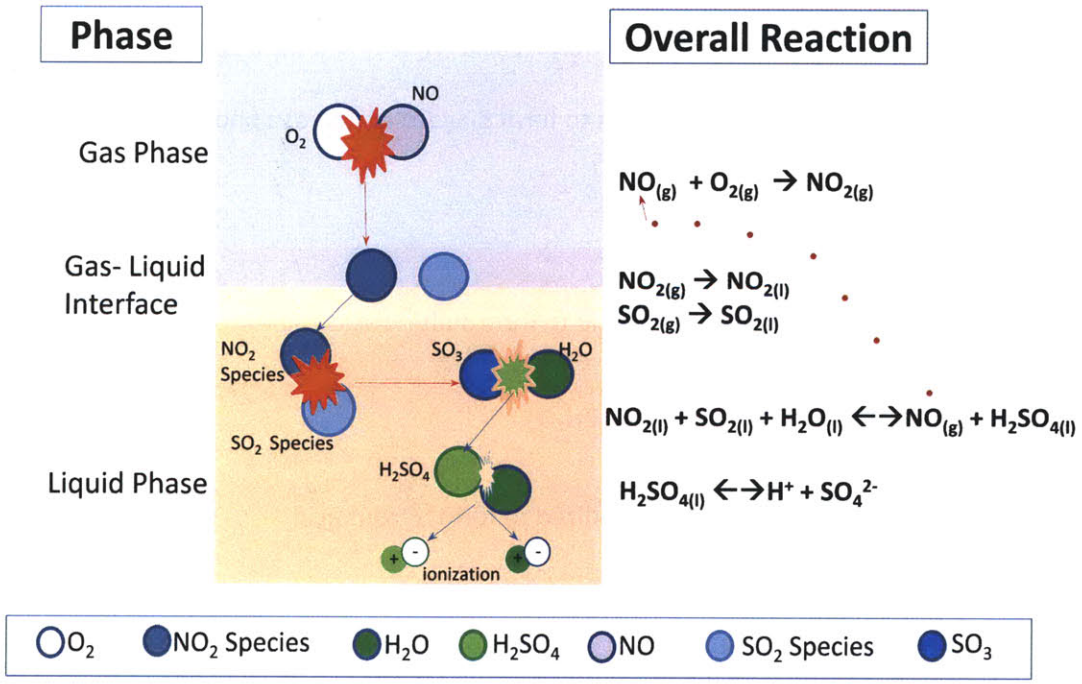

Figure 2.5. Liquid Phase oxidation route

It is generally accepted that all three processes play a role in the lead chamber production of sulfuric acid. However there are different perspectives regarding relative importance of each of them as well as the operating conditions that determine the significance of each route. Several authors like Jones, Raschig [27], Lunge [28] and Berl [29] have suggested theories describing this process. Others like Falgout [30]and Ellison [31]have independently studied some reactions which would be expected to take place in the lead chamber process. For some of the authors, the sulfuric acid process was not the purpose of their studies but their findings are considered relevant to understanding some aspects of the underlying chemistry. We will attempt to present a synopsis of the ideas proposed by a few of these prominent authors and subsequently draw some informed conclusions.

2.2.1.1. Raschig: Sulfuric acid chemistry theory [27]

According to Raschig's theory, sulfur dioxide and nitrogen dioxide are absorbed in the sprayed film in the chamber and react with water to form sulfurous acid (H_2SO_3) and nitrous acid (HNO_2). These two combine according to the following reaction to form dihydroxylaminesulphonic acid:

$$HNO_2 + H_2O + H_2SO_3 \rightarrow (OH)_2.N.SO_2.OH + H_2O \quad (2)$$

This product is decomposed by excess nitrous acid to form sulfuric acid and nitrogen oxide

$$(OH)_2.N.SO_2.OH + H_2O + HNO_2 \rightarrow H_2SO_4 + 2NO + 2H_2O \quad (3)$$

The nitrogen oxide formed is subsequently reoxidized to form nitrous acid

$$2NO + O + 3H_2O \rightarrow HNO_2 + H_2O \quad (4)$$

The major drawback of this theory, which has been highly criticized by Lunge is that it does not take into account the existence of nitrosyl sulfate and also the fact that nitrous oxide (N_2O), which would be expected to form if there is a deficiency of nitrous acid, has never been found in any significant amount in lead chamber gas[32].

2.2.1.2. Geo Lunge: Sulfuric acid chemistry theory [28]

Lunge presents two main pathways for the formation of sulfuric acid depending on the prevailing chamber conditions. Sulfur dioxide is either directly or indirectly converted to sulfuric acid.

Indirect conversion

This conversion route is generally of the type represented in figure 2.4. Sulfur dioxide, water vapor, nitrogen trioxide and oxygen react to form nitrosyl sulfuric acid mist as shown in the equation below:

$$2SO_2 + N_2O_3 + {}^3/_2O_2 + H_2O \rightarrow 2SO_5NH \qquad (5)$$

In a sulfur dioxide-rich chamber atmosphere, this product combines with excess steam to form sulfuric acid and nitrogen oxide and subsequently regenerate the nitrosyl sulfuric acid

$$2SO_5NH + SO_2 + 2H_2O \rightarrow 3H_2SO_4 + 2NO \qquad (6)$$

$$2NO + 2SO_2 + 3O + H_2O \rightarrow 2SO_5NH \qquad (7)$$

Otherwise in a sulfur dioxide –lean chamber atmosphere, sulfuric acid is formed as shown next

$$2SO_5NH + H_2O \rightarrow 2H_2SO_4 + N_2O_3 \qquad (8)$$

Direct conversion

This conversion route is generally of the type represented in figure 2.3. A significant proportion of the sulfuric acid formed by the lead chamber process is expected to be via this path. Here, sulfur dioxide is directly oxidized to sulfuric acid according to either of the two reactions below:

$$NO_2 + SO_2 + H_2O \rightarrow H_2SO_4 + NO \quad (9)$$

$$N_2O_3 + SO_2 + H_2O \rightarrow H_2SO_4 + 2NO \quad (10)$$

Lunge suggests that the NO formed is likely not directly oxidized by atmospheric oxygen to form NO_2 but rather by oxygen in the water vapor in the presence of sulfur dioxide to form nitrosyl sulfate. This might be the case at low pressures but at elevated pressures, direct oxidation by atmospheric oxygen is more likely.

Other prominent authors like Sorel [33]and Schertel [34] have either come up with very similar mechanisms to that of Lunge or experimentally verified several aspects of Lunge's theory. A salient paper by William Potter [32] which analyzed a number of existing theories of the sulfuric acid process arrived at the conclusion that Lunge has provided the best explanation of the formation of sulfuric acid in the lead chamber process at the time.

2.2.1.3. Ernst Berl: Sulfuric acid chemistry theory [29]

Ernst Berl, in his "Studies of the Lead Chamber Process" paper presented a similar but more detailed chemistry for the process which is supported by the extensive experimental work he carried out. He splits the reactions into homogeneous gas phase reactions, heterogeneous gas-

liquid surface reactions and homogeneous liquid phase reactions. The overall oxidation route presented here is best captured by figure 2.4.

Table 2.1: Lead Chamber Chemistry

11	$2NO + O_2 \rightarrow 2NO_2$	**Homogeneous Gas Phase**
12	$SO_{2(g)} + H_2O_{(l)} \rightarrow H_2SO_{3(l)}$	**Interfacial**
13	$H_2SO_{3(l)} + NO_{2(g)} \rightarrow H_2SO_4.NO_{(l)}$	
14a	$2H_2SO_4.NO_{(l)} + 1/2O_{2(g)} \rightarrow 2SO_5NH_{(l)} + H_2O_{(g)}$	
14b	$2H_2SO_4.NO_{(l)} + NO_{2(g)} \rightarrow 2SO_5NH_{(l)} + H_2O + NO_{(g)}$	
15	$2SO_5NH_{(l)} + SO_{2(g)} + 2H_2O_{(l)} \leftrightarrow 2H_2SO_4.NO_{(l)} + H_2SO_{4(l)}$	
16	$H_2SO_4.NO \leftrightarrow H_2SO_4 + NO$	**Liquid Phase**
17	$2SO_5NH + H_2O \leftrightarrow 2H_2SO_4 + NO + NO_2$	
18	$SO_5NH + HNO_3 \leftrightarrow H_2SO_4 + 2NO_2 / (N_2O_4)$	

$(H_2SO_4)NO$: Violet acid
$2SO_5NH$: Nitrosyl sulfuric acid

Reaction 11 is the well known third order NO oxidation reaction which is slow at atmospheric pressure but increases rapidly with pressure. Reactions 12, 13, 14 and 15 take place at the gas-liquid interface. Therefore, the rate of this reaction is greatly influenced by contact surface and consequently by pressure since increase in pressure increases the effective interfacial area. Ernst was able to show from experimental measurements that the yield per unit volume of sulfuric acid increased proportionally with the square of pressure.

In reaction 16, violet acid quickly decomposes to sulfuric acid and nitrogen oxide. This reaction is influenced by pressure in the sense that higher pressures decrease the ease of decomposition of the violet acid. However, violet acid is unstable at low sulfuric acid concentration. Decomposition of nitrosyl sulfate to sulfuric acid as shown in reaction 17 is rapid at lower acid concentration since nitrosyl sulfuric acid is unstable in dilute sulfuric acid

2.2.1.4. Ellison and Eckert: Insights on aqueous phase chemistry [31]

Ellison and Eckert studied the impact of NO_X on the aqueous phase oxidation of SO_2. They observed that the catalytic effect of NO_2 on SO_2 oxidation observed in the gas phase kinetics does not occur in the liquid phase. This view is also supported by Ernst Berl [29]. Instead direct reaction takes place which involves the two compounds and their aqueous species. What remains unresolved however is whether the chief oxidant is NO_2 at the gas-liquid interface, the absorbed NO_2 or the hydrolyzed nitrous acid. They however concluded from their experiments that it's more likely that the absorbed NO_2 hydrolyzes to nitrous acid before reacting with dissolved SO_2. Nitric acid is also formed with the absorption of NO_2 but unlike nitrous acid which quickly oxidizes the aqueous SO_2, nitric acid indirectly inhibits the oxidation by increasing the ionic strength of the liquid phase.

A closer look at relative solubilities of NO_2 and SO_2 suggests that in a typical flue gas cleanup scenario, aqueous NO_X does not significantly oxidize aqueous SO_2 to sulfuric acid. Based on a simplified computation presented by Ellison and Eckert, a typical flue gas stream at atmospheric pressure with 2000ppm SO_2 and 800ppm NO_X will result in a liquid phase with SO_2 concentration of about 2.5E-3 M and nitrous acid concentration of 3.2E-6 M. From this one can infer the following:

- Only a little sulfuric acid will be formed from oxidation of the aqueous sulfur species by nitrous acid
- The removal of sulfur oxides from the flue gas will be largely dependent on equilibrium solubility which will be proportionally inhibited by increasing liquid phase acidity.
- In the absence of some other catalyst, the aqueous phase oxidation of the sulfur dioxide to sulfuric acid will be relatively low

2.2.1.5. Robinson and Lindstedt[35]

Robinson and Lindstedt of Imperial College presented preliminary results from their study at the 1st Oxy-fuel Combustion Conference in Germany. The aim of their study was to develop a kinetic model for the reactions involved in the removal of sulfur and nitrogen oxides from oxy-combustion flue gases. They had not published the paper yet, since the work is still in progress, and the presentation they provided does not contain detailed information on their work. Some of the product distribution plots they presented show SO_2 build-up in the aqueous phase, which seems to suggest that there is not enough aqueous NO_X species to oxidize it, a conclusion that would be supported by Ellison et al [31]. According to the plots, as the gas phase SO_2 depletes, aqueous phase SO_2 and sulfurous acid grow proportionally (more SO_2 than sulfurous acid). Their plots do not show significant production of sulfuric acid. We will unable to draw any conclusions at the moment from their work and will have to wait for more detailed results from their studies.

2.2.1.6. Falgout: Insights on gas phase chemistry [30]

Allen Falgout in his PhD thesis carried out a detailed experimental study on the reactions of Sulfur and Nitrogen oxides in different environments. In his thesis he showed that the presence of water vapor has a striking effect on the rate of consumption of SO_2, an observation also confirmed by Schroeder [36]. Table 2.2 below summarizes his findings from an experiment carried out with inlet gas at room temperature and pressure:

Table 2.2: Influence of water vapor on the 1% SO_2 - 1% NO_2 air system

Initial relative humidity (%)	Initial concentration Water vapor (%)	Rate of SO_2 removal (%/hr)	Final SO_2 concentration (%)[a]	Amount of NO_2 remaining at the end[b]
100	2.77	715	0.025	Nearly all
75	2.08	340	.075	Most
50	1.39	184	0.046	half
25	0.69	99.7	0.392	Very little
Dry gas[c]	-	0.02 -0.07		

[a] Amount of SO_2 **remaining when the conversion rate flattened out**

[b] **Qualitative estimate based on visual observation**

[c] **Average value taken from a different data set – for comparison**

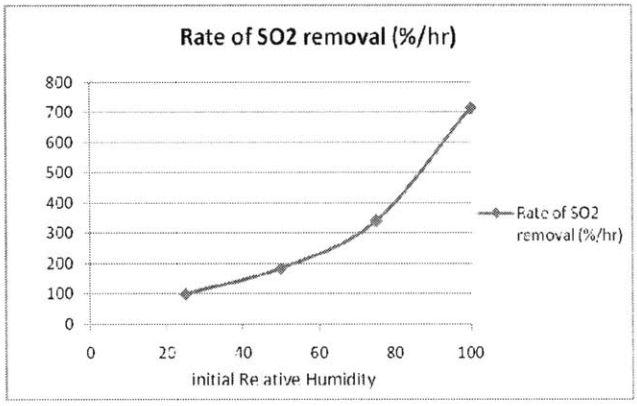

Figure 2.6: Variation of SO_2 gas phase oxidation with relative humidity [30]

It can be seen from table 2.2 and figure 2.6 above that addition of water vapor to the reacting mixture had a striking effect on the rate and extent of consumption of SO_2. There is a three order of magnitude jump in reaction rate from dry to 25% relative humidity and a further order of magnitude increase getting to 100% relative humidity. Even more interesting is the significance of the observation in the fifth column. It appears that with increasing water vapor, NO_2 is less and less

directly involved in the reaction but rather increasingly plays the role of a catalyst, confirming the view of several experts on the catalytic role of NO_2 in the gas phase oxidation of SO_2. Falgout suggested that atmospheric oxygen may need to be included in the reaction mechanism. This view is supported by other authors, including Hurter[37] and Sorel[33]. Jaffe and Klein [38] also observed that the rate of the gas phase reaction increased in proportion to third body (diluent gas) pressure.

The discussion presented so far show that the exact reaction pathway for the lead chamber process is still an unresolved issue. The dominant phase for the oxidation reaction depends on a number of issues, chief among which is the prevailing condition in the gaseous and liquid phases in the chamber environment and the design of the chamber vessel. Based on the work of Lunge and Ernst Berl, it is evident that the interfacial reactions play a very important role in this process and that these reactions become much more relevant as pressure increases. On the other hand, the relative importance of the gas and liquid phase kinetics depends on the relative rates of the gas reactions and the gas-to-liquid mass transfer of the sulfur dioxide. There thus appears to be a competition for the SO_2 between the homogeneous gas phase reaction pathway, interfacial reactions and absorption into the liquid phase. The survey done so far indicates that the interfacial reactions are extremely important and this position is supported both by theory and experience from industrial practice.

2.2.2. Relative Rate Comparison: justification for key modeling assumption

The purpose of this exercise was to determine the relative importance of each SO_2 oxidation route and to justify the modeling assumption regarding SO_2 oxidation. The model assumes that the SO_2

oxidation rate is fast enough to be considered as an equilibrium reaction relative to the kinetically limited NO oxidation reaction. A major hindrance to comparing the relative rates of the gas, interfacial and liquid phase oxidation reaction routes is the paucity of published data with relevant information. Due to the absence of publicly available data on the rates of the important interfacial reactions presented, it is not possible at the moment to make any direct comparison involving the interfacial reactions. Nonetheless, we can infer from the experimental work of Ernst Berl that the overall rate of of the lead chamber reactions is high and becomes especially so at elevated pressures (it was shown to be proportional to the square of pressure [29]). Figure 2.7 shows the normalized dependence of the rate of sulfuric acid production on pressure based on values reported by Ernst Berl.

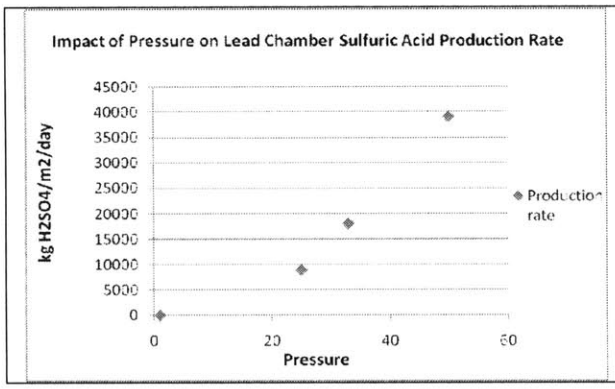

This is the variation of sulfuric acid production rate with pressure reported by Ernst Berl. This production rate is equivalent to the rate of consumption of SO_2. This relation with pressure supports the proposition that the interfacial oxidation pathway is very important at elevated pressures

Figure 2.7: Impact of Pressure on Sulfuric acid production in lead chamber process [29]

Therefore it is fair to assume that the interfacial oxidation route accounts for a significant removal of SO_2 from the gas stream.

We will then go ahead to compare the rate at which SO_2 is consumed by the gas phase reaction to the rate at which it is absorbed into the liquid phase to determine the relative importance of the

gas phase route compared to the liquid phase pathway. Due to lack of published data that could be directly applied to the system under consideration, we'll proceed to present an order of magnitude calculation to get a sense of how the two processes compare.

2.2.2.1 SO_2 Absorption vs. Gas Phase Consumption Rate

Rate of SO_2 absorption into the liquid phase

The rate of transfer of SO_2 from the gaseous to the liquid phase is given by the following expression:

$$Flux\ absorbed\ per\ unit\ volume\left(\frac{mol}{l\ hr}\right) = \frac{Interfacial\ Area\left(\frac{dm^2}{dm^3}\right)\ x\ Concentration\ Difference\left(\frac{mol}{l}\right)}{Mass\ transfer\ resistance(hr\ dm^{-1})} \quad (19)$$

Interfacial area

Benadda et al [39] studied the impact of pressure on effective gas liquid interfacial area in a countercurrent reactive packed column with pressure varying from 1.5 to 13bar. This study was done for a CO_2/N_2-NaOH system but is applicable to our case. Since we are also considering high pressure operation at about 30bar, the interfacial area will be estimated by extrapolating the model result from Benadda et al to 30bar as shown in figure 2.8.

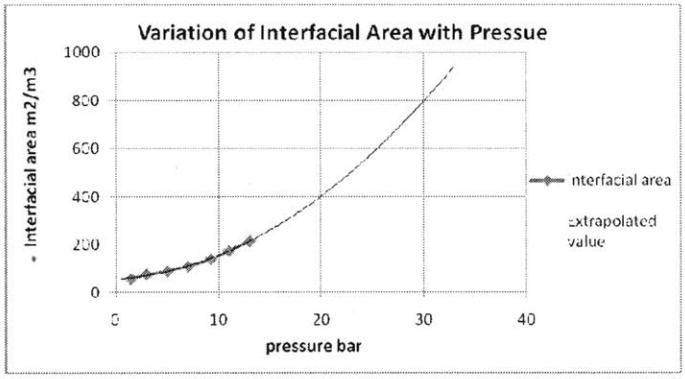

Pressure	**Estimated interfacial area**
1 bar	58 m^2/m^3 *(5.8dm^2/dm^3)*
30 bar	749 m^2/m^3 *(74.9 dm^2/dm^3)*

Figure 2.8: Extrapolated curve showing variation of gas-liquid interfacial area with pressure [39]

Mass Transfer Resistance

Starting with Dankwerts resistance equation [40], Liss [41] calculated the mass transfer rate between atmospheric sulfur dioxide and environmental water and showed how the mass transfer resistance varied with pH. The solubility of SO_2 is diminished due to the chemical reactivity of the gas in solution. For high pH liquid phase, SO_2 is quickly hydrated and ionized once it enters the liquid, enhancing the transport of SO_2 on the liquid side of the interface. His calculations were validated by experimental work carried out by Brimblecombe and Spedding [42]. Dankwerts relation which was used by Liss in his calculation is shown below:

Where:

K = gas flux/ concentration difference

(1/k = interface resistance to mass transfer)

$$H = Henry\ Law\ constant = \frac{equilibrium\ concentration\ in\ gas\ phase}{equilibrium\ concentration\ of\ dissolved\ gas\ in\ liquid\ phase} = 3.8 \times 10^{-2}$$

$$K_{l(SO2)} = \alpha\, K_{l\,(inert)} \quad **$$

$$\alpha = \frac{\tau}{\{(\tau - 1) + (tanh[(\frac{k^* \tau}{D})^{1/3} \frac{D}{K_{l\,(inert)}}] / (\frac{k^* \tau}{D})^{1/2} \frac{D}{K_{l\,(inert)}}\}} \quad ***$$

τ *is the ratio of total to ionic forms of the gas in solution and is a function of pH*

k^* *is the hydration rate constant for the gas* = $3.4 \times 10^6\ s^{-1}$ for SO_2

D is t molecular diffusivity of dissolved gas molecules = = $2 \times 10^{-5}\ cm^2\ s^{-1}$

$K_{l\,(inert)} = 10 cmh^{-1}$

$K_{gso2} = K_{gwater} = 3000 cmh^{-1}$ *(equivalent to water vapor, for best case scenario)*

** $K_{l(SO2)}$ is determined by multiplying the diffusion coefficient of an inert, sparingly soluble gas, $K_{l\,(inert)}$, by an enhancement factor, α, which is a function of pH, hydration constant and molecular diffusivity

*** *This expression was originally derived for CO_2 but is also applicable to SO_2* [41]

The following plot (figure 2.9) was created from the results table from Liss [41] and extrapolated down to pH of 1. Extrapolation errors are not an issue for these order of magnitude estimates.

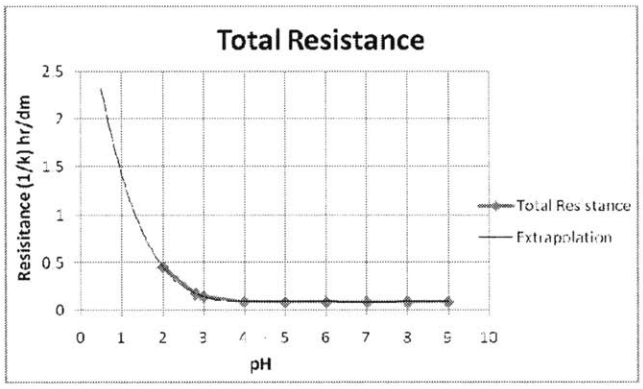

Figure 2.9: variation of gas-liquid interfacial resistance with pH

Concentration Difference

For best case scenario, it is assumed that the concentration of SO_2 in the liquid bulk is zero

Original SO_2 composition in bulk gas phase = 1000ppm

SO_2 gas phase Consumption Rate

There is little reliable documentation of the rate of the NO_2 catalyzed oxidation of SO_2 in humid air. One of the few documented experimental data is that from the work carried out by Falgout [30]. The actual value recorded by Falgout from a single experimental run is 715%/hr for an initial 1% SO_2 system. This value, though several orders of magnitude faster than the reaction in the absence of moisture is still believed to be slow compared to observations made about this same reaction by Lunge [28]. Another relevant observation is that the experimental setup may not match the conditions expected in an absorption tower where for example, an excess of water vapor ensures the air remains saturated everywhere throughout the process. Since we have no information about the actual form or order of this reaction rate, we will just take it as is and use it in this analysis. This

rate is converted to mol L^{-1} hr^{-1} basis and when necessary, adjusted to include the effect of pressure. The result is included in the table below. Tables 2.3A and 2.3B present the relative rates of SO_2 absorption and SO_2 consumption in the gas phase at 1 bar and 30bar respectively. The comparison of the NO oxidation reaction rate for typical flue gas with this pseudo SO_2 oxidation rate is shown in table 2.4. The 30 bar condition is chosen to match the operating condition in the absorber column of the CO_2 purification unit.

Table 2.3A: Comparison of SO_2 gas phase reaction and solution rates at 1bar

pH	$1/K_{total}$ **hr dm^{-1}**	SO_2 absorption rate **mol L^{-1} hr^{-1}**	SO_2 gas phase reaction rate @ 1bar **mol L^{-1} hr^{-1}**
1	1.488	1.73E-4	3.2E-3 *
2	0.458	5.6E-4	
7	0.0883	2.92E-3	

*Quasi rate taken from an experimental measurement from Falgout. Considered a conservative estimate.

Table 2.3B: Comparison of SO_2 gas phase reaction and solution rates at 30 bar

pH	$1/K_{total}$ **hr dm^{-1}**	SO_2 absorption rate **mol L^{-1} hr^{-1}**	SO_2 gas phase reaction rate @ 30bar **mol L^{-1} hr^{-1}**
1	1.488	0.0712	2.92 *
2	0.458	0.2314	
7	0.0883	1.1996	

* Based on Falgout quasi rate.

Table 2.4: Comparison of SO_2 gas phase reaction and solution rates at 30 bar

Pressure	NO gas phase odixation rate (**mol L^{-1} hr^{-1}**)	SO_2 gas phase oxidation rate (**mol L^{-1} hr^{-1}**)
1	4.64E-6	3.2E-3 *
15	1.5E-2	7.2E-1 *
30	0.125	2.92 *

* Based on Falgout quasi rate.

Note:

- The calculations made in the preceding section is based on data available from literature
- The rate of gas phase oxidation of SO_2 was estimated based on results from a single test run carried out by Allen Falgout under circumstances which may not have been designed to simulate lead chamber chemistry
- Jaffe and Klein stated that the rate of the SO_2 gas phase reaction is proportional to third body pressure but gave no quantitative relation.
- The correctness of the comparison is dependent on the accuracy of the input data used. The method however is reliable.
- The pH of the liquid stream from the bottom of the absorber column of the SO_X and NO_X removal unit is less than 1.

2.2.3. Discussion

Based on the results from the calculations shown in Tables 2.3 and 2.4, one can draw the following conclusions:

- For low pH values, SO_2 absorption and gas phase reaction are about the same order of magnitude.
- If a pH buffer is used to reduce the acidity of the absorbing liquid, then the mass transfer rate of the SO_2 to the liquid phase becomes more important.

- For the operating pressures considered, SO_2 oxidation rate is significantly higher than NO oxidation rate.

We did not bother to compare the rate of absorption of NO_2 into the liquid phase because we know that the rate of absorption of SO_2 is higher than that of NO_2. As demonstrated by Ellison[31], for a typical flue gas, the equilibrium concentration of SO_2 in the liquid phase will be about three orders of magnitude higher than that of NO_2, implying that no significant oxidation of SO_2 by NO_2 to H_2SO_4 is likely to take place in the liquid phase.

2.2.3.1. Synopsis

At this stage it would be helpful to note the basic differences between the traditional lead chamber process for the production of sulfuric acid and the use of the same chemistry in SO_X removal from oxy-combustion flue gases. In the oxy-combustion flue gas:

- The nitrogen oxide mole fractions are orders of magnitude lower than for the lead chamber process.
- The nitrogen oxide feed concentration is dominated by nitrogen monoxide (NO) while NO_2 dominates in the lead chamber feed gas,
- The flue gas temperature is typically lower than the gas stream temperature in a lead chamber
- The concentration of the sulfuric acid produced is far less than the concentration generated in the lead chamber process.

With the above in mind, we'll proceed to summarize the conclusions drawn from the discussion in the preceding section as it applies to lead chamber chemistry utilized in the removal of SO_2 from oxy-combustion flue gas:

Catalytic role of NO_2

I. There is general consensus on the fact that NO_2 has a catalytic effect on SO_2 oxidation reaction in the presence of moisture. This catalytic effect is only observed in gas phase or interfacial reactions and in the presence of H_2O. Dry gas phase reactions are slow and do not exhibit any catalytic effect. In the liquid phase, aqueous or hydrolyzed NO_X directly reacts with the aqueous SO_X species and does not play any catalytic role. In the dry gas phase, the reaction between NO_2 and SO_2 is very slow. Hence the observed catalytic effect of NO_2 on SO_2 oxidation requires the presence of H_2O. However, the NO_2 does not act as a pure catalyst and is actually consumed in the process, at least to some extent. Falgout showed that for gas phase reactions, the amount of NO_2 consumed depends on relative humidity. Based on his observation of the reaction at 100% humidity, one cannot rule out the possibility that in moist air, NO_2 reacts rapidly with SO_2 and also enhances the direct oxidation of SO_2 by atmospheric oxygen to form sulfuric acid.

Route

I. SO_2 removal from the flue gas takes place primarily via gas phase reactions, interfacial reactions and direct dissolution into the liquid phase.

II. SO_2 oxidation to sulfuric acid takes place via direct gas phase oxidation, interfacial reactions and liquid phase oxidation which is preceded by the solution of the SO_2 into the aqueous phase.

III. For the process that involves a typical oxy-combustion plant flue gas, there will be insufficient NO_X species in the liquid phase to directly oxidize the dissolved SO_2. This is so

because the equilibrium solubility of SO_2 is considerably higher than that for NO_X and the SO_2 gas phase composition is also higher than that of NO_X. Therefore, oxidation to sulfuric acid is expected to be dominated by gas phase and interfacial reactions. Most of the SO_2 transferred to the liquid phase will most likely leave as sulfurous or aqueous SO_2.

Rate Assumptions

I. Based on qualitative analysis of the studies by Ernst Berl and Geo Lunge and the evidence of industrial practice, it is evident that the interfacial reactions for the conversion of SO_2 to sulfuric acid are significantly faster than the rate limiting NO oxidation reactions.

II. The calculation using results from Falgout (which we believe to be conservative) show that the gas phase SO_2 oxidation reaction is three orders of magnitude faster than that of NO at 1 bar and is still about 20 times faster at 30 bar. Therefore, the assumption that the SO_2 reaction can be represented as equilibrium relative to the NO oxidation reaction is justified.

III. The mass transfer rate of SO_2 is in the same range as the gas phase oxidation reaction rate calculated based on results from Falgout (The pH values expected in the column range from 0.3 to 0.6). Therefore we can consider the following scenario for the removal of SO_2 from the flue gas stream. A good proportion (say 50%) of the SO_2 is consumed directly in the gas phase reaction. Of the remaining SO_2 that reaches the liquid boundary, most of it is consumed by interfacial the reactions and the balance will transfer to the liquid phase. Both the gas and interfacial reactions will be limited only by the rate of oxidation of NO to NO_2. Hence for low pH conditions in the liquid phase, as pressure increases and the rate

limiting effect of NO oxidation decreases, most of the SO_2 will be oxidized before getting into the liquid phase.

Overall reaction Mechanism

The most comprehensive mechanism provided for the lead chamber process was that by Ernst Berl in reactions 11 to 18. Taking into account that the acid concentration involved in the flue gas cleanup is much lower than in a traditional system reactions 11 to 18 can loosely be combined to give the following overall reaction mechanism:

A

$\mathbf{NO} + \frac{1}{2}O_2 \rightarrow NO_2$

$NO_2 + SO_2 + H_2O \leftarrow\rightarrow \mathbf{NO} + H_2SO_4$

A possible alternative that involves atmospheric oxygen in the SO_2 oxidation reaction is shown below:

B

$\mathbf{NO} + \frac{1}{2}O_2 \rightarrow NO_2$

$\frac{1}{2}O_2 + 2SO_2 + 2H_2O + NO_2 \leftarrow\rightarrow 2H_2SO_4 + \mathbf{NO}$

The direct overall reaction pathway of Geo Lunge is similar to mechanism A. From a thermodynamic point of view, we believe that either of the two options (A and B) can be used to model the SO_2 removal process. However, given the dependence of the SO_2 oxidation reaction on the presence and concentration NO_2, we chose the first option (A) as the overall reaction mechanism in the model developed for the process.

The selected reaction scheme for modeling SO_2 removal from oxy-combustion flue gas in our model is shown in table 2.5. Here, the second reaction in A is split into two steps.

Table 2.5: Overall SO_2 oxidation scheme adopted for this model

24	$\mathbf{NO}_{(g)}+½O_{2(g)} \rightarrow NO_{2(g)}$	Rate limited [43, 44]. See discussion on the Nitric Acid Process
25	$NO_{2(g)}+SO_{2(g)} \leftrightarrow \mathbf{NO}+ SO_{3(g)}$	Fast, Equilibrium
26	$SO_{3(g)} + H_2O_{(g/l)} \leftrightarrow H_2SO_{4(g/l)}$	Fast, Equilibrium

It has been shown that SO_2 removal from the gas phase will be via the three routes and as such will be a fast process relative to NO oxidation. This reaction scheme therefore is good enough for estimating how rapidly SO_2 is removed from the gas phase and can provide a good estimate of the composition of the acidic liquid discharged from the removal equipment. With the availability of more reaction chemistry data expected in the future, this modeling scheme can be improved to reflect any new information on the chemistry for SO_2 oxidation.

2.3. Nitric Acid Chemistry

NO_X absorption columns are used extensively in industry for production or recovery of nitric acid. The same chemistry used in the production of nitric acid is used to model the removal of the nitrogen oxides as nitric acid from the oxy-combustion flue gas. The discussion in this section will basically consist of a summary of the impressive work carried out by D. N. Miller [23] in determining the relevant reaction steps and quantifying the relative rates of the important overall reactions for this process, especially the gas-liquid mass transfer rates. Miller developed a rate method for predicting the performance of absorption columns which provides greater accuracy than the traditional method of using plate efficiencies. He determined the mass transfer constants from extensive plant data and developed correlations as functions of temperature and acid strength.

2.3.1. Reaction Mechanism

Miller identified a number of possible overall reaction routes. However, the dominant route shown in table 2.6 was adopted for our model (see further discussion in [23]. Miller showed that excluding the other pathways had little impact on the accuracy of the column simulations). This process is pictorially represented in figure 2.10.

Table 2.6: Nitric acid process reaction routes

	Route 1
1	$2NO_{(g)} + O_{2(g)} \leftrightarrow 2NO_{2(g)}$
2	$2NO_{2(g)} \leftrightarrow N_2O_{4(g)}$
3	$N_2O_{4(g)} \leftrightarrow N_2O_{4(l)}$
4	$N_2O_{4(l)} + H_2O_{(l)} \leftrightarrow HNO_{3(l)} + HNO_{2(l)}$
5	$3HNO_{2(l)} \leftrightarrow HNO_{3(l)} + H_2O_{(l)} + 2NO_{(g)}$

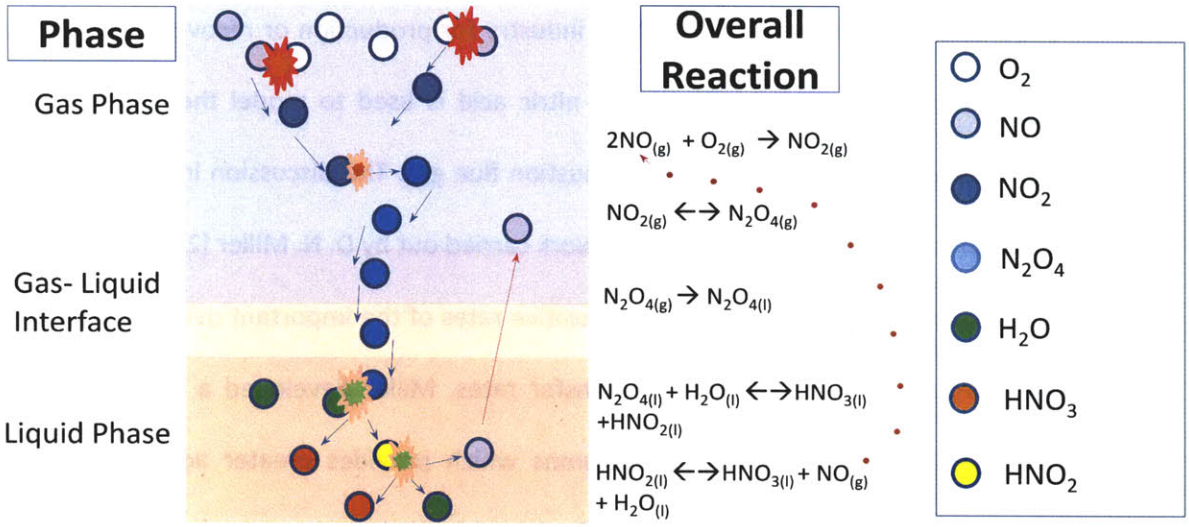

Figure 2.10: Nitric acid chemistry overall pathway

For reaction 1 and 2, Miller used the widely accepted rate expression and equilibrium constant of Bodenstein [43, 44]:

$$R_{(1)} = k_1 \left(p_{NO}^2 p_{O2} - \frac{p_{NO2}}{K1}\right), \text{kPa/s} \quad (6)$$

$k_1 = \exp\left(\frac{1,468}{T} - 10.9043\right)$, $kPa^{-2}.s^{-1}$

$K1 = \exp\left(-8.002 + 1.75lnT - 0.000217T - \frac{2.496}{T}\right)$, kPa^{-2}

p = partial pressure, kPa
T = temperature, K

$$K_2 = \frac{p_{N2O4}}{p_{NO2}^2}, \text{kPa-1} \quad (7)$$

Based on previous work by several prominent authors, Miller combined the mass transfer equation 3 and the liquid phase equations 4 and 5 into a single equation with an effective rate that accounts for both kinetic and transport limitations.

$3N_2O_4 + 2H_2O \leftarrow\rightarrow 4HNO_3 + 2NO$ (8)

$$R_{(8)} = H_{N2O4} \sqrt{(k_{4,5} D_{N2O4})} A \left[p_{N2O4} - \frac{\left(\frac{p_{NO}}{K_O}\right)2}{3}\right], \text{kmol/s} \quad (9)$$

$$K_{4,5} = \frac{(p_{NO} . a_{HNO3}^2)}{p_{NO2}^3 . a_{H2O}}, \quad \text{kmol/m}^3\text{.kPa}^2$$

$$K_O = \exp\left(\begin{matrix}23.39 - 134.98W_{HNO3} + 434.69W_{HNO3}^2 - 789.84\, W_{HNO3}^3 \\ + 675.65\, W_{HNO3}^4 - 221.89W_{HNO3}^5\end{matrix}\right), \text{kPa}^{-1/2}$$

A = Interfacial area
H = Henry's law coefficient $kmol/m^3$. kPa
D = effective diffusivity, m^2/s
a = activity, $kmol/m^3$
W = weight fraction

Miller determined the value of the mass transfer factor, $H_{N2O4}\ \sqrt{(k_{4,5}D_{N2O4})}$ from plant data. This factor, together with other relevant column parameters, is then used via an iterative procedure to calculate the mass transfer for each plate in the column. This rate expression is implemented in Aspen Plus.

2.4. Non-condensable Gas Removal Unit

The second stage in the CO_2 purification process is the non-condensable gas removal. The three major non-condensable gases to be removed are O_2, N_2 and Ar, but this process will also remove the majority of any other non-condensable gas. Removal is achieved by low temperature phase separation in a multistage distillation column. The separation of the non-condensable gases from the CO_2 is achieved in one multi-stage distillation column with a two-stage condenser. The distillation column is essential to reduce the O_2 concentration in the CO_2 to parts-per-million concentrations, while avoiding alternative O_2 removal methods such as adsorption and/or catalytic oxidation reactions. Before entering the low temperature region, the gas must be dehydrated by one of the available molecular sieve sorbents that are commercially available. The dehydration specifications will be dictated by requirements of the low temperature heat exchangers in this region. However, the high-pressure cooled absorption columns for NO_X and SO_X removal are very effective in reducing the water content in the flue gas by an order of magnitude thereby dramatically reducing the cost and energy consumption of the dehydration unit.

Two process configurations, A and B, have been developed for the removal of the non-condensable gases. The layouts of the two configurations are shown in figures 2.11 and 2.12 and a detailed description of each process follows.

2.4.1. Configuration A

The special feature of this design is the use of the Joule-Thompson (JT) effect and tight heat integration to provide the required low temperatures in the system and to increase CO_2 recovery from the vent gas, with minimal external cooling. This configuration is shown in figure 2.11.

The cooling of the inlet gas stream as well as the cooling load for the condenser is provided by a combination of the reboiler duty of the distillation column and the evaporation of the depressurized bottoms from the column. The distillate vapor stream leaving the column comprises about 60% CO_2. To increase CO_2 recovery, the vapor is partially condensed. The condensation cooling is provided primarily by depressurizing the liquid condensate. This is required to efficiently realize greater than 90% CO_2 recovery while achieving tight purity specs on the bottoms CO_2 stream. After being depressurized and vaporized, this stream is compressed to the distillation column pressure and cooled before being fed back in the appropriate stage. A detailed description of the process, based on Figure 2.11, follows.

Dry CO_2 stream 1 is first cooled to about -6C by heat exchange with evaporating fluid in the reboiler (M1) before further cooling to around -23C in the cold box (M2) and the supplemental refrigeration unit (M7). Most of the cooling in the cold box is provided by the evaporation of depressurized high purity (99.99%) CO_2 streams 7 and 11 at 14bar (-31C) and 21.3bar (-18C) respectively. Bottoms stream 6 is used to provide the required evaporative cooling in the condenser (M4). More CO_2 is

recovered from the vapor distillate stream 16 by partially condensing it in the cold box (M5) to yield a two-phase stream 17 which is then separated in the flash drum (M6). The low temperature vapor stream 24 (-42C) and the throttled stream 19 (-50C, 12.2bar) provide the requisite cooling in M5.

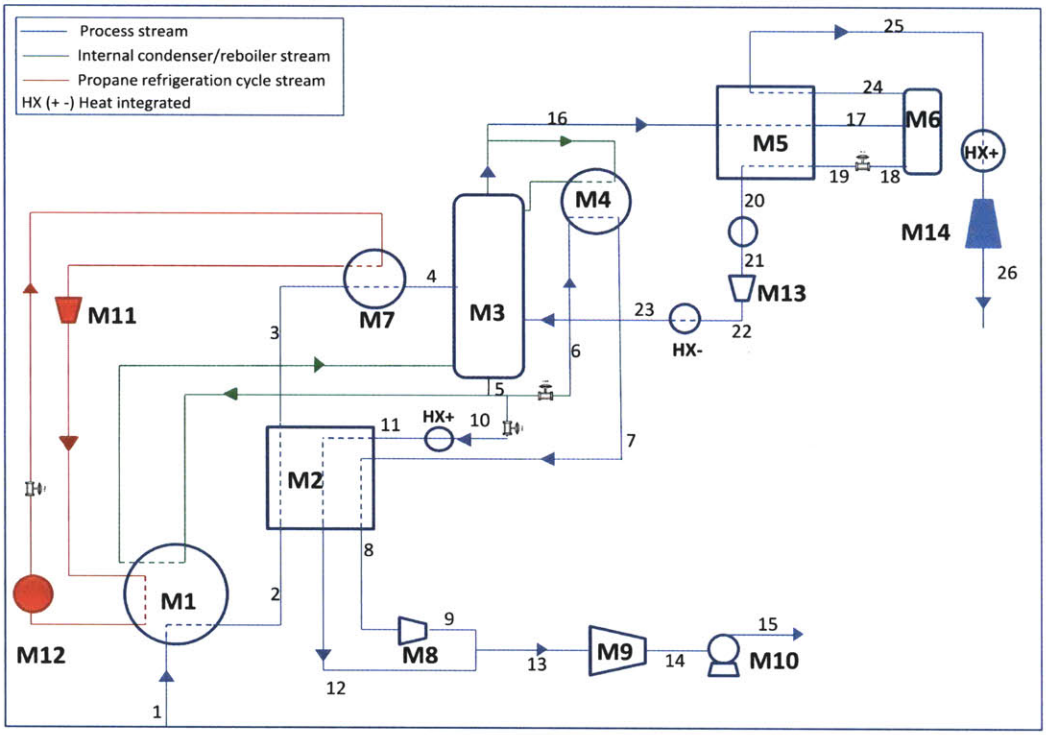

Figure 2.11: Non-Condensable Gas Removal Unit – Configuration A

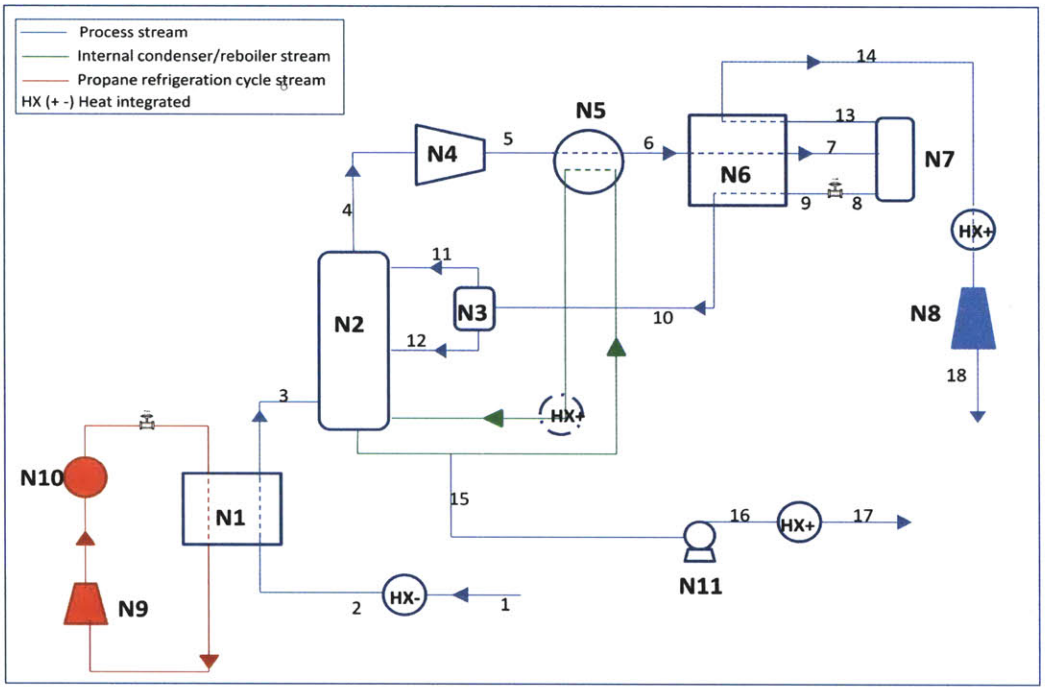

Figure 2.12: Non-Condensable Gas Removal Unit – Configuration B

Table 2.7: Equipment List

M2	Reboiler
M2	Cold Box for inlet CO_2 cooling
M3	Distillation column
M4	Condenser
M5	Cold Box for distillate cooling
M6	Flash drum
M7	Propane refrigeration cycle evaporator for inlet CO_2 supplemental cooling
M8, M9	Compressor
M10	CO_2 Pump
M11	Propane refrigeration cycle compressor
M12	Propane refrigeration cycle condenser
M13	Reflux CO_2 compressor
M14	Integrated Expander*

N1	Cold Box for inlet CO_2 cooling
N2	Distillation column
N3	Vapor-Liquid Separator
N4	Distillate compressor
N5	Reboiler/1st stage Condenser
N6	Cold Box -2nd stage Condenser
N7	flash drum
N8	Integrated Expander
N9	Propane refrigeration cycle compressor
N10	Propane refrigeration cycle condenser
N11	CO_2 pump

***Integrated expander**: Multistage expansion system with reheat

The 96% pure CO_2 stream 21 is first compressed then cooled and fed back into the distillation column. Stream 8 is then compressed up to 21.3bar to match the pressure of stream 12 and the two streams are combined, compressed to 75bar (safely in the supercritical state) and then pumped up to the pipeline pressure of 110bar. The operating condition and states of the various streams described can be adjusted to optimize performance.

2.4.2. Configuration B

The second non-condensable gas removal process configuration also uses Joule-Thompson cooling of the CO_2-rich stream but relies on an external refrigeration cycle to provide most of the cooling required for the low temperature phase separation. The major advantage is that the purified CO_2 is extracted as bottoms liquid and pumped directly to sequestration pressure, eliminating the cost and energy penalty of gas phase compression of the purified stream. However this configuration eliminates the cooling potential from vaporization of the CO_2 and requires the large external refrigeration load. Previous systems designed to extract liquid CO_2 utilize large external refrigeration cycles for cooling both the inlet gas and also for providing cooling duty to the condenser. This configuration was developed to replace the use of external refrigeration for providing cooling duty to the condenser and to lower the overall energy requirement by optimizing internal heat integration. The cooling load for the condenser is now provided in part by the reboiler and in part by a Joule-Thompson expansion of the reflux distillate stream. Ordinarily, the condenser temperature is lower than that of the reboiler, making it impossible to integrate the two units. Therefore to enable heat integration between the condenser and the reboiler, this system employs vapor recompression on the vapor distillate from the column.

The balance cooling is then provided by the Joule-Thompson expansion of the liquid condensate. The two phase reflux stream is separated and fed into appropriate stages in the distillation column. A detailed description of the process, based on figure 2.12, follows:

Dry CO_2 stream entering at about 27C is first optionally pre-cooled to 5C by heat exchange with the exiting vent stream 14 (-3C), the sequestration CO_2 streams 16 at -3C or by heat exchange with evaporating reboiler fluid. The cool inlet stream now enters the cold box (N1) where it is further cooled to about -30C by an external propane refrigeration cycle. The two-phase stream 3 is fed into an appropriate stage in the distillation column (determined by the stage composition) where separation results from the interaction between the down-coming liquid and the up-rising vapor stream. High purity (99.9%) CO_2 is extracted from the column bottoms at about -11C and 25.9bar and then pumped directly to pipeline pressure of 110bar. To utilize reboiler duty in providing partial cooling in the condenser, the distillate vapor is first compressed to about 50bar and then passed through the reboiler/condenser heat exchanger (N5) where the vapor fraction drops to about 0.73. The two-phase stream 6 then proceeds to the heat exchanger (N6) where further cooling condenses more of the CO_2 till a vapor fraction of about 0.28 is achieved. The flash drum (N7) is then used for phase separation and the resulting vent (13) and depressurized reflux (9) streams provide the cooling duty for the heat exchanger (N6). The two-phase, 90% CO_2 stream 10 at -10C and 31.6bar is then recycled back to the distillation column. The two phases might first be separated and optimally fed into appropriate stages of the distillation column.

2.5. Conclusion

The proposed CO_2 purification unit comprises of the NO_X and SO_X removal section and the non-condensable gas removal section. NO_X and SO_X removal is achieved by taking advantage of lead chamber and nitric acid chemistry used in industrial production of sulfuric and nitric acid. This removal process takes place in absorber columns operating at elevated pressure. The use of high pressure columns is determined by the rate limiting NO oxidation reaction which is a third order reaction and speeds up rapidly with increasing pressure. Contaminants like mercury are also removed in this section.

The nitric acid chemistry has been extensively studied and the reaction rates are well documented. The approach used to model this process is a rate based method for predicting performance of absorption columns developed by Miller. This method properly accounts for the gas to liquid mass transfer resistance which is the rate determining step in the process. He validated the accuracy of the method using extensive data from industrial columns.

The lead chamber chemistry however is not as well documented. The two key reactions central to this process are the NO and SO_2 oxidation reaction. We found from in-depth analysis of existing literature that the oxidation of SO_2 can take place in the gas phase, gas-liquid interface and liquid phase. Catalyzed oxidation of SO_2 takes place only in the gas phase and interfacial reactions. Also, formation of sulfuric acid depends more on these two processes because of the relatively high gas-to-liquid mass transfer resistance for NO_X compared to SO_2. Given that the overall reaction path is the same for all, what really matters is how the rates compare with that of the NO oxidation reaction.

We adopted the gas phase oxidation route in developing this model. The accuracy of the model is then hinged on the assumption that the SO_2 oxidation reaction is sufficiently faster than the NO oxidation reaction to be modeled as equilibrium relative to the NO reaction. This we were able to show in the relative rate calculations of section 2.2.

Two thermally integrated process configurations were developed for the removal of non-condensable gases downstream of the NO_X and SO_X section. Removal is achieved by low temperature phase separation in a multistage distillation column which has been demonstrated to be the only feasible way to achieve parts per million O_2 concentration using VLE.

The first configuration utilizes Joule-Thompson cooling and a tight heat integration of the process stream to provide all the required low temperatures in the process. This eliminates the need for an external refrigeration cycle and the extra fire control installations required when inflammable refrigerants are used. However, the high purity CO_2 stream is delivered as a gas and requires a compression train to take it to pipeline pressure.

The second configuration achieves the same separation using an external refrigeration system and delivers the CO_2 as liquid. That way, it eliminates the need for compressors as the CO_2 is directly pumped up to pipeline pressure.

Chapter 3 Results and Sensitivity Analysis

In the previous chapter, a detailed discussion of the thermodynamics and chemistry of the CO_2 purification unit was provided. We were able to shed some light on key aspects of the process and provided a basis for our underlying assumptions. The Purification train model was then developed using Aspen Plus and for the base power cycle which has been described in detail by Hong et al [6]. The base power cycle is a pressurized oxy-coal plant designed with coal flow rate of 30 kg/s (HHV: 874.6MWth, LHV: 839.1MWth) with flue gas flow rate of 87.4kg/s, typical composition as shown in table 3.1 and operating at combustor pressure of 10bar.

Table 3.1: Flue gas composition for a pressurized oxy-coal system at inlet of Purification Unit

Component	CO_2	H_2O	O_2	N_2	Ar	CO	NO	NO_2	SO_2
Mole fraction	0.86	.015	.057	.015	.047	.0004	.0003	.00008	.002

3.1 NO_X and SO_X Removal Unit

3.1.1. Chemistry

The sulfuric acid (lead chamber) and nitric acid chemistry schemes are shown in table 3.2:

Table 3.2: sulfuric and nitric acid chemistry schemes

Sulfuric acid Chemistry
Gas Phase Reactions
$NO+½O_2 \rightarrow NO_2$
$NO_2+SO_2 \leftarrow\rightarrow NO+ SO_3$
Liquid Phase Reactions
$SO_3 + H_2O \leftarrow\rightarrow H_2SO_4$

Nitric acid Chemistry
Gas Phase Reactions
$NO+½O_2 \rightarrow NO_2$
$2NO_2 \leftarrow \rightarrow N_2O_4$
Interfacial Reactions
$N_2O_{4(g)} \leftarrow \rightarrow N_2O_{4(l)}$
Liquid Phase Reactions
$N_2O_4+ H_2O \leftarrow \rightarrow HNO_3+ HNO_2$
$3HNO_2 \leftarrow \rightarrow HNO_3+ H_2O+ 2NO$

In the base case model the flue gas is first compressed to 15bar before entering the first absorber column. This column is referred to as the SO_X removal column because it is designed such that the SO_2 in the flue gas is completely knocked out. However, at that pressure, there is increased NO oxidation to NO_2 which is required both by the 'sulfuric acid' and the 'nitric acid' processes. Therefore, it is expected that both will be taking place simultaneously, though at different rates. Therefore a combined reaction scheme is defined for the model and is shown in table 3.3.

Table 3.3: combined reaction scheme implemented in model

	Reactions	Comments
1	**$NO+½O_2 \rightarrow NO_2$**	Rate limited, 3rd order gas phase reaction. Rate increases with Pressure. Forward reaction favored at low temperatures
2	$NO_2+SO_2 \leftarrow\rightarrow$**$NO$**$+ SO_3$	Fast equilibrium reaction
3	$SO_3 + H_2O \leftarrow\rightarrow H_2SO_4$	Fast equilibrium reaction
4	$2NO_2 \leftarrow \rightarrow N_2O_4$	Fast equilibrium dimerization reaction
5	$3N_2O_4 + 2H_2O \leftarrow \rightarrow 4HNO_3 +$ **$2NO$**	Mass transfer limited reaction - (Miller's correlation)

Reactions 1,2,3 represent the sulfuric acid process while reactions 1,4,5 represent the nitric acid process which is implemented using D.N Miller's model. This combined scheme is also used in the second 30bar column though only the nitric process is expected to take place there. The absorber column is modeled using a Radfrac[3] block in Aspen Plus [45]. The sulfuric acid reactions are provided as inputs to the simulation. Miller's model is implemented using a Radfrac User-Kinetic model through a user subroutine that calculates the required reaction rates as well as the rate of generation for each species per stage.

3.1.2. Thermodynamic Property Method

The ELECNRTL property method is specified to describe liquid phase solution equilibrium. This method has been determined to be accurate for the dilute acid conditions that we expect in the absorber columns. Dissociation reactions for the acids are also included as part of the chemistry definition of the absorber column block associated with the ELECNRTL method in Aspen Plus.

3.1.3 Column Specifications

Table 3.4 lists the specifications for the absorber columns used in the double column model. The number of stages was selected based on results from earlier simulations.

Table 3.4: Column Specifications

Low Pressure Column	High Pressure Column
Top stage pressure: 14.76 bar	Top stage pressure: 30 bar
Pressure drop per stage: 0.04bar	Pressure drop per stage: 0.04bar
Number of stages: 5	Number of stages: 8
Flue gas feed stage: (bottom)	Flue gas feed stage: (bottom)
Water Feed stage: (top)	Water Feed stage: (top)

[3] RadFrac is a rigorous model in Aspen for simulating all types of multistage vapor-liquid fractionation operations and facilitates the simulation of tray and packed columns.

Condenser/Reboiler: None	Condenser/Reboiler: None
On-stage cooling: Bottom stage	On-stage cooling: bottom stage
Vapor holdup per stage: 20 m^3	Vapor holdup per stage: 20 m^3
Water flow rate: 2kg/s	Water flow rate: 2kg/s
Flue gas flow rate: 87kg/s	Flue gas flow rate: 87kg/s
Column diameter: 4.5m	Column diameter: 4.5m

3.1.4 Stream Results

Tables 3.5 and 3.6 show the state and composition of the inlet and exit streams to the Low pressure and High pressure absorber columns respectively. As shown, SO_2 is practically completely removed in the first column and more of the unconverted NO_X is removed in the high pressure column to ensure that transport and sequestration specifications for these components are achieved.

Table 3.5: Low Pressure (15 bar) Column Stream Results

	Flue Gas in	Flue Gas out	Bottoms Liquid
Total Flow kg/sec	86.91	86.64	2.27
Total Flow kmol/sec	2.028	2.025	0.108
Temperature K	298.15	305.62	296.19
Pressure bar	15.24	14.76	15.00
Mole Fraction			
NO	2.63E-04	2.96E-04	7.41E-07
NO_2	7.64E-05	1.90E-05	-
N_2O_4	-	1.91E-08	-
N_2	0.015148	0.01517	1.10E-06
O_2	0.05742	0.056525	8.15E-06
H_2O	2.32E-03	3.89E-03	0.921257
HNO_3	-	2.20E-10	4.78E-05
H_3O+	-	-	0.041025
NO_3-	-	-	4.15E-04
CO_2	0.875265	0.876503	1.23E-05
CO	4.24E-04	4.25E-04	4.63E-08
AR	0.047104	0.047171	7.38E-06
H_2SO_4	-	-	3.21E-12
SO_2	1.98E-03	-	1.72E-04
HSO_4-	-	-	0.033496
SO_4--	-	-	3.56E-03

pH	0.31839

Mole fractions less than 1E-20 are considered negligible

Table 3.6: High Pressure (30 bar) Column Stream Results

	Flue Gas in	Flue Gas out	Bottoms Liquid
Total Flow kg/sec	86.64	86.51	3.47
Total Flow kmol/sec	2.025	2.018	0.117
Temperature K	293.15	292.47	291.52
Pressure bar	30.38	30.00	30.36
Mole Fraction			
NO	2.96E-04	8.28E-06	7.90E-07
NO_2	1.90E-05	2.25E-06	1.08E-06
N_2O_4	1.91E-08	1.27E-09	9.48E-07
N_2	0.0151698	0.01522	3.93E-06
O_2	0.0565246	0.056491	2.86E-05
H_2O	3.89E-03	1.10E-03	0.989796
HNO_3	2.20E-10	1.24E-13	4.40E-04
H_3O+	-	-	4.82E-03
NO_3-	-	-	4.82E-03
CO_2	0.8765031	0.879429	6.06E-05
CO	4.25E-04	4.26E-04	1.63E-07
AR	0.0471706	0.047327	2.63E-05
H_2SO_4	4.09E-21	-	-
SO_2	-	-	-
HSO_4-	-	-	-
SO_4--	-	-	-
pH			0.375251

mole fractions less than 1E-20 are considered negligible

3.1.5. Stage Composition Profiles

The following plots show the composition profile of the important components – SO_2, NO_2 and NO – across the stages of the two columns.

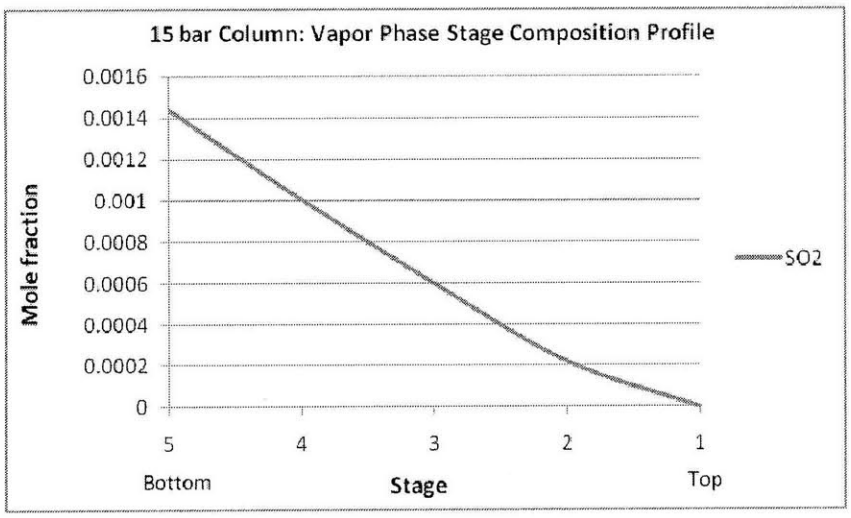

Fig 3.1: SO_2 vapor phase profile @ 15bar

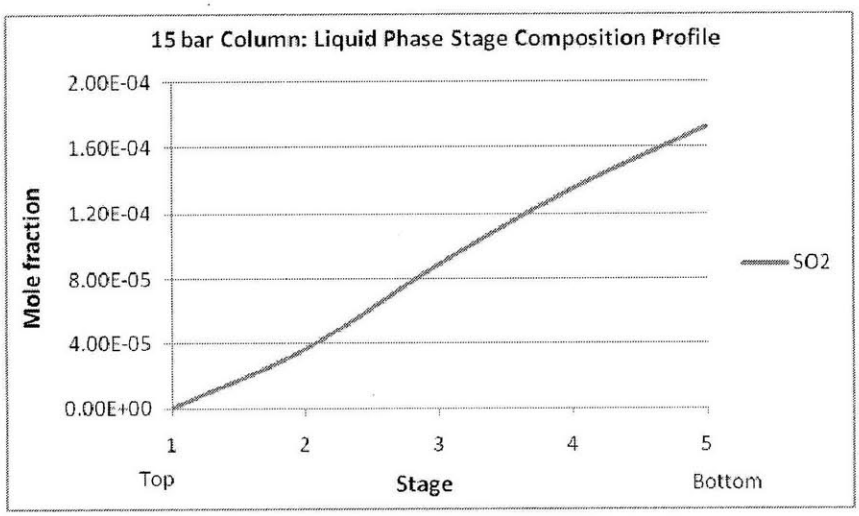

Fig 3.2: SO_2 liquid phase profile @ 15bar

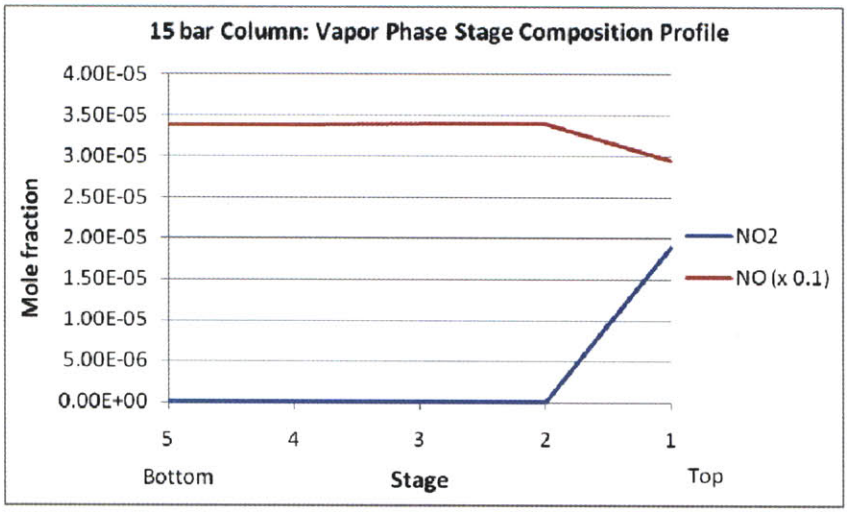

Fig 3.3: NO and NO_2 vapor phase profile @ 15bar

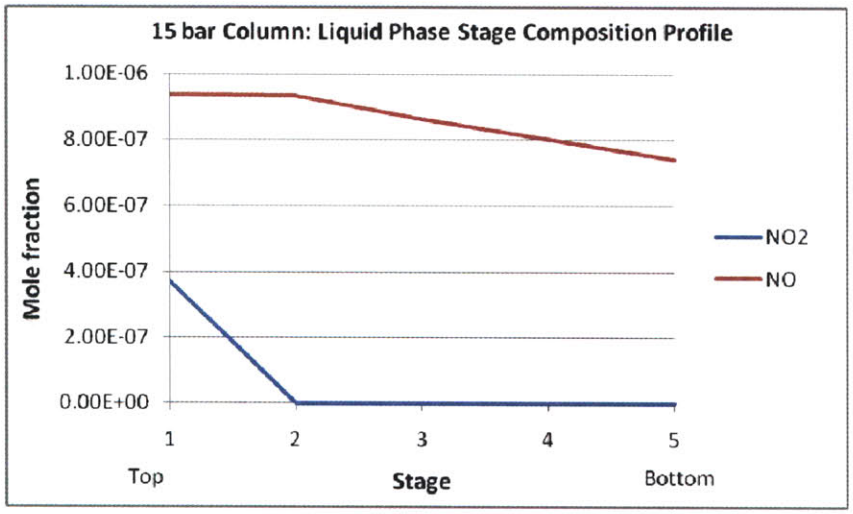

Fig 3.4: NO and NO_2 liquid phase profile @ 15bar

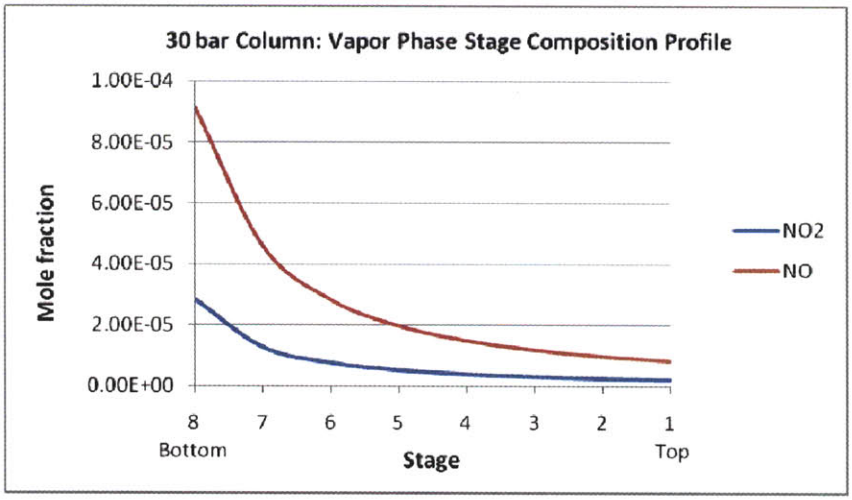

Fig 3.5: NO and NO_2 vapor phase profile @ 30bar

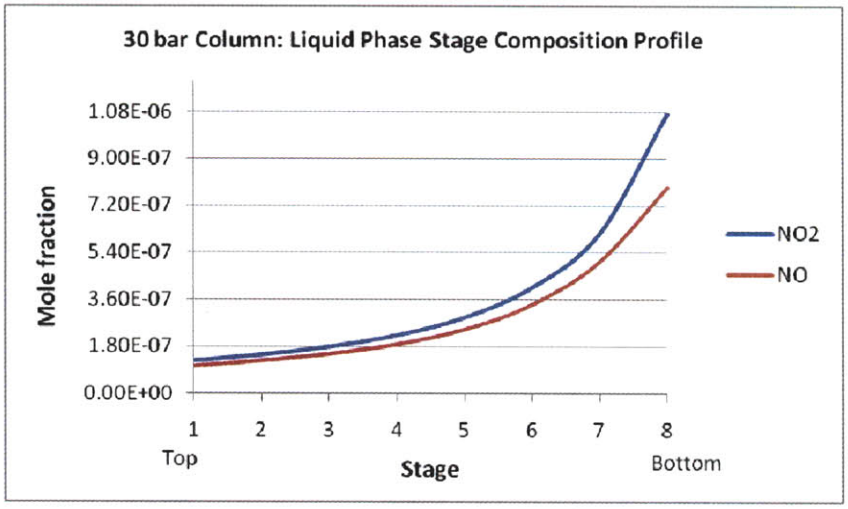

Fig 3.6: NO and NO_2 liquid phase profile @ 30bar

Figures 3.1 and 3.2 show SO_2 composition profile in the vapor and liquid phases across the stages of the low pressure (15bar) column. It is seen that the SO_2 is completely removed from the gas phase by the end of the 5^{th} stage. A closer look at figure 3.2 indicates that some amount of the SO_2 stays dissolved and un-reacted in the liquid phase and that this amount increases almost linearly from the top stage to the bottom. SO_2 transfer to the liquid phase is limited by phase equilibrium and the dissolved SO_2 leaving with the bottoms liquid is about 10% of the captured SO_2. This is because at 15 bar, the oxidation reaction of SO_2 to SO_3 is limited by the rate of generation of NO_2 from NO which is still not fast enough at that pressure..

In figure 3.3, the composition of NO and NO_2 in the vapor phase remain fairly constant. This is mainly because the rate of consumption of NO in the NO oxidation reaction is approximately equal to the rate of production of NO from the SO_2 oxidation and liquid phase reaction. Similarly, NO_2 consumption is approximately equal to NO_2 generation in the gas phase. However, nearer the top of the column (1-2), NO concentration drops while that of NO_2 increases. A possible explanation is that at this stage, most of the SO_2 has been eliminated from the gas phase, resulting in an increase in the amount of unused NO_2 and a drop in the amount of NO recycled.

Figures 3.5 and 3.6 show the NO and NO_2 composition profile in the high pressure (30 bar) column. Most of the NO_X is removed in this column as HNO_3 down to parts per million values. The liquid phase plots for NO and NO_2 show that inevitably, less than 1% of the NO_X will simply remain in solution in the liquid phase while more than 99% of the captured NO_X is in the form of nitric acid.

3.1.6 Sensitivity analysis

The main modeling parameters that define the performance of the absorber column include:

- Operating pressure
- Vapor Holdup Volume
- Water flow rate

A sensitivity analysis was carried out on the absorber column to determine how these factors influence the extent of removal of the major pollutant species as well as the state and composition of the exit streams. The objective is to determine the optimal specifications for each of these controlling factors. The specification of the column used for the study is shown in tables 3.7, 3.10 and 3.11 while the results of the sensitivity studies are shown in the following plots.

3.1.6.1. Pressure Sensitivity analysis

The operating pressure of the column has a significant effect on the performance of the column. This is because the key oxidation reaction of NO to NO_2 is a third order reaction and thus the rate increases rapidly with pressure.

Table 3.7: Absorber Specs in Pressure Sensitivity Study

No. of stages	9	Vapor holdup per stage	20m3
Inlet gas temperature	25C	Water flow rate	4kg/s

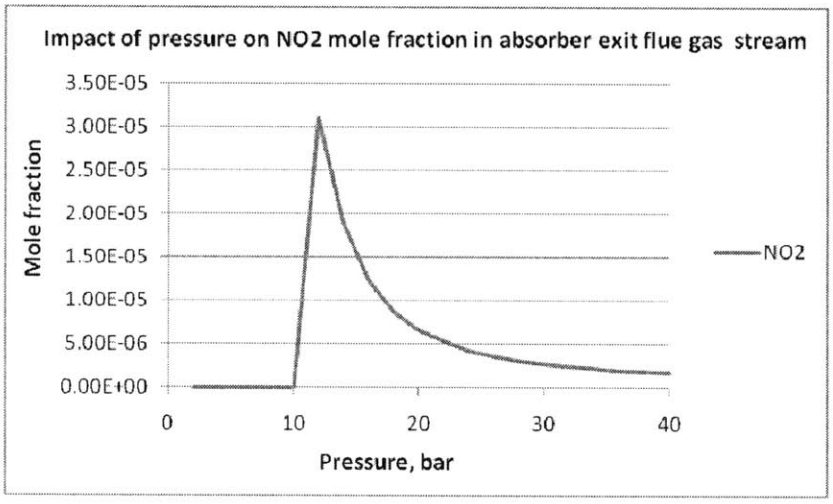

Fig 3.7: Impact of Pressure on NO_2 mole fraction

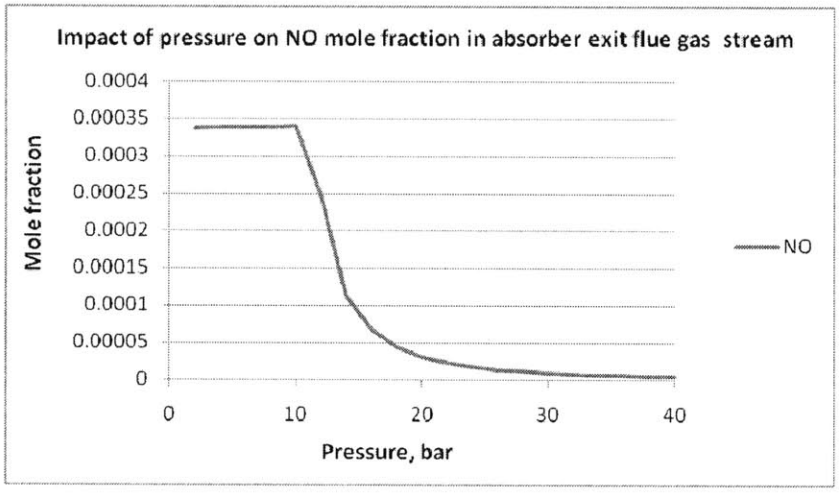

Fig 3.8: Impact of Pressure on NO mole fraction

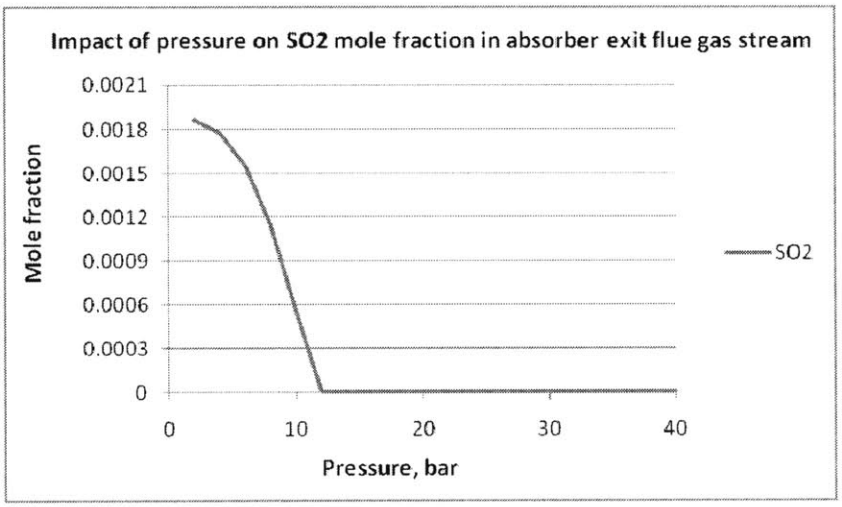

Fig 3.9: Impact of Pressure on SO_2 mole fraction

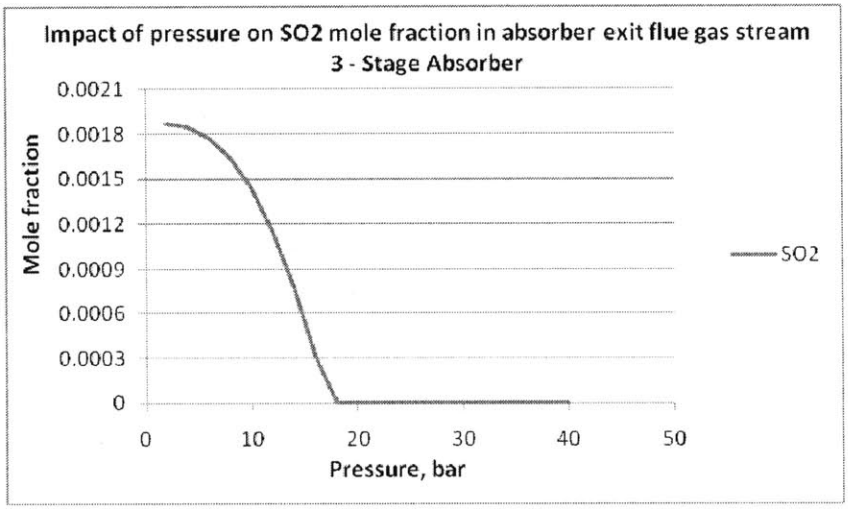

Fig 3.10: Impact of Pressure on SO_2 mole fraction (3 stage column)

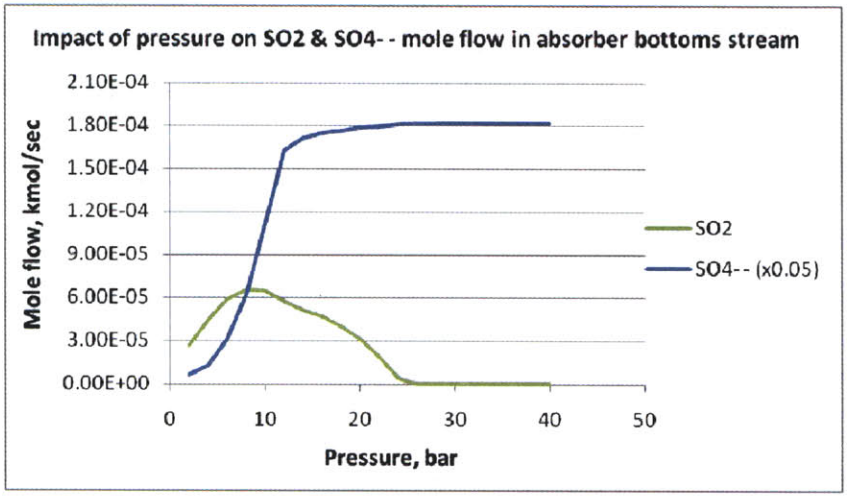

Fig 3.11: Impact of Pressure on liquid phase composition

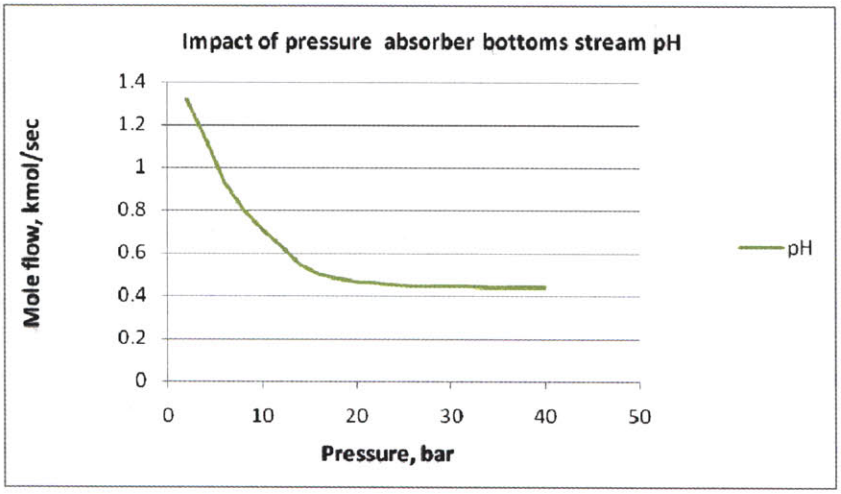

Fig 3.12: Impact of Pressure on pH

Also, pressure increases the gas-liquid interfacial area providing more vapor-liquid contact area and therefore speeding up the overall process.

Figures 3.7 – 3.9 show the variation in the composition of the exit flue gas stream from the reactive absorber with operating pressure. In figure 3.7, the NO_2 composition remains stays close to zero

from 1 to 10 bar before spiking and then gradually decaying as pressure increased. The flat profile from 1 to 10 bar is explained by the fact that at these pressures, there is sufficient SO_2 in the gas phase to rapidly consume the NO_2 produced from the slower NO oxidation reaction. Beyond 10bars, the SO_2 in the gas phase is completely consumed and there is not sufficient residence time in the column for the nitric acid chemistry to use up the NO_2. This becomes possible at higher pressures, as indicated by the decay observed in the plot.

Figure 3.9 shows the impact of operating pressure on SO_2 mole fraction in the exit flue gas stream. SO_2 decreases rapidly with pressure since increasing pressure greatly favors its removal. Slightly below 12 bar, all the SO_2 is removed from the gas phase in the 9-stage column. In order to gain a better understanding of how pressure impacts SO_2, the column specification for the sensitivity study was changed from 9 to 3 stages and the plot of pressure vs. SO_2 composition obtained is shown in figure 3.10. From this figure, it is seen that at about 20 bar operation, all the SO_2 will be removed from the 3 stage column. This is a very interesting result. The NO oxidation reaction is a third order reaction and its rate increases with pressure. Therefore, at higher pressures, NO_2 is produced at a faster rate to be utilized by the rapid SO_2 oxidation reaction, requiring lower residence times with increasing pressure. A direct implication of this is that it is therefore possible to achieve both NO_X and SO_X removal in a single column operating at high pressure, say 30 bar. A simulation of a single column operating at 30 bar showed complete SO_2 removal as early as the first stage. Adopting a single column design will also result in savings in process energy requirements [46]– resulting from lower overall pressure drop in the columns - as well as in equipment cost.

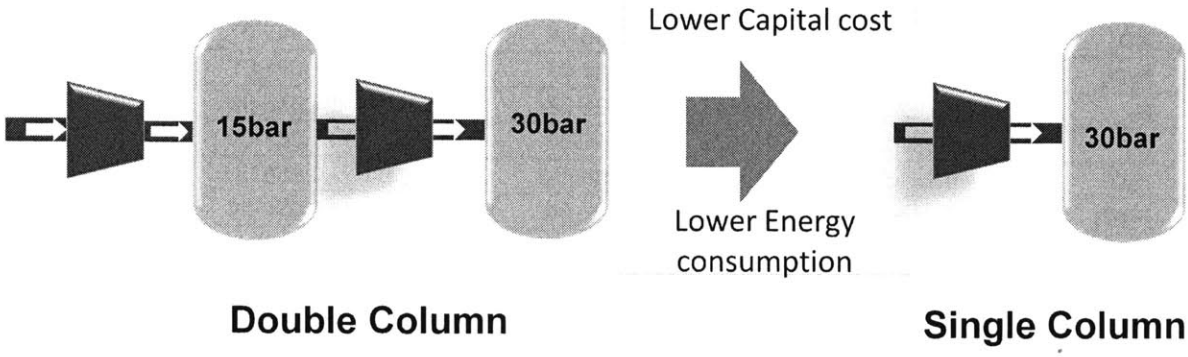

Figure 3.13: Single vs. Double column configuration

The reduction in material cost depend to some extent on whether the eventual composition of the bottoms acid from the single high pressure column is significantly different from that of the low pressure column of the double column setup to warrant additional consideration for construction material. Table 3.9 shows the composition of the exit streams from the two options.

Table 3.8: Single and Double column specs

	Double Column		Single Column
Operating Pressure	**15 bar**	**30 bar**	**30 bar**
Inlet temperature	25C	25C	25C
Vapor holdup per stage	$20m^3$	$20m^3$	$20m^3$
Water flow rate	2kg/s	4kg/s	2kg/s
Number of stages	5	9	7

Table 3.9: Exit Flue Gas Stream data from the two options

	Double Column (15bar)		Double Column (30bar)		Single Column (30bar)	
	Bottoms Liquid	Flue Gas Out	Bottoms Liquid	Flue Gas Out	Bottoms Liquid	Flue Gas out
Total Flow kg/sec			3.47	86.51		
Temperature K	296.19	298.15	291.52	292.47	301.4	298.15
Pressure bar	15	14.76	30.36	30.00	30.4	30
Mole Fraction						

NO	7.41E-07	2.96E-04	7.90E-07	8.28E-06	1.14E-06	9.12E-06
NO_2	-	1.90E-05	1.08E-06	2.25E-06	3.96E-07	2.77E-06
N_2O_4	-	1.91E-08	9.48E-07	1.27E-09	1.04E-07	1.26E-09
N_2	1.10E-06	0.01517	3.93E-06	0.01522	2.63E-06	0.015214
O_2	8.15E-06	0.056525	2.86E-05	0.056491	1.88E-05	0.056465
H_2O	0.921257	3.89E-03	0.989796	1.10E-03	0.956251	1.50E-03
HNO_3	**4.78E-05**	2.20E-10	**4.40E-04**	1.24E-13	**1.03E-04**	6.36E-14
H_3O+	0.041025	-	4.82E-03	-	0.022645	-
NO_3-	**4.15E-04**	-	**4.82E-03**	-	**2.88E-03**	-
CO_2	1.23E-05	0.876503	6.06E-05	0.879429	3.33E-05	0.879072
CO	4.63E-08	4.25E-04	1.63E-07	4.26E-04	1.10E-07	4.26E-04
AR	7.38E-06	0.047171	2.63E-05	0.047327	1.73E-05	0.047308
H_2SO_4	3.21E-12	-	-	-	2.95E-12	-
SO_2	1.72E-04	-	-		-	-
HSO_4-	**0.033496**	-	-	-	**0.016334**	-
SO_4--	**3.56E-03**	-	-	-	**1.72E-03**	-
pH	**0.31839**		**0.375251**		**0.4446627**	

Any value less than 10^{-21} is considered negligible

The results from table 3.9 show that the bottoms stream for the single high pressure (30 bar) column and the first low pressure (15 bar) column are similar in acid composition, though the 30 bar column has more nitric acid. Both also have pH less than 1. Therefore the material requirement for dealing with the acidic liquid in these absorber columns would be similar.

Figures 3.11 and 3.12 show how pressure affects the acid and SO_2 composition as well as the pH of the liquid bottoms stream. The pH is related to the formation and dissociation of sulfuric acid as well as nitric acid in the liquid stream. The SO_2 content of the liquid stream initially increases with pressure since the rate of solution of SO_2 increases with the increased gas-liquid interfacial area which is a function of pressure. However, as pressure increases, more of the SO_2 is consumed to form sulfuric acid, resulting in a drop in direct SO_2 dissolution in the liquid.

3.1.6.2. Holdup Sensitivity analysis

The vapor holdup volume serves as a handle for providing sufficient room and residence time for the rate limited reactions to take place. Increasing the holdup volume results in increased removal of the targeted components. Figures 3.14 and 3.15 show the impact of increasing stage vapor holdup on NO and NO_2 removal from the flue gas stream. At a vapor holdup of about $20m^3$, the NO_X composition falls below the 10ppm required specification for transport and storage and is the value adopted for this model. Increasing the holdup volume further does not result in commensurate increase in degree of removal of the NO_X components. The impact of holdup volume on SO_2 removal is not shown because all the SO_2 is removed at 30 bar for all the holdup values presented.

Table 3.10: Absorber Specs in Holdup Sensitivity Study

No. of stages	9	Operating Pressure	30 bar
Inlet gas temperature	25C	Water flow rate	4kg/s

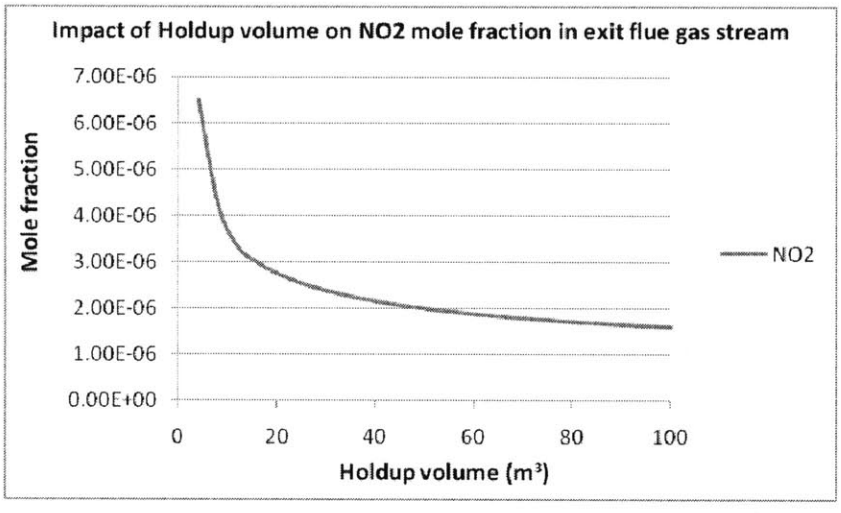

Fig 3.14: Impact of Holdup volume on NO_2 mole fraction

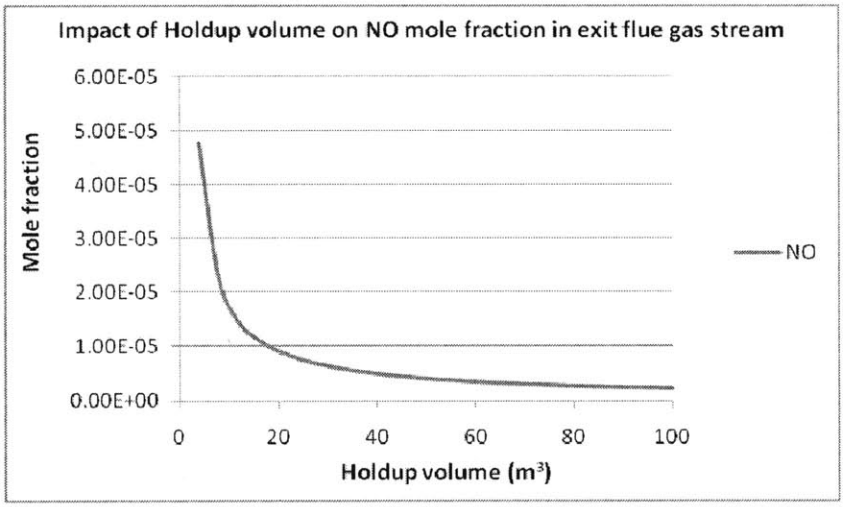

Fig 3.15: Impact of Holdup volume on NO mole fraction

3.1.6.3 Water flow rate Sensitivity analysis

Table 3.11: Absorber Specs in Water flow Sensitivity Study

No. of Stages	9	Operating Pressure	30 bar
Inlet temperature	25C	Vapor holdup per stage	$20m^3$

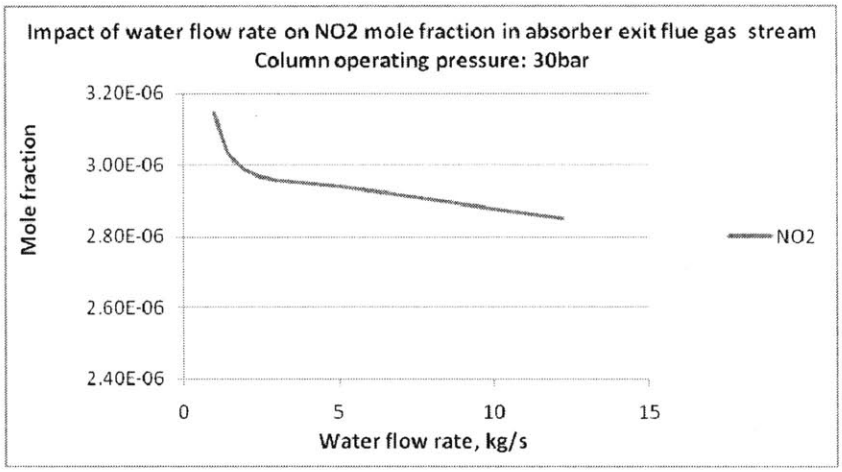

Fig 3.16: Impact of water flow rate on NO_2 mole fraction

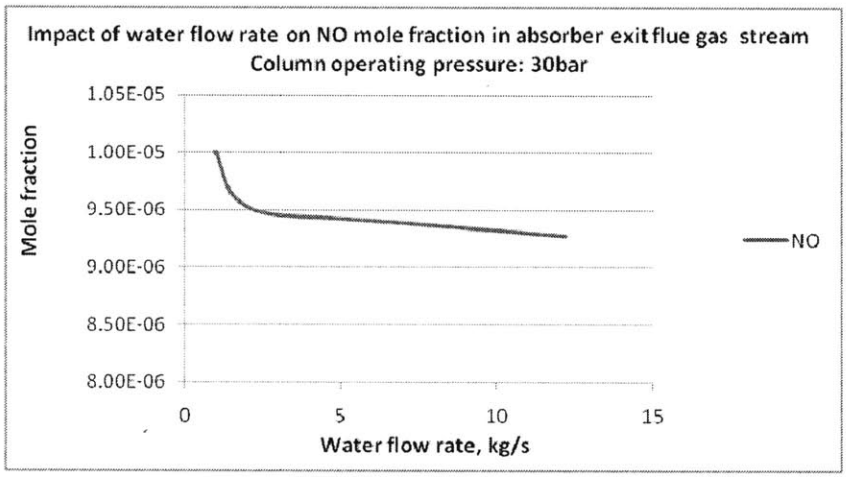

Fig 3.17: Impact of water flow rate on NO mole fraction

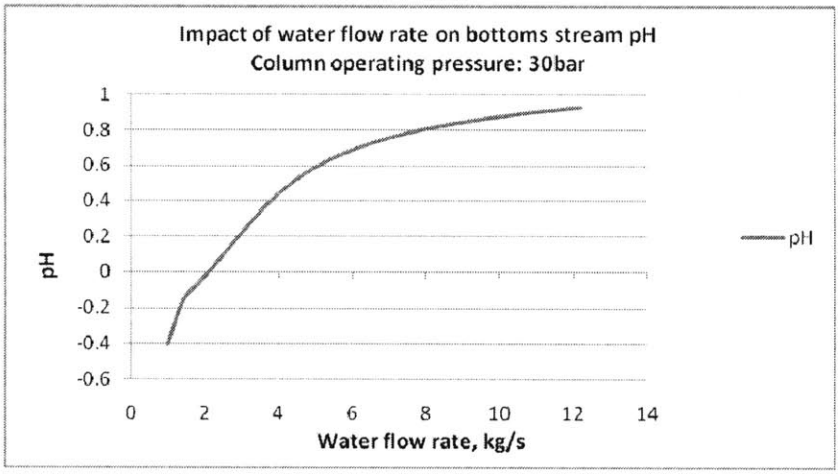

Fig 3.18: Impact of water flow rate on bottoms stream pH

The impact of varying the water flow rate on the performance of the absorber column was also studied. Figures 3.16 - 3.17 show the results obtained. It was found that increasing the water flow rate beyond 2kg/s did not have a significant impact on the composition of the exit flue stream. Figure 3.18 however shows the reason why a higher water flow rate might be considered. For a flow rate of 1kg/s, the pH is as low as -0.4. Doubling the flow rate gives in a pH of about 0.6. Though

the pH range represented is still low, the choice of water mass flow rate into the column will come as a reasonable balance between water consumption and material requirements for the absorber column. Moreover, further recycling of the feed water back into the column will greatly reduce the fresh water requirement, though the acid concentration will be higher.

3.2 Non-condensable Gas Removal Unit

Two configurations (described in chapter 2) were developed for the non-condensable gas removal unit. Configuration A (Auto-cooling) utilizes process stream to provide cooling duty for the system and delivers a high purity gas phase CO_2 which is compressed up to supercritical pressure and subsequently pumped to pipeline pressure (110bar). Configuration B (External Cooling) utilizes an external refrigeration cycle to provide the required cooling duty and delivers a high purity liquid CO_2 stream which is pumped directly to pipeline pressure. The major equipment in the non-condensable gas removal unit are the low temperature distillation column (modeled in Aspen Plus using a Radfrac block) and the heat exchangers.

3.2.1. Thermodynamic Property Method

RK-Aspen property method was selected for this modeling work. This property method is based on the Redlich-Kwong-Aspen equation of state model and is good for modeling mixtures of non-polar and slightly polar compounds [47]. Oxygen is by far the most important non-condensable contaminant because of its stringent transport and storage specification for CO_2. To evaluate the predictive accuracy of the selected property method, Pressure – Temperature – Liquid phase composition – Gas phase composition (PTXY) simulations were carried out for CO_2-O_2 binary

systems and the results compared with literature data from Aage, Zenner and Muirbrook [48-50]. The simulation was run for temperatures ranging from -50C to 10C which covered the range of temperatures expected in the distillation equipment. Some deviation was noticed between the simulation results and the data from literature, especially with respect to composition in the liquid phase. To improve the predictive accuracy of RK-Aspen, the values of the binary interaction parameters were improved by regression using data from the referenced source and some results from this activity are shown in figure 3.19:

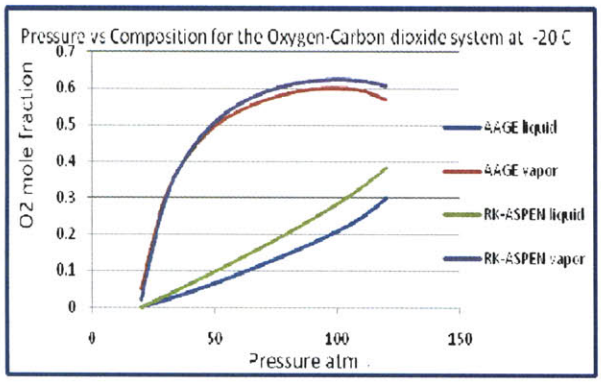

a: Results Before Property Regression @ -20C

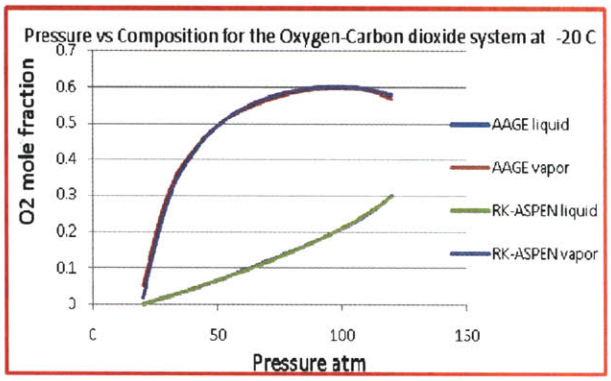

b: Regressed Prediction Results @ -20C

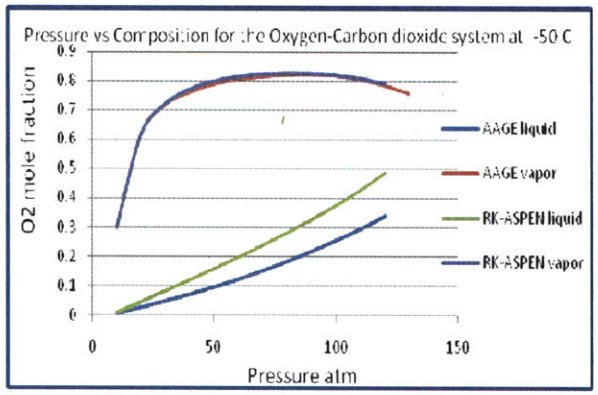

c: Results Before Property Regression @ -50C

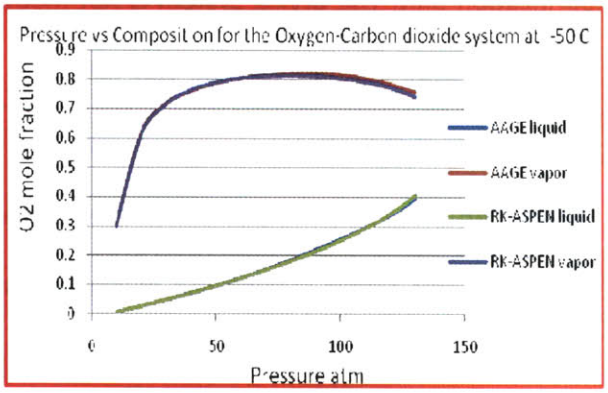

d: Regressed Prediction Results @ -50C

Figure 3.19: Sample Pressure-Temperature-Composition (PTXY) simulation results for CO_2-O_2 binary system

Higher predictive accuracy was achieved by data regression, as shown in the preceding figure. This higher accuracy obtained had the favorable side effect of resulting in a decrease in the number of column stages required for achieving the O_2 parts per million target.

3.2.2. Model Results

Two processes for non-condensable gas removal were developed, both employing low temperature phase separation in a multistage distillation column. Modeling of various strategies to achieve the O_2 target demonstrated that a distillation column is the only practical option for a separation design based on vapor-liquid equilibrium. Pipeline specifications for other non-condensable gases like nitrogen and argon are relatively easy to achieve. The specification for water is typically dependent on the solubility of water in supercritical CO_2. Studies have shown that the solubility of water in supercritical CO_2 increases with pressure and results of about 4000ppm at 40C and 110bar has been published [51].However, in the design presented in this work, it is also likely that the specifications for water will be set by the requirements of the low temperature heat exchangers in this part of the purification unit. The drying system is not modeled in this work since standard high performance molecular sieve dryers exist and can easily be picked off the shelf. For modeling purposes, we assumed the H_2O is almost completely removed in the molecular sieve dryer. The most challenging target then is the 10 parts per million specification for oxygen. Both processes developed are able to achieve this target making use of components selected based on mature technologies. Non-condensable gases make up slightly over 10% of the flue gas stream. This means that about 10% of total compression energy is wasted on gases which we still wish to eliminate from our system. Later

we will show how some of this "wasted" energy is recovered via vent gas expansion. The purified CO_2 stream composition data for the two processes are shown in the table 3.12 alongside the pipeline/storage target specifications adopted for this work.

Table 3.12: Exit stream composition for the non-condensable gas removal process

	Inlet Stream	Configuration A: External Cooling (Exit)	Cofiguration B: Auto-cooling (Exit)	Pipeline Specifications
Phase	Vapor	Supercritical	Supercritical	
Mole Fraction				
NO_X (ppm)	12.2	3.19	3.8	< 20
SO_2 (ppm)	-	-	-	<10
CO_2 (%)	88.03	99.99	99.99	> 95.5
O_2 (%)	5.67	4.28 ppm	4.65 ppm	< 10 ppm
N_2 (%)	1.52	1.4E-01 ppm	2.44E-01	< 4
CO (%)	4.27E-02	8.5E-03ppm	1.25E-02	
AR (%)	4.74	43ppm	28.1 ppm	

A more detailed stream data table for the non-condensable gas removal process is included in Appendix A.

3.3. Conclusion

The complete CO_2 purification Unit with the NO_X & SO_X and the non-condensable gas removal sections was developed and implemented in Aspen plus. All process equipment were sized to match the required performance for handling the flue gas stream from a pressurized oxy-combustion power plant. The performance of the system was analyzed and shown to be consistent with underlying theory. A sensitivity analysis was carried out on the NO_X and SO_X removal unit. Having identified holdup volume, number of stages, water flow rate and pressure as important

control parameters, sensitivity analysis was carried out by fixing the number of stages and varying the other parameters. The study revealed that pressure has a greater impact on column performance than holdup volume and water flow rate. This is primarily because the key rate limiting reaction in the process ($NO + \frac{1}{2}O_2 \rightarrow NO_2$) is heavily pressure dependent. This fact was taken advantage of in redesigning the process to optimize performance while cutting down on cost. The results presented show that replacing the two column process with a single column operating at 30bar achieved same performance and will later be shown to result in cost savings. Higher pressures generally result in better performance for the columns, but negatively impacts energy consumption because of the non-condensable gases. For every KW of energy expended in compressing the gas stream, a fraction (about 10% in this case) is wasted in compressing the non-condensable gases which still have to be removed. However, this can be offset by extracting energy from the vent gas stream, which will be discussed in the next chapter.

Chapter 4 Analysis of Cycle Integration Options

CO_2 purification increases parasitic power demand for the oxy-combustion cycle. This increase is mainly due to the cooling requirements in the process as well as the extra energy for flue gas recompression. Performance improvements can however be achieved by the proper integration of the purification cycle with the base power cycle. Cycle performance can be improved via:

- heat integration of the purification unit with the base cycle
- Energy recovery from the vent gas stream
- material integration between the purification unit and the base cycle

4.1. Integration Options

The only feasible opportunity for heat integration between the purification unit and the base cycle is in reheating the vent gas stream in-between expander stages to increase power output and avoid very low exit temperatures. The impact of this option is not analyzed because it has already been included in the system model. The following options have been considered to possibly offset the power consumption requirement of the purification train, optimize raw material usage and improve overall cycle performance:

- **Reducing ASU oxygen purity requirements:** A look at the stream tables in chapter 3 shows a very low N_2 concentration in the purified stream (5E-8 compared to the 4% transport/storage requirement). This presents the possibility of using a lower purity O_2

from the ASU while still meeting pipeline and storage requirements for N_2. ASU separation power is a function of required oxygen purity and increases with increasing oxygen purity specification as shown in figure 4.1.

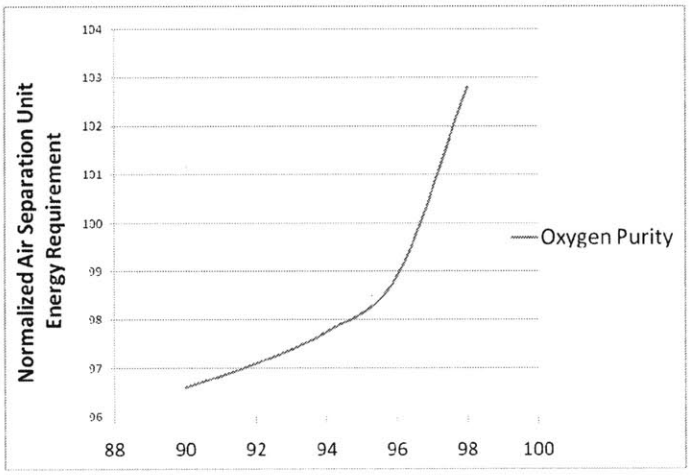

Figure 4.1: Variation of normalized cryogenic air separation unit energy requirement with oxygen purity (100%-energy at 97%-oxygen purity) [52]

- **Total expansion of vent gas from the purification system for power recovery.** This is the case of expanding all the vent gas which leaves the purification unit at a high pressure in order to recover some of the Availability in the stream. This expansion is modeled as consisting of multistage expanders with inter-heating.
- **Partial vent gas recycle:** In this case, a fraction of the vent gas is recycled to the combustor while the rest is expanded to produce power. The recycled vent stream contains about 30% oxygen, 40% CO_2 and 20% Argon. The recycled O_2 will thus reduce ASU power requirement. This option could also provide extra combustor cooling, reduce the recycled flue gas requirement and hence, drop the power consumption of the flue gas recirculation fan.

- **Oxygen recycle:** In this case, oxygen is separated from the vent stream via a membrane and recycled to the combustor. The oxygen-free vent gas is then expanded for power. This would also reduce ASU power requirement though it will require more capital investment for the membrane.
- **Using water from the acid condenser in the absorber columns:** This is possible given that the acid concentration of the condensate from the acid condenser is relatively low. This option has the potential to reduce the overall water consumption for the cycle.

4.2. Results

ASU Oxygen Purity

Figure 4.2 – 4.8 show results from simulation of the integration options. From figure 4.2, we see as expected that reducing the purity requirement of the ASU reduces the ASU separation power[5]. However, the overall ASU power increases as shown in figure 4.3. This is because given that lower oxygen purity implies that the same amount of oxygen is accompanied by a larger amount of nitrogen, the savings in separation power is offset by the additional compression work required to deliver the low pressure oxygen stream leaving the ASU to the combustor at 10bar. Therefore, the overall effect is to decrease the cycle efficiency by about 0.1% for an ASU purity reduction from 95% to 92%. This reduction is depicted in figure 4.4.

[5] For pressurized oxy-combustion, overall ASU power constitutes both the separation energy for delivering oxygen at near atmospheric pressure and the compression power for bringing it up to combustor operating pressure.

Vent Expansion/Recycle

Total vent gas expansion results in a 0.3% increase in overall cycle efficiency by recovering useful work from the high pressure (26 bar) vent gas stream. Total vent expansion is considered as the base configuration. However, extracting some of the vent gas from the vent stream and recycling it to the combustor negatively impacts cycle efficiency. Figure 4.5 shows that vent gas recycle of up to 50% results in approximately 0.1% decrease in efficiency from the value obtained with total vent expansion. The power production/consumption breakdown for the different sections of the process provides some insight into understanding how this came about. From Figures 4.6 and 4.7, one can see that the decrease in cycle efficiency for vent gas recycle results mainly from increased power consumption in the CPU even though it saves on ASU power - ASU power requirement is lower because oxygen is also recycled to the combustor, requiring less oxygen supply from the ASU. Vent gas recycle requires more CPU power because the flue gas stream contains higher impurity fractions. Therefore, larger pressure drops are needed to provide the cooling load requirements of the purification system

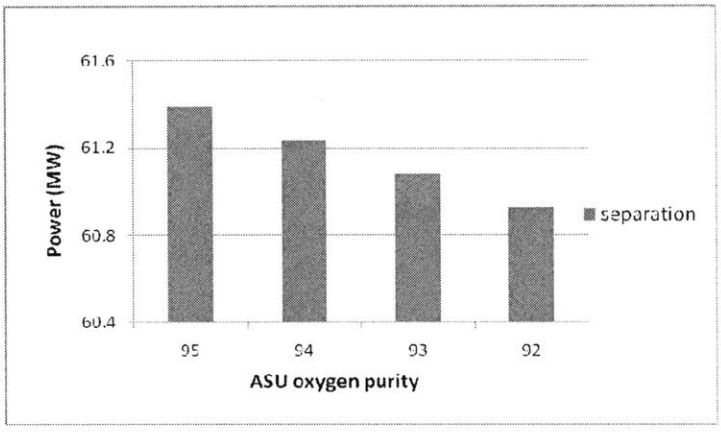

Fig 4.2: Impact of ASU oxygen purity on ASU separation power

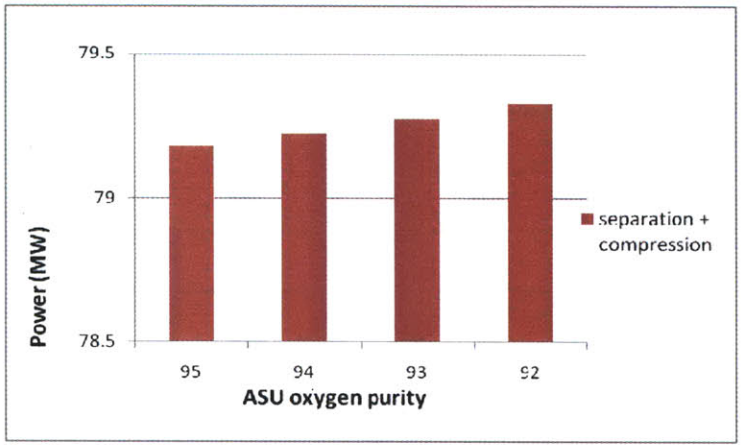

Fig 4.3: Impact of ASU oxygen purity on overall ASU power

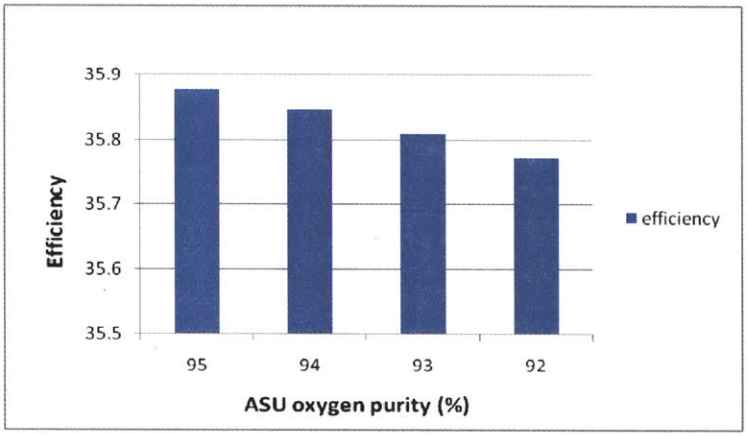

Fig 4.4: Impact of ASU oxygen purity on net cycle efficiency

O_2 Recycle

From an energy perspective, a better option than recycling vent gas is to utilize a membrane to separate out only the oxygen and recycle it to the combustor. This option increases the efficiency by about 0.3% beyond that of the case for total vent gas expansion as shown in figure 4.8.

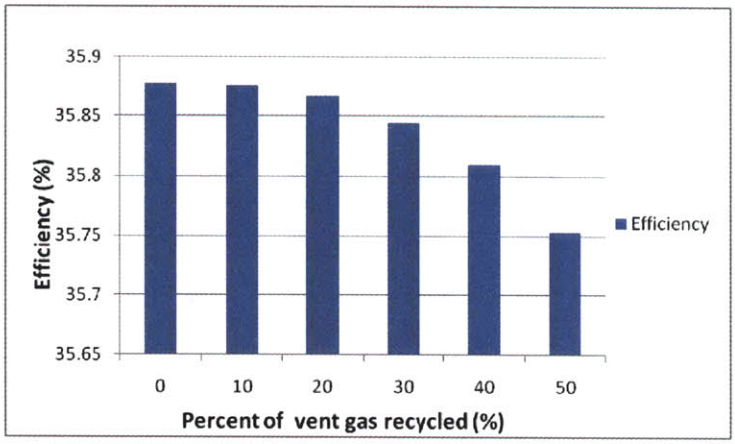

Fig 4.5: Impact of vent gas recycle on net cycle efficiency

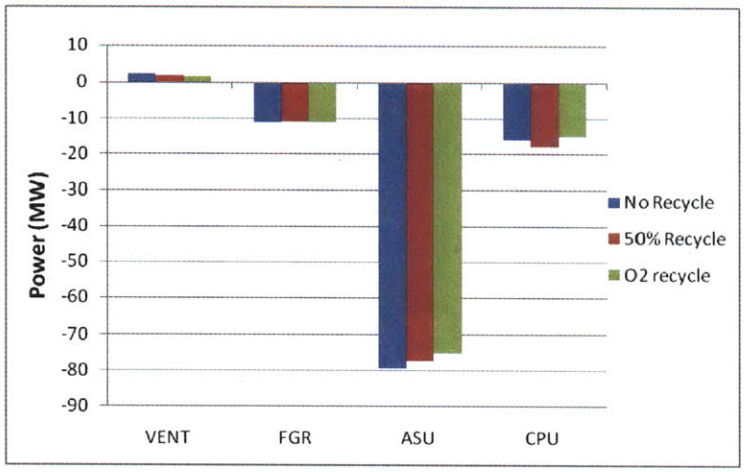

Fig 4.6: cycle power output breakdown by section

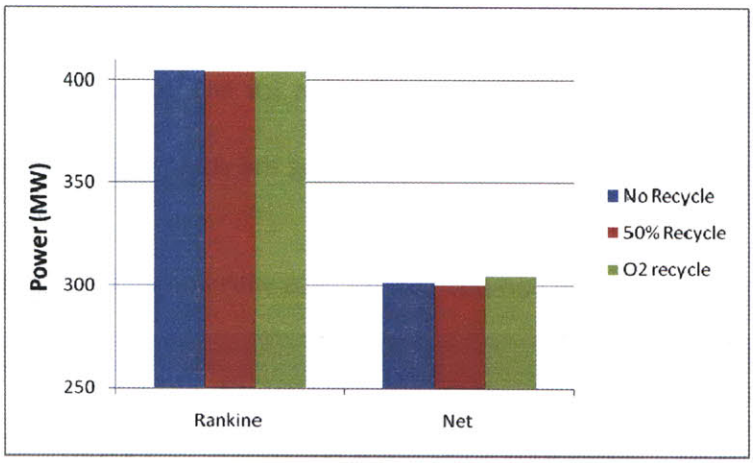

Fig 4.7: cycle power output breakdown by section

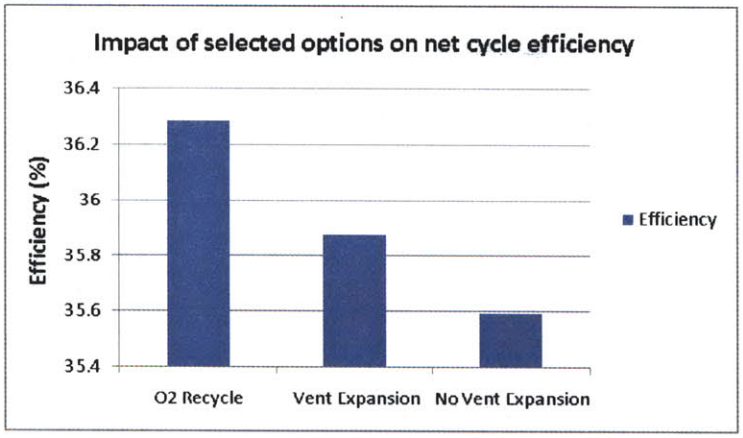

Fig 4.8: Comparison of cycle efficiency for selected options

From the Figures

FGR:	Flue gas recirculation fan work. This makes up for HRSG and recirculation duct pressure drop
VENT:	This is the recovered work from vent gas expansion
ASU:	Total power consumption in the Air Separating Unit (separation + compression power)
CPU:	Power consumption in the CO_2 Purification Unit
Rankine:	Total power output from the steam cycle

Acid water Reuse

Table 4.1 compares the exit stream composition for the absorber columns for the cases with and without the use of acid water from the acid condenser. Using the same configuration for

fresh water operation, the performance of the column when operating with acid water does not quite achieve the parts per million specification for NO. In this case, this target can be achieved by including an additional stage or increasing the stage vapor holdup volume.

Table 4.1: Exit stream composition for case with and without acid water

		Exit Flue gas composition		Bottoms liquid composition	
	Acid water composition	Using Acid Water	Using Fresh Water	Using Acid Water	Using Fresh Water
NO	3.07E-07	1.33E-05	9.25E-06	7.82E-07	7.79E-07
NO_2	6.79E-07	7.38E-07	2.80E-06	6.62E-07	6.57E-07
N_2O_4		8.95E-11	1.31E-09	4.20E-07	4.07E-07
N_2	1.27E-06	0.015214	0.015215	1.81E-06	1.81E-06
O_2	8.84E-06	0.056462	0.056464	1.29E-05	1.29E-05
H_2O	0.999409	1.50E-03	1.49E-03	0.91675	0.917505
HNO_3		1.34E-13	2.61E-13	2.86E-03	2.84E-03
H_3O+	2.16E-04			0.040725	0.040355
NO_3-				3.04E-03	3.08E-03
CO_2	3.24E-06	0.87907	0.879082	1.91E-05	1.92E-05
CO	5.18E-08	4.26E-04	4.26E-04	7.54E-08	7.54E-08
AR	7.91E-06	0.04731	0.04731	1.19E-05	1.19E-05
H_2SO_4	7.27E-17			2.07E-11	2.12E-11
SO_2	1.43E-04				
HSO_4-	5.71E-06			0.035267	0.035065
SO_4--	7.31E-06			1.11E-03	1.10E-03
SO_3--	1.30E-09			1.30E-09	
HSO_3-	1.96E-04			1.98E-04	

Any value less than 10^{-21} is considered negligible

Table 4.2: Simulation Column Specs

Inlet temperature	Vapor holdup per stage	Water flow rate	Number of stages
25C	$20m^3$	2kg/s	9

4.3. Conclusion

The CO_2 purification unit adds to the parasitic power demand of the oxy-combustion cycle. The analysis performed showed that opportunity exists for offsetting this power consumption requirement by proper integration of the CPU with the power cycle. Energy can be recovered from the high pressure vent gas by expanding it in turbo-expanders. Given that the CPU vent gas stream is at a relatively low temperature, better performance can be achieved by staging the expansion and reheating the gas via compressor intercooling. Further improvement in performance can be achieved by selectively extracting oxygen from the vent stream and recycling it to the combustor to offset ASU oxygen requirement. However, all these incremental improvements amount to a total of about 0.7 points increase in efficiency. This gain will have to be measured against the associated cost (e.g., the cost of a membrane for O_2 separation).

In addition, water use can be improved by utilizing acid water from the acid condenser and thereby avoiding the use of fresh water in the absorber columns of the CPU.

Chapter 5 Cost Estimation

5.1. Overview

The CO_2 purification unit (CPU) for the oxy-combustion plant constitutes an additional cost to the base power plant. Therefore estimating the cost of this process becomes necessary in analyzing the economic viability of the overall oxy-combustion system. The CPU presented in this work consists of the acid removal section (double column configuration or single column configuration) and the non-condensable gas removal section (Auto cooling configuration A or external cooling configuration B). These can be combined to give four possible options for the CPU configuration:

Option A Double column acid removal with auto cooling configuration for non-condensable gas removal

Option B Double column acid removal with external cooling configuration for non-condensable gas removal

Option C Single column acid removal with auto cooling configuration for non-condensable gas removal

Option D Single column acid removal with external cooling configuration for non-condensable gas removal

In this section, we estimate the purification unit costs for each the four options in order to perform a comparative cost analysis. The absolute cost figures presented are design estimates and are useful as a process engineer's estimate prior to detailed engineering of the system.

5.2. Methodology

A bottom-up cost estimation approach is adopted in this study. Based on data from the process model, each process equipment is sized and its cost is then estimated. Installation costs are applied to each component and the results are summed up to give the total equipment cost. Then other costs (e.g. site preparation, labor, materials, etc) and factors (e.g. escalation, contingency, etc) are applied to determine the overall capital cost for the process. Equipment sizing and cost estimation is handled mainly by Aspen Process Economic Analyzer™ which is integrated with Aspen Plus™ and is able to read most process and equipment performance data directly from Aspen Plus™. Bulk materials and related labor costs for the installing the equipment were determined following the Association for the Adcancement of Cost Engineering AACE recommended standard [53] which can also be found in the DOE/NETL cost estimation report[54]. All capital costs were escalated to January 2009 dollars. The total project cost determined is also compared with data from Air Products on the CO_2 purification unit cost (which had already been scaled down and escalated to January 2009 USD value by Hong [55]). Details of the underlying cost assumptions are presented in section 5.4. The sizing and costing strategy for different equipment categories are presented next.

5.2.1. Pressure vessels, Compressors and Turbines

Equipment performance and process stream data are transferred directly from Aspen Plus™ to Aspen Economic Analyzer™ which is then used to to size and costs the equipment item.

5.2.2. Shell and Tube Heat Exchangers

Equipment performance and process stream data are transferred directly from Aspen Plus™ to Aspen Economic Analyzer™. Aspen Economic Analyzer™ is integrated with Aspen Exchanger Design

and Rating™ and uses this capability to size the exchanger. It costs the equipment based on the size data which includes number of tubes, tubve length, shell dimensions, etc.

5.2.3. Multi-stream Plate-Fin Heat exchangers

Equipment performance and process stream data are externally transferred from Aspen Plus™ to Aspen Muse™ for sizing since there is currently no integration between Aspen Muse and the other Aspen packages in the version used. Determining the cost of Plate-fin exchangers presented considerable challenge. The current version of Aspen Economic Analyzer™ does not evaluate the cost of Plate-fin exchangers. There is also very limited, publicly available data on cost/cost correlations for these multi-stream plate exchangers. In this study, cost data (provided as $/heat transfer area) from Lunsford [56] and Polasek et al [57] were used to cost these exchangers. The calculated costs were escalated to 2009 using the CEPCI index.

5.2.4. Molecular Sieve Dryers

Molecular sieve dryers are not part of the Aspen Economic Analyzer™ equipment library. Therefore, this equipment was first evaluated as a dual tower desiccant air dryer operating at atmospheric pressure. Then a pressure factor as well as a material factor applied to determine the expected cost. Vendor data for the cost of the molecular sieve desiccants was also included. The pressure and material factors were obtained from ASME standards for pressure vessels[58] and the DOE/NETL cost estimation report [54]

5.3. Material Selection

Selecting the appropriate materials for the different sections of the CO_2 purification unit is essential to ensure performance reliability and eliminate or grossly reduce chances of part failure. Given that different parts of the system operate under very different conditions, care must be taken in identifying suitable materials for each unique condition. The general criteria applied in selecting materials considered three main aspects:

- Flue gas composition
- Acid corrosion
- Operating temperature

Based on these criteria, the equipment for the CO_2 purification unit are broken down into the SO_2 equipment, acid equipment, low temperature equipment and others. The corresponding materials for these equipment are determined based on recommendations from literature and known properties of selected materials.

5.3.1. SO_2 Equipment

SO_2 equipment refer to the CO_2 compressor and other accessories between the acid condenser and the NO_X and SO_X absorber column and in the case of the double column acid removal process, also includes the compressor between the two absorber columns. The compressor is susceptible to corrosive attack from wet CO_2, SO_2 and perhaps some carry-over SO_3 mist. Wilkinson et al [59]suggested the use of G X5 Cr Ni 13.4 (1.4313) stainless steel for casting the volutes and X 6 Cr Ni Ti 8.10 (1.4541) for the intercooler shells, tubes and piping. Thomas et al [60] suggested the use of the corrosion resistant alloy 20CB-3 (Carpenter Alloy®) austenitic stainless steel for impact areas

or cold areas such as volutes, impeller, intercoolers and internals. The latter was selected for compressor costing in this study.

5.3.2. Acid Equipment

The primary component in this section is the absorber column with all its accessories. The absorption process in the column as described in previous chapters results in the removal of SO_X and NO_X as sulfuric and nitric acid. The model results presented show that the pH of the absorber liquid is very low so the absorber environment is expected to be very aggressive. An interesting characteristic of this system is that both sulfuric and nitric acid are produced in the absorber. This raises both a challenge as well as a potential advantage. The challenge is that the mixture of the two acids can create local oxidizing and reducing conditions, requiring a material with resistance to a broad range of aggressive environments. Furthermore, the potential presence of halides raises the corrosion resistance requirement. On the other hand, the mixture of nitric and sulfuric acid results in passivation of the metallic surface, increasing the corrosion resistance of the metal. This was verified experimentally by Adugina et al [61]. However, to stay on the safe side, the choice of materials in this study was conservative. Based on results of experimental comparison of the corrosion resistance of some stainless steel metals presented by Shoemaker et al [62], the material selected for the absorber shell cladding and trays is Alloy 686 (Iconel®). Iconel alloy 686 was shown to be very stable in highly corrosive environments subject to aggressive attack from sulfuric and nitric acid with high halide concentration (which is not the case for our system). Its high nickel and chromium content provide protection from reducing and oxidizing media respectively and is

maintains high resistance to very low pH (< 1) media [63]. Carbon Steel was specified for the Absorber column shell material.

5.3.3. Low Temperature equipment

The affected components include the low temperature heat exchangers, the distillation column, flash vessels and compressors associated with the non-condensable gas removal section. These components typically operate at temperatures ranging from -8C to -45C. Possible materials are typically limited to austenitic stainless steels which do not become brittle at low temperatures. For heat exchangers operating below -15C, shell and tube materials selected were typically A516 and 304 respectively (in most cases, the tube contained the hot fluid while the shell had the cold fluid). Other materials like A333C and A179 were also considered. For other components, A516 was typically used for operating temperatures below -10C. Aluminum was also considered as an option for plate-fin exchangers. See footnote for references consulted in making these selections[6].

5.3.4. Others

Carbon steel was used for all other equipment items which did not fall under the previous classifications. The choice of carbon steel even for the compression/pumping of the purified CO_2 stream to supercritical pipeline pressure is largely based on the studies which showed that the corrosion rate of carbon steel in dry supercritical CO_2 is low [64]. The process design already incorporates a molecular sieve dryer which is used to reduce the water fraction way below the pipeline transport and storage specifications. Therefore, we do not expect any danger from

[6]Some references consulted for metal properties
http://www.astm.org/Standards/A179.htm
http://www.aec-design.com/EN/pdf/A179-1250M3.pdf
http://www.keytometals.com/articles/art61.htm

corrosion by wet CO_2. Typical material choices made for different equipment groups are shown in figure 5.1.

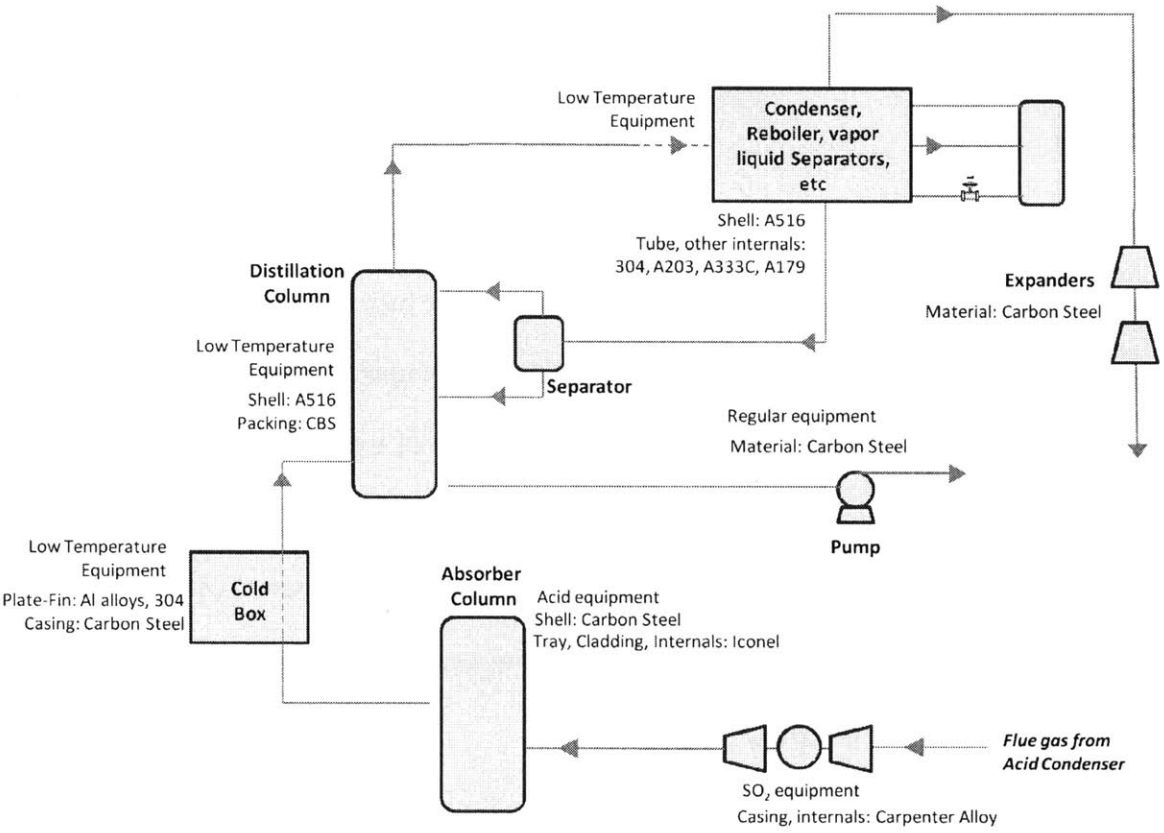

Figure 5.1: Material Selection Summary for CO_2 Purification Unit

5.4. Cost Estimation Basis

5.4.1. Basis for capital cost

The cost basis for the CO_2 purification process presented in this study was based on AACE recommended standards and DOE/NETL cost estimation report. The equipment cost estimate was evaluated using Aspen Economic Analyzer. The bulk material and labor costs were evaluated using

AACE recommended factors for gas processes. The first year of plant construction is assumed to be 2009 and the capital and O&M costs are expressed in January 2009 dollars. The project site is generic with no special conditions. The design is based on ASME standards. Labor costs are based on North American Midwest values and is based on a 50-hour week. No additional incentives were specified.

The process is considered as a new process since no commercial scale demonstration exists. In Aspen, process complexity is specified as high because of the high pressures, low temperatures and tight thermal integration required. The above specifications impact the design allowance applied to the process equipment (15%). The overall process contingency is set to 25%. This is in line with the AACE international contingency guideline presented in the NETL "Quality guidelines for Energy System Studies" report which recommends 20-40% as the range for new technology with little or prototype test data [65]. Table 5.1 summarizes the capital cost estimation methodology and parameters selected for this study

Table 5.1: Major Capital Cost Estimation Parameters

Equipment material and setting cost	Aspen Economic Analyzer™
Bulk labor and material costs	AACE Recommended Practice [53] DOE/NETL Report [54]
Sales Tax (average value)	7% of Equipment cost
Indirects on Labor	115% of Bulks
Contractor Engineering costs	20% of Direct Costs
Contingency	25%
Operating life of Project	30 years

Economic life of project	20 years
Project Capital Escalation	5% per year
Raw Material Escalation	3.5% per year

5.5. Cost Estimation Results

5.5.1. Results Discussion

Figure 5.1 shows the overall specific capital cost ($/KW) for the CO_2 purification systems computed for the four different purification strategies listed in section 5.1. As already stated, the base oxy-combustion plant is a 400MW (gross) power plant with a 30kg/s coal feed rate. This base cycle has been described in detail by Hong et al [55]. The overall Specific capital cost includes equipment material and setting costs, all associated installation costs, instrumentation, contingency, as well as sales tax and other indirect costs.

As can be seen from figure 5.2, Option A involves the highest capital expenditure (about $308/KW) while Option D has the lowest capital cost ($246/KW). This difference arises from two factors; The first is that Option A utilizes the double column setup for NO_X and SO_X removal while Option D uses the single column process. This constitutes a significant cost difference because the absorber tower used here requires special cladding, tray and drainage materials. Specifically, Iconel™ was specified because of its resistance to reducing and oxidizing acid environments which is expected in this process. The use of this material adds significantly to the cost of the absorber tower and accessories which come in contact with the acid. The second contribution to the cost difference is the non-condensable gas removal process adopted for each of the options. Option A employs the

Auto-Cooling process and is able to provide most of the required cooling duty from the expansion of the process fluid. However, this option delivers the purified CO_2 stream in the gas phase, requiring a train of compressors to raise it to supercritical pressures before employing a pump. Also, the level of heat integration involved requires the use of customized multi-stream cold boxes which also add to the cost of the process. Option D utilizes an external refrigeration cycle to provide most of the required cooling. Though this involves a larger cost for the refrigeration, it eliminates all the compressors in the compression train since it delivers the purified CO_2 as liquid which is then pumped directly to pipeline pressure.

Figure 5.3 to 5.5 present equipment cost break-down for the CO_2 purification unit by category. Note that this cost is only for the equipment materials, setting and installation. Figure 5.3 presents a break down based on the different sections of the purification process while figures 5.4 and 5.5 categorize the cost by equipment type. This is done for each of the four options and the combined results are shown in the figures. Table 5.2 identifies the major equipment groups contained in each of the process sections.

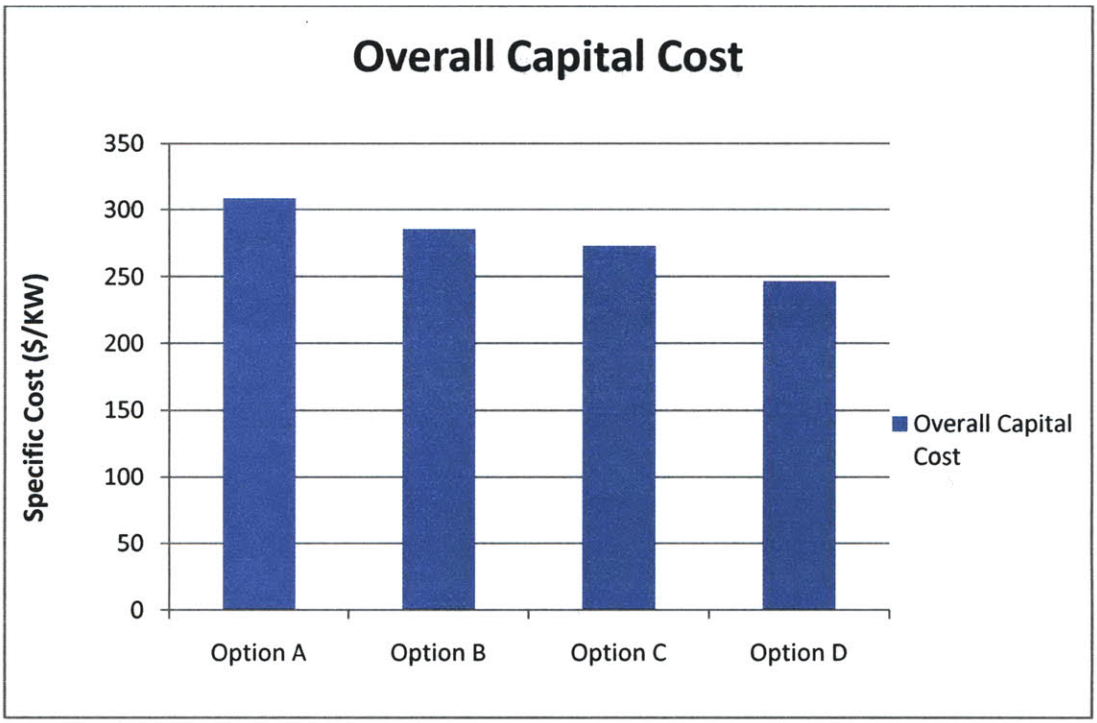

Figure 5.2: Overall Capital Cost For the CO_2 Purification Process Options A to D

We can see from figure 5.3 that the largest proportion of the capital investment is accounted for by the NO_X and SO_X removal section because of the special material requirements for acid handling. For options B and D, the compression train cost is seen to be very small because the CO_2 stream only requires pumping. The Vent gas power recovery section basically comprises re-heaters and expanders for power recovery from the high pressure vent gas. Figure 5.4 and 5.5 show that the pressure changing equipment (compressors and pumps) contribute the most to capital cost, followed by the towers and then the heat transfer equipment.

Table 5.2: Major equipment categories in CPU Sections

NO_X & SO_X Removal	Non-condensable Gas Removal	Compression Train	Vent Gas Power Recovery
Absorber Towers and Accessories	Distillation Column	Compressors	Heat exchangers
Compressors	Cold boxes/Heat Exchangers	pumps	Expanders
Molecular sieve Dryer	Refrigeration Unit		
	Pressure Vessels		
	Reboiler/Condensers		

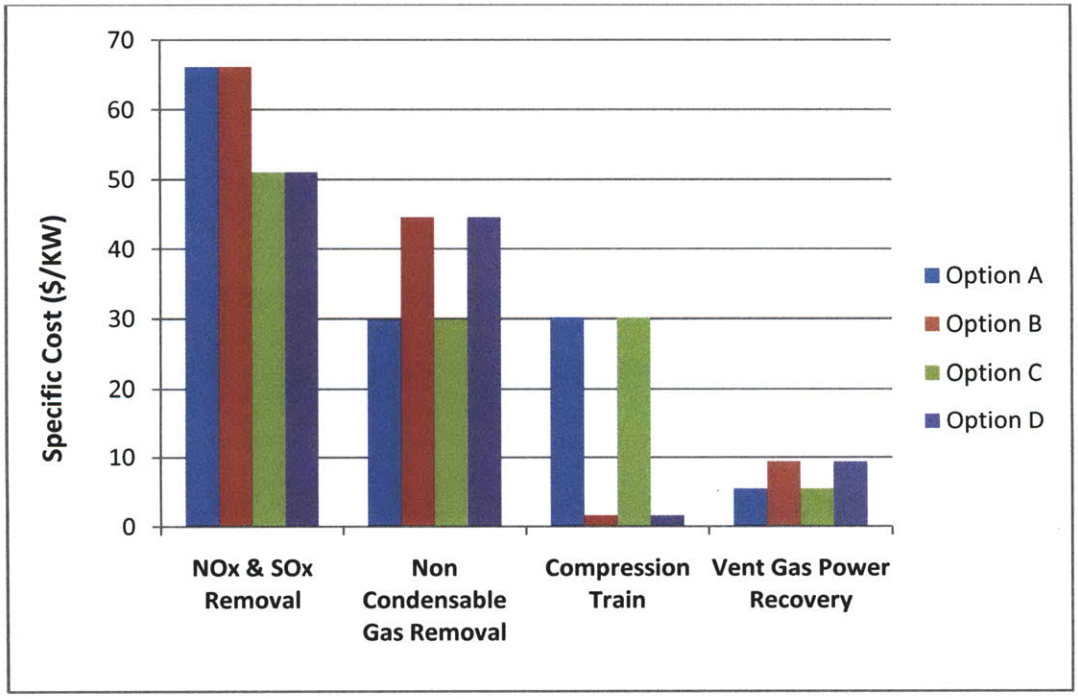

Figure 5.3: Capital Cost Breakdown by CPU Section

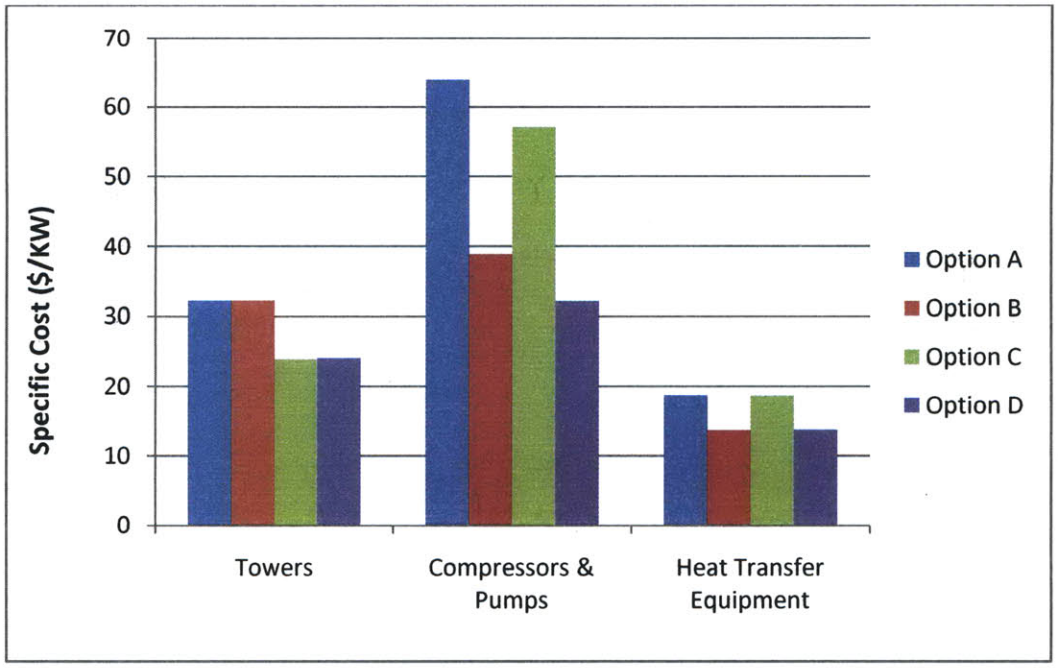

Figure 5.4: Capital Cost Breakdown by Equipment Groups

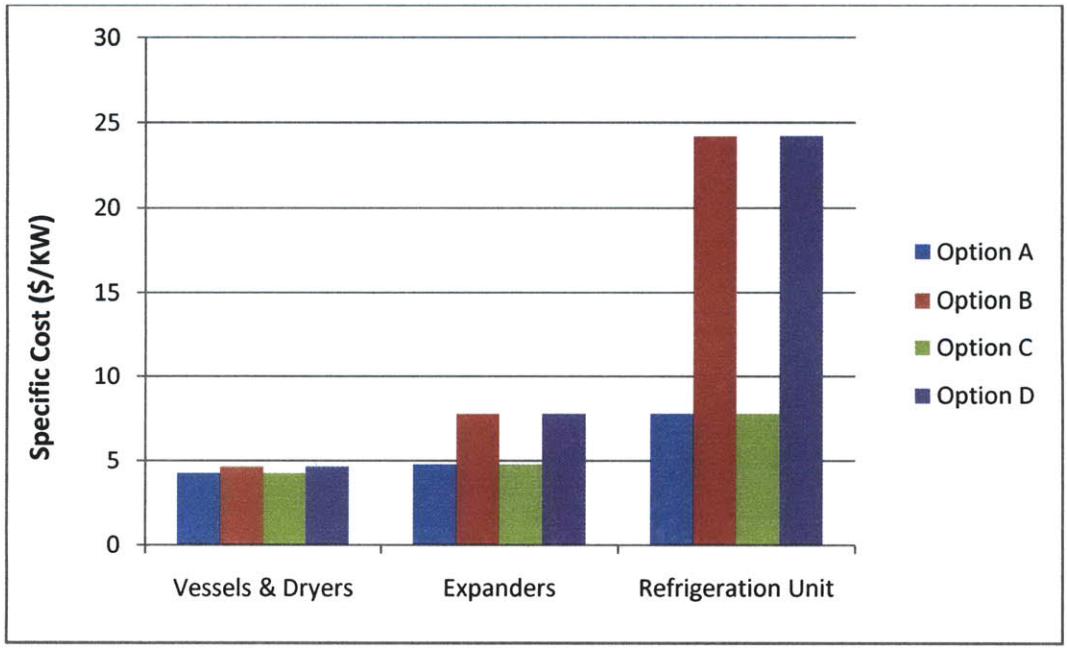

Figure 5.5: Capital Cost Breakdown by Equipment Groups continued

5.5.2. Cost Comparison

To get a better sense of where our cost estimates lie compared to other estimates for flue gas purification systems, we compare the capital cost estimate from this study to some reference estimates for CO_2 purification. The estimates selected for comparison include the CO_2 purification unit estimate for pressurized oxy-combustion by Hong [55], CO_2 purification unit estimate for atmospheric oxy-combustion by NETL and post combustion flue gas purification and CO_2 capture system estimate for an air-fired power plant also by NETL. The base power plant for each of these systems has a gross power output of 400MW and calculated values were escalated to January 2009 when necessary. The capital cost estimates are presented in table 5.3 and depicted graphically in figure 5.6.

Table 5.3: CO_2 Purification Unit Capital Cost Comparison

	Overall Capital Cost ($/KW)
NETL Air-fired System	913
NETL Atmospheric Oxy-fuel	514
Hong (MIT-ENEL)Pressurized Oxy-fuel	448
Auto Cooling CPU	272-308
External Cooling CPU	247-284

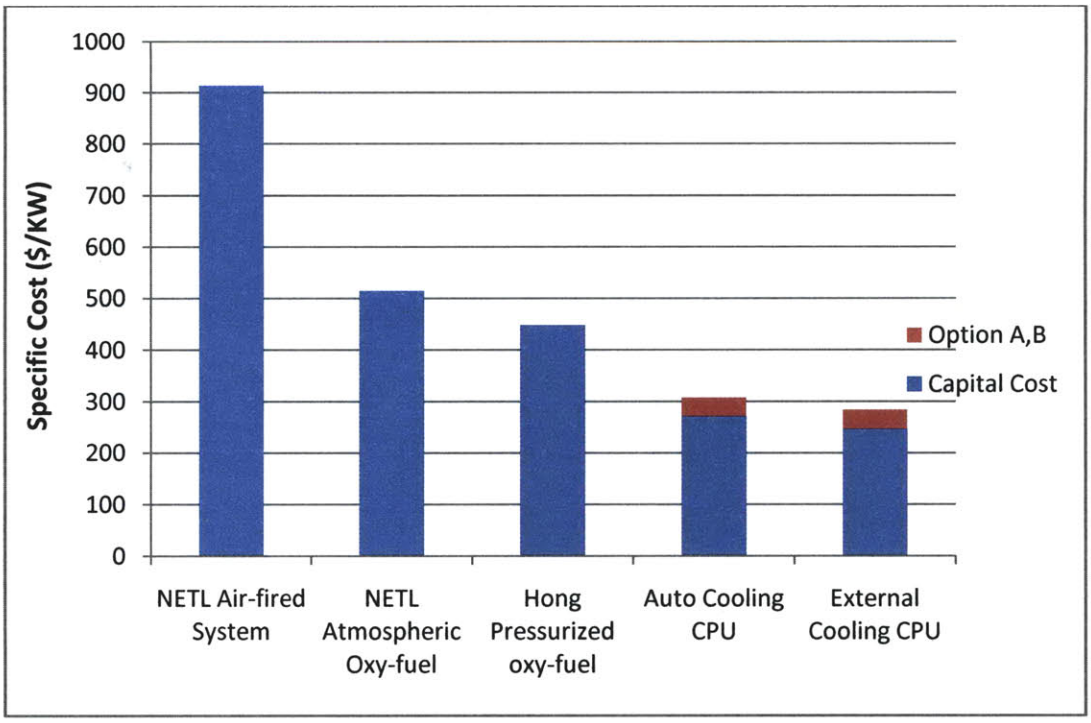

Figure 5.6: CO_2 Purification Unit Capital Cost Comparison

Figure 5.6 shows that the capital cost estimates from this study for the Auto and External Cooling processes is significantly lower than that of Hong for a similar pressurized oxy-combustion system. There might be a number of reasons for this. First is that the estimates arrived at in this study are design estimates with an error margin of about -15% to +35%. Secondly, this estimate was based on sizing the individual components of the CO_2 purification unit in Aspen and determining the overall capital cost from there. The study presented by Hong obtained cost estimate from literature which is based on a system that might have a different process setup than ours. Thirdly, the estimate presented in this study does not include the cost of valves, connectors, separators, acid handling equipment, and site preparation beyond the equipment installation space. In addition, the level of optimization of the CPU processes might also be different. Finally, the choice of 25% for

contingency provides a conservative estimate. Given the novelty of the process, higher values like 35% could be used. Based on the costing assumptions made for this study and taking into account the error margin, the estimates presented here for the Auto and External Cooling processes are consistent and expected to be within the right ballpark. It can also be seen from the figure that the estimate for the Auto and External Cooling processes are much lower than that for an air fired system. This is largely because the pressurized oxy-combustion system deals with a much smaller flue gas volume and also does not require the installation of expensive traditional FGD and SCR and Amine systems in the purification train.

5.6. Conclusion

The cost estimate results for the NO_X and SO_X removal unit show that moving from the double column to the single column setup results in about 12-14% savings in overall CPU capital cost. The single column setup eliminates the additional cost associated with a second absorber column and compressor. This is particularly significant given that these equipment require special acid resistant material that adds to the cost of the plant. Also, the External Cooling concept for the non-condensable gas removal section results in a 7-9% saving in overall CPU cost compared to the Auto Cooling process. The chief contributor to this savings is the elimination of a relatively expensive compression train even though it comes at the cost of a larger refrigeration unit. It also utilizes fewer multi-stream cold boxes compared to the Auto Cooling model.

Chapter 6 Conclusion

6.1. Summary

An analysis of the CO_2 purification process developed for an oxy-combustion power system has been presented. NO_X and SO_X removal is achieved via the use of reactive absorber columns operating at elevated pressure while other non-condensable gases are removed in a low temperature multistage distillation column. The process developed is capable of delivering high purity CO_2 that meets pipeline and storage requirements at lower cost and lower energy penalty than traditional technologies. Sensitivity analysis conducted on the NO_X and SO_X purification system to determine the effect of key control parameters showed the impact of operating pressure, water flow rate and column stage holdup on the performance of the system. From the sensitivity results, ideal operating parameters as well as optimal process configurations which resulted in improvement over the base case were identified. A number of options for integration with the base power cycle were explored and the marginal impact of each on overall process performance was presented. The preliminary cost analysis provided a refined estimate of the capital cost for the purification system and identified the key components that are the major cost drivers in the process.

6.2. Future Work and Challenges

6.2.1. Detailed Kinetics for NO_X and SO_X removal

The process employed for the removal of NO_X and SO_X from the CO_2 stream utilizes the lead chamber and nitric acid chemistry. The lead chamber chemistry, especially as it applies to the conditions encountered in CO_2 purification, is not fully understood and there is sparse documentation on the reaction pathways and reaction rates involved. In particular, the SO_2 oxidation reaction in the presence of NO_2 and H_2O is assumed to be an equilibrium reaction relative to the NO oxidation reaction in the model. The major limitation of this assumption is that at higher pressures, the rate of the NO oxidation reaction increases significantly and this increase will result in a decrease in the relative rates of the two reactions. Therefore, at pressures higher than those presented in this study, this assumption will likely to be called into question. More accurate results will be obtained if the actual rate of the SO_2 oxidation reaction(s) were known and included in the model. In addition, knowledge of the reaction mechanism will provide the model with the capacity to predict more accurately the composition of the acidic liquid leaving the column. Therefore, there is need for further investigation to determine, with the aid of experimental measurements, accurate reaction mechanisms and associated reaction rates for the process.

6.2.2. Cycle Integration

Several integration options with the base power cycle have already been analyzed to determine their impact on overall cycle performance. However, some other options for integration exist and need to be studied. One such option is the use of supercritical CO_2 obtained from the purification

process for delivering the coal to the combustor, instead of the water slurry feed strategy currently employed. This reduces the water demand for the overall oxy-combustion cycle and should be evaluated to see if it also yields efficiency improvements.

6.2.3. Acid Disposal

The disposal of the dilute acidic water from the purification system was not discussed in detail in this study. One of the possibilities already mentioned is the partial recycle of the acidic liquid for reuse in the column. This still leaves the question of what to do with the balance dilute acid that is not reused. A major opportunity involves the use of dilute acid in lignocellulosic biomass pretreatment for biofuel applications. This pretreatment is necessary to liberate the cellulose from the lignin so as to facilitate subsequent hydrolysis of the cellulose. Dilute acid hydrolysis has been used successfully for the pretreatment of a wide range of biomass feedstock [66]. Therefore, the possibility of using dilute acid from the purification system in biomass pretreatment is worth investigating. The potential challenges which will need to be addressed include the impact of the presence of other components in the acid stream on its usability and the economics of the strategy (whether it requires collocation of the biofuel and oxy-combustion plant to be economically beneficial).

6.2.4. Cost Estimation

The cost estimates presented in this study are still preliminary and require updating. Some of the special pieces of equipment like the multi-stream cold boxes could not be sized in Aspen Plus® and cost data for these equipment are sparse and often dated in open literature. Access to more

accurate cost data for these equipment will improve the capital cost estimate. In addition, the underlying basis for material selection and capital cost estimation need to be validated by further comparison with other published cost estimates for similar systems.

6.2.5. Process Optimization

Two processes were developed for the removal of non-condensable gases from the CO_2 stream using different strategies. There is still room to come up with alternative process configurations and to optimize the performance parameters of the existing processes in order to minimize the energy penalty involved.

Appendix Sample Stream Data for Non-condensable Gas Removal Process

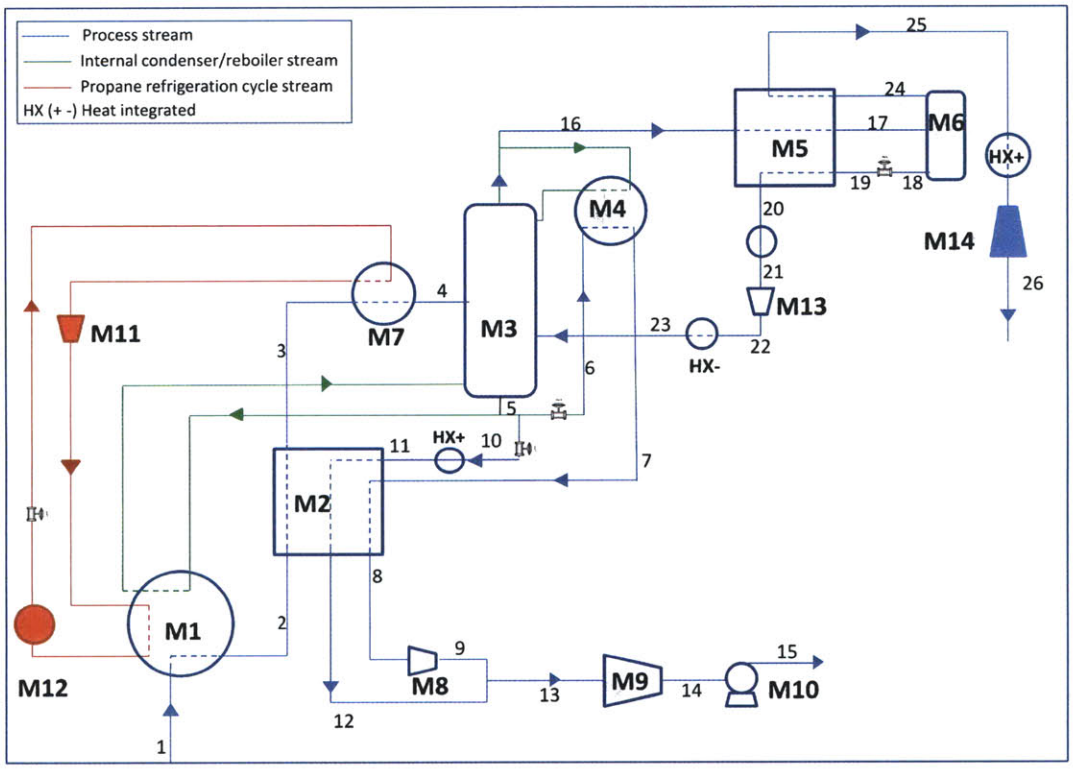

Figure A1: Non-Condensable Gas Removal Unit – Configuration A

Table A1: Stream Data for Non-condensable gas process A

	1	2	3	4	5	6
Total Flow kg/sec	86.47	86.47	86.47	86.47	70.70	43.87
Temperature C	27.92	-6.33	-15.63	-23.00	-8.52	-30.63
Pressure bar	28.60	28.60	28.50	28.50	27.80	14.00
Vapor Fraction	1.00	1.00	0.70	0.34	0.00	0.16
Phase	VAPOR	VAPOR	MIXED	MIXED	LIQUID	MIXED
			Mole Fraction			
NO	9.83E-06	9.83E-06	9.83E-06	9.83E-06	2.95E-09	2.95E-09
NO_2	2.98E-06	2.98E-06	2.98E-06	2.98E-06	3.74E-06	3.74E-06
N_2O_4	1.37E-09	1.37E-09	1.37E-09	1.37E-09	1.72E-09	1.72E-09
N_2	0.0152	0.0152	0.0152	0.0152	2.44E-07	2.44E-07
O_2	0.0565	0.0565	0.0565	0.0565	4.65E-06	4.65E-06
CO_2	0.8804	0.8804	0.8804	0.8804	0.99996	0.99996
CO	4.27E-04	4.27E-04	4.27E-04	4.27E-04	1.25E-08	1.25E-08
AR	0.047379	0.047379	0.0474	0.0474	2.81E-05	2.81E-05

Table A1 continued.

	7	8	9	10	11	12
Total Flow kg/sec	43.87	43.87	43.87	26.82	26.82	26.82
Temperature C	-30.63	-12.00	22.67	-16.89	-16.88	-12.00
Pressure bar	14.00	14.00	21.76	21.76	21.76	21.76
Vapor Fraction	0.90	1.00	1.00	0.07	0.25	1.00
Phase	MIXED	VAPOR	VAPOR	MIXED	MIXED	VAPOR
			Mole Fraction			
NO	2.95E-09	2.95E-09	2.95E-09	2.95E-09	2.95E-09	2.95E-09
NO_2	3.74E-06	3.74E-06	3.74E-06	3.74E-06	3.74E-06	3.74E-06
N_2O_4	1.72E-09	1.72E-09	1.72E-09	1.72E-09	1.72E-09	1.72E-09
N_2	2.44E-07	2.44E-07	2.44E-07	2.44E-07	2.44E-07	2.44E-07
O_2	4.65E-06	4.65E-06	4.65E-06	4.65E-06	4.65E-06	4.65E-06
CO_2	0.99996	0.99996	0.99996	0.99996	0.99996	0.99996
CO	1.25E-08	1.25E-08	1.25E-08	1.25E-08	1.25E-08	1.25E-08
AR	2.81E-05	2.81E-05	2.81E-05	2.81E-05	2.81E-05	2.81E-05

Table A1 continued

	13	14	15	16	17	18
Total Flow kg/sec	70.70	70.70	70.70	25.94	12.00	10.17
Temperature C	10.68	25.00	32.94	-28.63	100.00	-42.21
Pressure bar	21.76	75.00	110.00	27.50	26.50	26.50
Vapor Fraction	1.00	0.00	0.00	1.00	1.00	0.00
Phase	VAPOR	Supercritical	Supercritical	VAPOR	VAPOR	LIQUID
Mole Fraction						
NO	2.95E-09	2.95E-09	2.95E-09	3.26E-05	6.73E-05	4.99E-06
NO_2	3.74E-06	3.74E-06	3.74E-06	2.82E-09	5.45E-11	7.71E-09
N_2O_4	1.72E-09	1.72E-09	1.72E-09	1.29E-12	2.47E-14	3.52E-12
N_2	2.44E-07	2.44E-07	2.44E-07	0.0489	0.1043	3.01E-03
O_2	4.65E-06	4.65E-06	4.65E-06	0.1834	0.0194	0.0166
CO_2	0.99996	0.99996	0.99996	0.6099	0.5555	0.9587
CO	1.25E-08	1.25E-08	1.25E-08	1.37E-03	2.92E-03	9.70E-05
AR	2.81E-05	2.81E-05	2.81E-05	0.1564	0.3178	0.0216

Table A1 continued

	19	20	21	22	23	24
Total Flow kg/sec	10.17	10.17	10.17	10.17	10.17	15.77
Temperature C	-49.63	-36.01	5.00	75.68	-14.00	-42.21
Pressure bar	12.19	12.19	12.19	28.00	28.00	26.50
Vapor Fraction	0.07	0.98	1.00	1.00	0.28	1.00
Phase	MIXED	MIXED	VAPOR	VAPOR	MIXED	VAPOR
Mole Fraction						
NO	4.99E-06	4.99E-06	4.99E-06	4.99E-06	4.99E-06	4.84E-05
NO_2	7.71E-09	7.71E-09	7.71E-09	7.71E-09	7.71E-09	3.91E-11
N_2O_4	3.52E-12	3.52E-12	3.52E-12	3.52E-12	3.52E-12	1.77E-14
N_2	3.01E-03	3.01E-03	3.01E-03	3.01E-03	3.01E-03	0.074979
O_2	0.0166	0.0166	0.0166	0.0166	0.0166	0.2782
CO_2	0.9587	0.9587	0.9587	0.9587	0.9587	0.4116
CO	9.70E-05	9.70E-05	9.70E-05	9.70E-05	9.70E-05	2.10E-03
AR	0.0216	0.0216	0.0216	0.0216	0.0216	0.2330

Table A1 continued.

	25	26
Total Flow kg/sec	15.77	12.00
Temperature C	-36.01	-26.81
Pressure bar	26.50	1.20
Vapor Fraction	1.00	1.00
Phase	VAPOR	VAPOR
Mole Fraction		
NO	4.84E-05	6.73E-05
NO_2	3.91E-11	5.45E-11
N_2O_4	1.77E-14	2.47E-14
N_2	0.074979	0.104333
O_2	0.2782	0.0194
CO_2	0.4116	0.5555
CO	2.10E-03	2.92E-03
AR	0.2330	0.3178

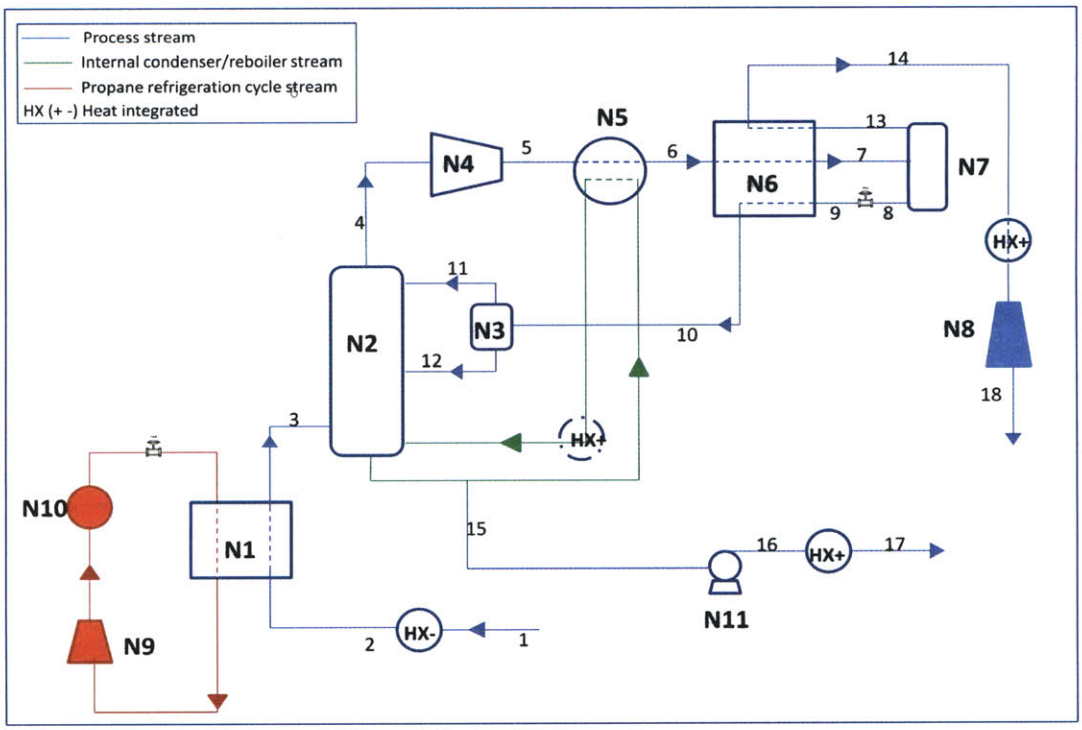

Figure A2: Non-Condensable Gas Removal Unit – Configuration B

Table A2: Stream Data for Non-condensable gas process B

	1	2	3	4	5	6
Total Flow kg/sec	86.48	86.48	86.48	61.73	61.73	61.73
Temperature C	27.55	6.05	-30.05	-22.02	35.61	-5.00
Pressure bar	26.00	26.00	26.00	25.50	50.50	50.50
Vapor Fraction	1	1	0.26	1	1	0.73
Phase	Vapor	Vapor	Mixed	Vapor	Vapor	Mixed
			Mole Fraction			
NO	1.33E-05	1.33E-05	1.33E-05	2.64E-05	2.64E-05	2.64E-05
NO_2	3.17E-06	3.17E-06	3.17E-06	9.85E-08	9.85E-08	9.85E-08
N_2O_4	1.47E-09	1.47E-09	1.47E-09	4.54E-11	4.54E-11	4.54E-11
N_2	0.0152	0.0152	0.0152	0.0259	0.0259	0.0259
O_2	0.0567	0.0567	0.0567	0.1032	0.1032	0.1032
CO_2	0.8803	0.8803	0.8803	0.775	0.775	0.775
CO	4.27E-04	4.27E-04	4.27E-04	7.41E-04	7.41E-04	7.41E-04
AR	0.0474	0.0474	0.0474	0.0951	0.0951	0.0951

Stream 1 refers to the flue gas stream after drying

Table A2 continued.

	7	8	9	10	11	12
Total Flow kg/sec	61.73	45.88	45.88	45.88	28.21	17.67
Temperature C	-27.57	-27.57	-32.50	-10.02	-10.02	-10.02
Pressure bar	50.50	50.50	31.97	31.97	31.97	31.97
Vapor Fraction	0.28	0	0.08	0.62	1	0
Phase	Mixed	Liquid	Mixed	Mixed	Vapor	Liquid
			Mole Fraction			
NO	2.64E-05	1.14E-05	1.14E-05	1.14E-05	1.73E-05	1.81E-06
NO_2	9.85E-08	1.36E-07	1.36E-07	1.36E-07	1.65E-08	3.31E-07
N_2O_4	4.54E-11	6.27E-11	6.27E-11	6.27E-11	7.59E-12	1.53E-10
N_2	0.0259	6.96E-03	6.96E-03	6.96E-03	0.0108	7.17E-04
O_2	0.1032	0.0355	0.0355	0.0355	0.0543	4.72E-03
CO_2	0.775	0.9154	0.9154	0.9154	0.8716	0.9869
CO	7.41E-04	2.17E-04	2.17E-04	2.17E-04	3.36E-04	2.46E-05
AR	0.0951	0.0420	0.0420	0.0420	0.0630	7.60E-03

Table A2 continued.

	13	14	15	16	17	18
Total Flow kg/sec	15.85	15.85	70.63	70.63	70.63	15.85
Temperature C	-27.57	-10.02	-10.96	-2.81	18.00	2.99
Pressure bar	50.50	50.50	25.92	110.00	110.00	1.20
Vapor Fraction	1	1	0	0	0	1
Phase	Vapor	Vapor	Supercritical	Supercritical	Supercritical	Vapor
			Mole Fraction			
NO	6.50E-05	6.50E-05	2.58E-09	2.58E-09	2.58E-09	6.50E-05
NO_2	2.14E-09	2.14E-09	3.98E-06	3.98E-06	3.98E-06	2.14E-09
N_2O_4	9.84E-13	9.84E-13	1.84E-09	1.84E-09	1.84E-09	9.84E-13
N_2	0.0746	0.0746	5.62E-08	5.62E-08	5.62E-08	0.0746
O_2	0.2776	0.2776	1.91E-06	1.91E-06	1.91E-06	0.2776
CO_2	0.4136	0.4136	0.99997	0.99997	0.99997	0.4136
CO	2.09E-03	2.09E-03	3.56E-09	3.56E-09	3.56E-09	2.09E-03
AR	0.2320	0.2320	2.25E-05	2.25E-05	2.25E-05	0.231976

References

[1] International Energy Agency Key World Energy Statistics. http://www.iea.org/textbase/nppdf/free/2010/key_stats_2010.pdf.

[2] MIT. The Future of Coal: An Interdisciplinary Study. 2007.

[3] U.S Department of Energy Press Release: FutureGen 2.0: http://www.energy.gov/news/9309.htm (accessed September 15, 2010).

[4] Erika de Visser; Hendriks, C.; Barrio, M.; Mølnvik, M. J.; Gelein de Koeijer; Liljemark, S.; Yann Le Gallo. Dynamis CO_2 Quality Recommendations. International Journal of Greenhouse Gas Control 2 2008, 478-484.

[5] Wall, T.; Gupta, R.; Buhre, B.; Khare, S. Oxy-fuel (O_2/CO_2, O_2/RFG) Technology for Sequestration-ready CO_2 and Emission Compliance; The 30th international technical conference on coal utilization and fuel systems, coal technology: yesterday,- today-tomorrow; 2005; .

[6] Hong, J.; Chaudhry, G.; Brisson, J. G.; Field, R.; Gazzino, M.; Ghoniem, A. Analysis of Oxy-fuel Combustion Power Cycle utilizing a Pressurized Coal Combustor. Energy 2009, 9, 1332-1340.

[7] Zheng, L.; Pomalis, R.; Clements, B. Technical Feasibility Study of TIPS Process and Comparison with other CO_2 Capture Power Generation Processes. The 32nd international technical conference on coal utilization and fuel systems.

[8] Hong, J.; Field, R.; Gazzino, M.; Ghoniem, A. F. Operating Pressure Dependence of the Pressurized Oxy-fuel Combustion Power Cycle. Energy 2010.

[9] Intergovernmental Panel on Climate Change (IPCC), Carbon Dioxide Capture and Storage: Summary for Policymakers and Technical Summary, 2005.

[10] Wang, C. S.; Berry, G. F.; Chang, K. C.; Wolsky, A. M. Combustion of Pulverized Coal using Waste Carbon Dioxide and Oxygen. Combustion and Flame 1988, 3, 301-310.

[11] Croiset, E.; Thambimuthu, K.; Palmer, A. Coal Combustion in O_2/CO_2 Mixtures Compared with Air. Canadian Journal of Chemical Engineering 2000, 2, 402-407.

[12] Liu, H.; Zailani, R.; Gibbs, B. M. Comparisons of Pulverized Coal Combustion in Air and in Mixtures of O_2/CO_2. Fuel 2005, 7-8, 833-840.

[13] Bachu, S. CO_2 Storage in Geological Media: Role, Means, Status and Barriers to Deployment, Progress in Energy and Combustion Science 2008, 254-273.

[14] Aya, I.; Yamane, K.; Shiozaki, K. Proposal of Self Sinking CO_2 Sending System: COSMOS; Proceedings of the 4th International Conference on Greenhouse Gas Control Technologies; Pergamon: 1999; pp 269-27.

[15] Steinberg, M. Decarbonization and Sequestration for Mitigating Global Warming; First National Conference on Carbon Sequestration; 2001.

[16] Ohsumi, T. CO_2 Disposal Options in Deep Sea. Marine Technology Science Journal 1995, 3, 58-66.

[17] Seibel, B. A.; Walsh, P. J. Potential Impacts of CO_2 Injection on Deep-sea Biota. Science 2001, 294, 319-320.

[18] Pipitone, G.; Bolland, O. Power Generation with CO_2 Capture: Technology for CO_2 Purification. International Journal of Greenhouse Gas Control 2009, 5, 528-534.

[19] Klara, Julianne M. et al. Cost and Performance Baseline for Fossil Energy Plants: Volume 1: Bituminous Coal and Natural Gas to Electricity. DOE/NETL-2007/1281 2007.

[20] DePriest, W.;Gaikwad, R. P. Economics of Lime and Limestone for Control of Sulfur Dioxide. http://www.carmeuse.com/

[21] Keilin, B.; Walitt, A. L. Method of Converting Sulfur Dioxide to Sulfuric Acid: Patent Application, 3649188, 1972.

[22] White, V.; Torrente-Murciano, L.; Sturgeon, D.; Chadwick, D. Purification of Oxyfuel-derived CO_2. Energy Procedia 2009, 1, 399-406.

[23] Miller, D. N. Mass Transfer in Nitric Acid Absorption. AIChE Journal 1987, 8, 1351-1358.

[24] Shafeen, A.; Zanganeh, K. E. Experimental Assessment of Lead-chamber Reactions in an Integrated CO_2 Capture and Compression Unit (CO_2CCU) for Oxy-fuel Plants; 2010; .

[25] Jones, E. M. Industrial and Engineering Chemistry 1950, 11, 2208-2210.

[26] Dewolf, P.; Larison, E. L. American Sulfuric Acid Practice; Kessinger Publishing: 2007; , pp 280.

[27] Raschig Ann. D. Chem. 1887, 242-250.

[28] Lunge, G.; Berl, E. Estimation of the Oxides of Nitrogen and the Theory of the Lead-chamber Process, Zeitsch Angew. Chem. 1907.

[29] Berl, E. *In* Studies of the Lead Chamber Process; 1935; Vol. 31, pp 193-227.

[30] Falgout, A. The Reactions of Nitrogen and Sulfur Oxides in Air. PhD Thesis, University of Florida, 1972.

[31] Ellison, T. K.; Eckert, C. A. The Oxidation of Aqueous SO_2. The Influence of Nitrogen Dioxide at Low pH. Journal of Physical Chemistry 1984, 2335-2339.

[32] Potter, W. *In* Recent Theories of the Sulfuric Acid Process; 1892; .

[33] Sorel, E. Bulletin de la Societe Industrielle de Mulhouse 1889.

[34] Schertel, A. Chemische Industrie 1889, 80.

[35] Robinson, R. K.; Lindstedt, R. P. Detailed Chemical Kinetic Modeling of Pollutant Conversion in Flue Gases from Oxycoal Plant. 1st OXYFUEL COMBUSTION CONFERENCE, Cotbus, Germany, 2009.

[36] Schroeder, W. H. Thermal and Photochemical Reactions of Sulfur Dioxide in Air. PhD Thesis, University of Colorado, Boulder, 1971.

[37] Hurter, F. Dynamic Theory of the Manufacture of Sulphuric Acid. The Journal of the Society of Chemical Industry 1882, 1, 8-8-12, 49-55, 83-85.

[38] Jaffe, S.; Klein, F. S. Photolysis of NO_2 in the Presence of SO_2 at 3660 A. Trans. Faraday Soc. 1966, 2150.

[39] Benadda, B.; Kafou, K.; Monkam, P.; Otterbein, M. Hydrodynamics and Mass Transfer Phenomena in Counter-current Packed Column at Elevated Pressures. Chemical Engineering Science 2000, 6251-6257.

[40] Dankwerts, P. V. Gas–Liquid Reactions; 1970; .

[41] Liss, P. S. Exchange of SO_2 between the Atmosphere and Natural Waters. Nature 1971, 327-329.

[42] Brimblecombe, P.; Spedding, D. J. Rates of Solution of Gaseous Sulfur Dioxide at Atmospheric concentrations. Nature 1972, 225.

[43] Bodenstein, M. Formation and Dissociation of the Higher Nitrogen Oxide. Zeit. Physik. Chem 1922.

[44] Bodenstein, M. Zeit. The Rate of the Reaction between Nitric Oxide and Oxygen. Elektrochem 1918, 183,.

[45] Aspen Inorganics. Nitric Acid Package Report. 2004.

[46] Iloeje, C.; Field, R.; Gazzino, M.; Ghoniem, A. Process Modeling and Analysis of CO_2 Purification for Pressurized Oxy-coal Combustion; 2010; .

[47] Aspen Technology, Inc. Aspen Physical Property System: Physical Property Models. 2009.

[48] Fredenslund, A.; Sather, G. A. J. Gas-Liquid Equilibrium of the Oxygen-Carbon Dioxide System. Chem. Eng. Data 1970, 1, 17-22.

[49] Zenner, G. H.; Dana, L. I. Chem. Eng. Liquid-Vapor Equilibrium Compositions of Carbon Dioxide-Oxygen -Nitrogen Mixtures. Progr. Symp. Ser. 1963, 44, 36.

[50] Muirbrook, N. K.; Prausnitz, J. M. Multicomponent Vapor-liquid Equilibria at High Pressures: Part I. Experimental Study of the Nitrogen—Oxygen—Carbon dioxide System at 0°C. 1965, 11, 1092.

[51] Sabirzyanov, A. N.; Il'in, A. P.; Akhunov, A. R.; Gumerov, F. M. Solubility of Water in Supercritical Carbon Dioxide. High Temperature 2002, 2, 203-206.

[52] Darde, A.; Prabhakar, R.; Tranier, J. P.; Perrin, N. Air Separation and Flue Gas Compression and Purification Units for Oxy-coal Combustion Systems; 2009; Vol. 1, pp 527-534.

[53] Douglas, F. R.; Brown, D.; Cobb, R. A.; George, T. J.; Hackney, J. W.; Humphreys, K. K.; Wellman, P. AACE International Recommended Practice No. 16R-90 1991, 1-62.

[54] Loh, H. P.; Lyons, J.; White , C. W. Process Equipment Cost Estimation: Final Report. DOE/NETL-2002/1169 .

[55] Hong, J. Techno_Economic Analysis of Pressurized Oxy-Fuel Combustion Power Cycle for CO_2 Capture, Massachusetts Institute of Technology, June 2009.

[56] Lunsford, K. M. Advantages of Brazed Heat Exchangers in the Gas Processing Industry. Proceedings of the 75th GPA Annual Convention, Tulsa, OK: Gas Processors Association 1996, 100-106.

[57] Polasek, J. C.; Donnelly, S. T.; Bullin, J. A. Process Simulation and Optimization of Cryogenic Operations Using Multi-Stream Brazed Aluminum Exchangers. Proceedings of the 68th GPA Annual Convention, Tulsa, OK: Gas Processors Association 1989, 100-106.

[58] American Society of Mechanical Engineers. ASME Boiler and Pressure Vessel Code. 1989.

[59] Wilkinson, M. B.; Boden, J. C.; Panesar, R. S.; Allam, R. J. CO_2 Capture via Oxyfuel Firing: Optimization of a Retrofit Design Concept for a Refinery Power Station Boiler. First National Conference on Carbon Sequestration. 2001.

[60] Thomas, D. C. Carbon Dioxide Capture for Storage in Deep Geologic Formations; Elsevier B.V: 2005 .

[61] Adugina, N. A.; Kristal, M. M.; Lazarev, G. E. Corrosion-Erosion Resistance of Stainless Steels in Sulfuric Acid Media. Chemical and Petroleum Engineering 1972.

[62] Shoemaker, L. E.; Crum, J. R. Experience in Effective Application of Metallic Materials for Construction of FGD Systems. Special Metals Corporation Technical Papers

[63] Schweitzer, P. A. Metallic Materials Physical, Mechanical, and Corrosion Properties; CRC Press: 2003.

[64] Seiersten, M. Materials Selection for Separation, Transportation and Disposal of CO_2; NACE Corrosion Conference and Expo 2001; NACE International: 2001.

[65] U.S Department of Energy ;2005.

[66] Kumar, P.; Barret, D. M.; Delwiche, M. J.; Stroeve, P. Methods for Pretreatment of Lignocellulosic Biomass for Efficient Hydrolysis and Biofuel Production. Ind. Eng. Chem. Res. 2009, 3713-3729.